University of Nebraska Medical Center
BREAKTHROUGHS FOR LIFE

University of Nebraska Medical Center
DigitalCommons@UNMC

Theses & Dissertations

Graduate Studies

Summer 8-14-2015

Role of the C-terminus of the Catalytic Subunit of Translesion Synthesis Polymerase ζ (Zeta) in UV-induced Mutagensis

Hollie M. Siebler
University of Nebraska Medical Center

Follow this and additional works at: https://digitalcommons.unmc.edu/etd

 Part of the Genetics Commons, and the Other Microbiology Commons

Recommended Citation

Siebler, Hollie M., "Role of the C-terminus of the Catalytic Subunit of Translesion Synthesis Polymerase ζ (Zeta) in UV-induced Mutagensis" (2015). *Theses & Dissertations*. 6.
https://digitalcommons.unmc.edu/etd/6

This Thesis is brought to you for free and open access by the Graduate Studies at DigitalCommons@UNMC. It has been accepted for inclusion in Theses & Dissertations by an authorized administrator of DigitalCommons@UNMC. For more information, please contact digitalcommons@unmc.edu.

ROLE OF THE C-TERMINUS OF THE CATALYTIC SUBUNIT OF TRANSLESION SYNTHESIS POLYMERASE ζ (ZETA) IN UV-INDUCED MUTAGENESIS

By

Hollie M. Siebler

A DISSERTATION

Presented to the Faculty of

The University of Nebraska Graduate College

In Partial Fulfillment of the Requirements

For the Degree of Doctor of Philosophy

Cancer Research Graduate Program

Under the Supervision of Professor Youri. I. Pavlov

University of Nebraska Medical Center
Omaha, Nebraska

May, 2015

ROLE OF THE C-TERMINUS OF THE CATALYTIC SUBUNIT OF TRANSLESION SYNTHESIS POLYMERASE ζ (ZETA) IN UV-INDUCED MUTAGENESIS

Hollie M. Siebler, Ph.D.

University of Nebraska, 2015

Supervisor: Youri I. Pavlov, Ph.D.

Cellular DNA is under constant attack by endogenous and exogenous DNA damaging agents that threaten genome integrity. Unrepaired DNA lesions often stall replicative DNA polymerases and are bypassed by translesion synthesis (TLS) to prevent replication fork collapse. TLS mechanisms are lesion- and species-specific, with prominent roles of specialized DNA polymerases with relaxed active sites. After incorporation of nucleotide(s) across from the lesion, the distorted primer termini are typically extended by DNA polymerase ζ (Pol ζ). As a result, Pol ζ is responsible for most DNA damage-induced mutations. Mechanisms of sequential polymerase switches and regulation of Pol ζ access to DNA *in vivo* remain unclear. Pol ζ shares two accessory subunits, called Pol31/Pol32 in yeast, with replicative Pol δ. Inclusion of Pol31/Pol32 in both holoenzymes requires a [4Fe-4S] cluster in the catalytic subunit C-terminal domains (CTDs). Disruption of the Pol ζ cluster or deletion of the *POL32* gene attenuates induced mutagenesis.

Here we describe a novel mutation affecting Pol ζ, *rev3ΔC*. Rev3ΔC lacks the entire CTD, the binding platform for Pol31/Pol32. This mutation provides insight into regulation of polymerase switches and further defines regulatory roles of the Pol ζ CTD.

rev3ΔC strains are partially proficient in Pol32-dependent UV-induced mutagenesis. This suggests a role for Pol32 in TLS beyond binding Pol ζ, related to Pol δ. We examined several TLS regulatory proteins, including Mgs1 which can compete with Pol32 for binding PCNA. Overproduction of Mgs1 suppressed induced mutagenesis, but had no effect in *rev3ΔC* suggesting Mgs1 exerts its inhibitory effect by acting specifically on Pol32 of Pol ζ. This evidence for differential regulation of Pol δ/ζ Pol32 emphasizes complexity of polymerase switches. Spectra of mutations induced by UV in *rev3ΔC* were examined to further define the regulatory role of Pol ζ CTD. Rev3ΔC produced different mutational spectra than WT, progressively deficient first in transversions/frameshifts, then transitions, and altered upon increasing UV doses. This supports a fine-tuned role for the CTD in regulating Pol ζ function and highlights differential mechanisms activated by different UV doses.

DEDICATION

To God

And my wonderful parents,

Calvin and Tereasa Siebler

Table of Contents

List of Figures and Tables

ACKNOWLEDGEMENTS

Graduate school has, by far, been the most challenging thing I have done in my life. I learned many lessons about hard work, perseverance, determination, and working through complex problems. I also learned about the thrill of discovery and all there still is to discover and understand. I owe my completion of this degree to many people, without whom I know I would have never made it. Here, I would like to share my thanks to many of them, although the list is endless.

First of all, I would like to thank God for giving me all of the skills necessary to pursue this career and Ph.D. degree. I would like to thank Him for always being there beside me and helping me through the tough times (for hundreds of prayers heard!). I really have a new understanding for the complex and beautiful nature of the world He made. I always can find strength through prayer.

I do not have near enough space or time to thank my mentor, Dr. Youri Pavlov, for all that he has done for me. I thank him for accepting me into his laboratory and for being an excellent mentor. When I first started, I had no idea how to be an independent researcher. He gave me a lot of direction when I started, and as I progressed through my career he continued to guide me but gave me more and more freedom to come up with and test my own ideas. He was always accessible if I needed to discuss results or writing with him (even when he was overseas). He is a great inspiration to me both as a scientist and as a mentor. I have seen him tailor his mentoring style to each individual student according to their needs, a skill that I would love to acquire in both my research mentoring and teaching in the future. Thank you Dr. Pavlov for helping me become the scientist that I am today, and for adding a positive light and a laugh to even the most upsetting results and situations.

I would like to thank all the past and present members of the Pavlov and Shcherbakova labs, who I have had the privilege to work alongside: Miriam Menezes, Corinn Grabow, Olga Kochenova, Tony Mertz, Liz Moore, Krista Brown, Artem Lada, Irina Vaysertreyger, Matt Northam, Yinbo Zheng, Lena Stepchenkova, Dan Kane, Stephanie Ives, Chelsea Bulock, Sarah Hill, and Xuanxuan Xing. I have spent a great deal of time with many of them over the last five years and owe them a lot. I thank them for creating an ideal work environment, for sharing and discussing many scientific ideas back and forth with me, and for all of the advice that they have given me during my time here. I especially want to thank Tony for his help with protein purification, Miriam for being one of my role models as a new student, and Corinn for all that she taught me.

I owe my thanks to many people in the Eppley department as well. I want to thank my wonderful committee members Polina Shcherbakova, Gloria Borgstahl, and Tahir Tahirov for all of their guidance and advice. I would especially like to thank Polina for all of her wonderful comments and criticism of my project and the manuscript for my first-author paper, I learned so much about my field from her. I also thank Michel Ouellette for serving as the chair on my comprehensive exam committee. I would like to thank Joyce Solheim for all of the time she gave me to answer any questions I had, whether they were about jobs, our department, classes or anything else. She has been a wonderful professor to work alongside on committees as well.

I would like to thank the professors who helped me gain teaching experience and become a better educator. I would like to thank Dr. William Tapprich and Dr. Karen Murch-Shafer for welcoming me into their classrooms to teach lectures in undergraduate biology courses. I thank Dr. Ying Yan for being my mentor while I taught for the Human Disease course at UNO and for her valuable feedback. I especially want to thank Dr. Richard McDonald, who served as my mentor when I was a Teaching Assistant for the graduate course 821: Macromolecular Structure and Function. He taught me many things about writing and grading quiz and exam questions, as well as offered advice on many different ways to help students internalize material. I am very grateful for all of the time that these exceptional professors took out of their busy schedules to help me better prepare and deliver lectures and problem-based recitation sections.

I would like to thank my fellow UNMC students. There are too many to name them all. I especially want to thank the older students that showed me the way: Miriam Menezes, Amanda Hawley, and Jamie Arnst. I always wanted to be the kind of senior student that all of you were. I would like to thank my wonderful friend and roommate Mercury Wu. I want to thank her for all of the hard work she put in when we were TAs, and for all of the fun times that we shared as roommates.

I would like to thank all of the wonderful staff, especially Darcy Jackson, Diane Torrey, and Misty Pocwierz. They made everything in Eppley run smoothly. I thank Darcy for always answering my questions and booking all my travel. I would like to thank Sherry Martin for all the work she did and for being a wonderful volleyball teammate and bible study buddy. I would like to thank Charlotte Stalnaker for helping me get my Russian visa to attend a conference in St. Petersburg, it was so much work! I thank Ed Rau and Roger White for always keeping our equipment working and Mike Berney for always delivering our packages and being so pleasant to talk to. I also want to thank Debi Griffith for her help tracking down my reimbursements and helping with the Eppley picnic. I am very grateful to the Graduate Studies office as well, especially Terri Vadovski for help with scheduling and getting all paperwork in throughout grad school.

I would like to thank the CRGP program for being my home while at UNMC. I thank the GAANN and UNMC fellowships and their committees for supporting me through my graduate career. I thank the DNA sequencing core facility for aiding in my research. I thank my collaborators Tahir Tahirov, Andrey Baranovskiy, and Javier Seravalli for their help and teaching me different techniques.

I would like to thank my wonderful family members, especially my parents and my sisters, Sara and Emma. They have patiently comforted and listened to me complain about my experiments not working, even though they had no idea what I was talking about most of the time. They shared in my successes and triumphs, and encouraged me to keep going when things were difficult. I want to specifically thank my parents for raising me to be hard-working and dedicated to whatever I pursue. Also, all of my other family members (grandparents, cousins, aunts, uncles) and wonderful friends, especially Erin Smith and Kiley Schroeder, have always been there for me and provided me a well-needed break and additional support.

Finally, I want to thank Krista Brown, Stephanie Ives, Chelsea Bulock, and Elizabeth Moore for critical reading of sections of this dissertation.

1 Introduction

For individual organisms to survive and remain healthy, it is critical that genetic information is properly maintained and transmitted faithfully to the next generation. This task is far from trivial because cellular DNA is under constant attack by both endogenous and exogenous (environmental) DNA damaging agents that threaten the integrity of the genome.

1.1 Sources and Types of DNA Damage

Human cells can acquire up to 100,000 spontaneous lesions per cell per day [1]. Without repair, this damage would be of huge negative consequence to the cell. DNA acquires spontaneous damage in a variety of ways (reviewed in [2, 3]). Due to the chemical nature of DNA present in an aqueous environment, its bases are subject to spontaneous hydrolysis. This can lead to bases being lost from nucleic acids, forming abasic sites (also called AP (apurinic/apyrimidinic) sites). Aerobic metabolism generates reactive oxygen and nitrogen species, as well as other products that can damage DNA. Reactive oxygen species (ROS) lead to a variety of types of damage: chemically altered bases such as thymine glycol and 8-oxoguanine (8-oxoG), AP sites, and single stranded breaks (SSBs) in the DNA backbone. Endogenous alkylating agents present in cells also chemically alter the bases of DNA. Another prevalent source of spontaneous DNA damage is deamination of bases. This can occur spontaneously or enzymatically and can lead to mutations by miscoding. Base analogs or damaged bases present in DNA precursor pools can be incorporated into DNA during replication, leading to mispairing and mutations.

The environment is a tremendous source of DNA damage (reviewed in [2]). UV radiation from the sun can link adjacent pyrimidines, forming 6,4 photoproducts (6-4PPs) and cyclobutane pyrimidine dimers (CPDs) which are difficult to replicate past. Ionizing radiation causes many different lesions, including oxidized bases and dangerous double stranded breaks (DSBs). Much of the DNA damage is caused by chemical agents in the environment. Examples include Aflatoxin B1 from fungi, which can cause bulky covalent links to guanine, and N-2-acetyl-2-aminoflurene (AAF, originally designed as an insecticide) and benzo[a]pyrene (cigarette smoke, car exhaust) that can form adducts with DNA. Therefore, in the presence of detrimental endogenous and environmental factors, cells must deal with the challenges of heavy loads of DNA damage.

1.2 Consequences of DNA damage

The type of DNA damage and how it is processed affect the biological outcome (reviewed in [3]). Some specific lesions are primarily mutagenic, others are cytotoxic (cell death) or cytostatic (inhibition of cell growth), and some can give rise to any one of these effects depending on the conditions present. Correspondingly, DNA damage can lead to cell death, cessation of cell division (replicative senescence), or mutations leading to uncontrollable growth and cell division. By causing senescence or death, unrepaired DNA damage can play a role in aging. This is evidenced by the fact that defects in DNA repair lead to progeroid syndromes such as Werner's or Cockayne's syndrome, which are characterized by premature aging.

Damage-induced mutations in the DNA of germ cells lead to hereditary diseases and mutations in the DNA of somatic cells lead to the development of cancer, arising from loss-of-function mutations in tumor suppressor genes or activation of oncogenes.

Mutations in genes involved in DNA repair can predispose cells to transformation. Well-known examples include skin, colon, breast, and ovarian cancers (mentioned in 1.3 under respective DNA repair pathways) [4]. Genome instability is a hallmark of all cancers [5]. In addition to cancer predisposition, many other specific diseases arise in the absence of efficient DNA repair pathways. Several of these are listed in Table 1.1. DNA damage has also been shown to contribute to a variety of neurodegenerative diseases and psychiatric disorders (reviewed in [6]).

Given that the genome can suffer a huge spectrum of damage either spontaneously or as a result of exposure to genotoxic environmental agents, it is not surprising that cells contain many systems designed to deal with DNA damage (Figure 1.1). Collectively they are called the DNA damage response (DDR). There are two major ways cells deal with DNA damage: the first is through DNA repair and the second is through DNA damage tolerance.

1.3 DNA Repair Mechanisms

DNA repair results in the restoration of damaged DNA and preservation of genome integrity (reviewed in [2, 7, 8]). DNA repair contains several pathways belonging to one of three fundamental mechanisms: reversal of DNA damage, excision of damaged elements, and repair of breaks in the DNA backbone. Direct reversal is the simplest and most accurate form of repair. In bacteria and yeast, CPDs can be split back to two normal pyrimidines by photolyase (discussed more in chapter 5) and some methylated bases can be restored by a methyltransferase. The two major DNA repair pathways involve excision of damaged elements, and are called base excision repair (BER) and nucleotide excision repair (NER). Mismatch repair (MMR) is another

Table 1.1 Some of the Diseases caused by defective DNA repair

Proteins Affected by Mutation	Repair Pathway	Human Disease
XPD helicase	NER	Xeroderma Pigmentosum; Trichothiodystrophy; Cockayne's Syndrome
Pol η	Error-free TLS	Xeroderma Pigmentosum Variant form
Pol γ	Mitochondria DNA replication/repair	Progressive External Opthalmoplegia
MRE11, NBS1	HR, NHEJ	Ataxia Telangiectasia like Disease; Nijmegen Breakage Syndrome
LIG4	NHEJ	Lig4 Syndrome
ATM	DSB repair	Ataxia Telangiectasia
APTX	SSB repair	Ataxia Oculomotor Apraxia 1; Spinocerebellar Ataxia; Microencephaly
FANCA-G, D1 (BRCA2), D2, L	Crosslink repair	Fanconi Anemia
BLM	RecQ helicase	Bloom's Syndrome
WRN	RecQ helicase	Werner's Syndrome

Information in table from [2, 3, 6, 9-13]

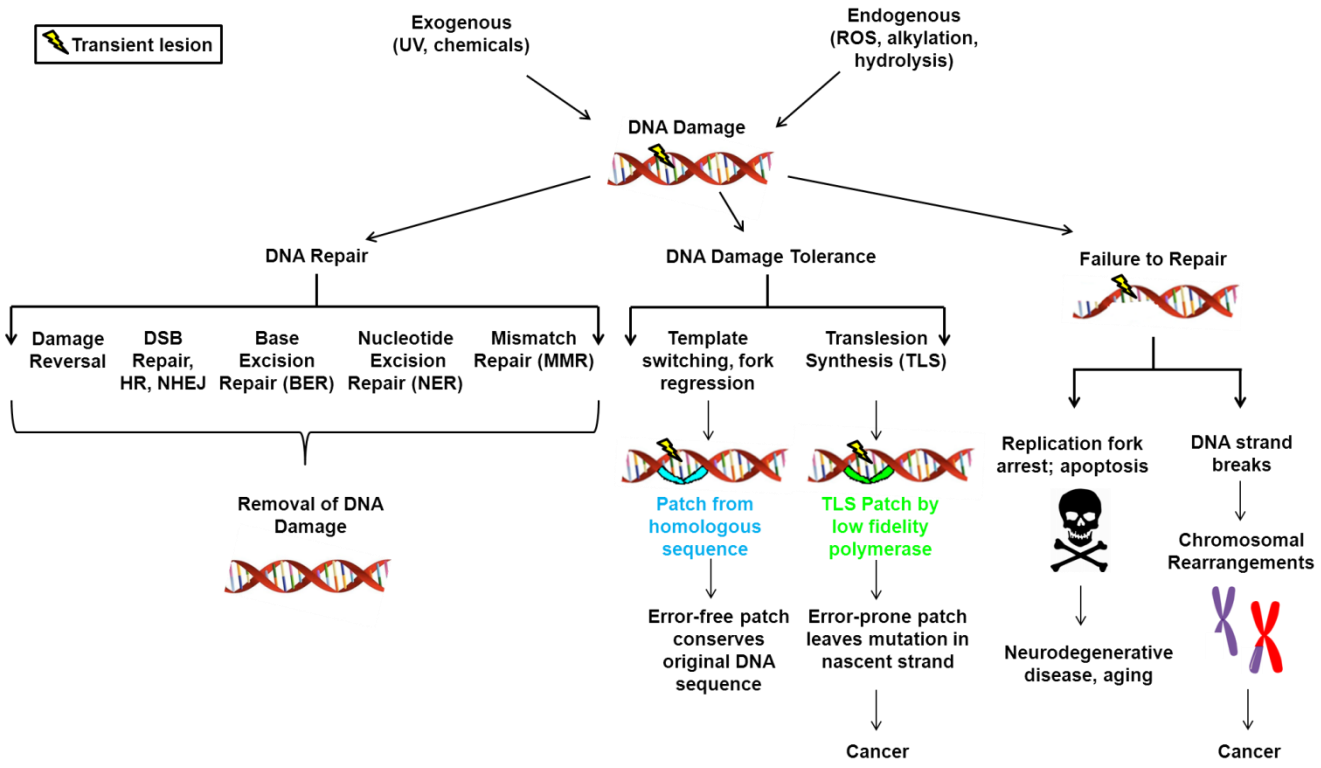

Figure 1.1 DNA Damage Response

The genome is under constant threat of damage, both spontaneously and as a result of exposure to genotoxic environmental agents. Cells contain many mechanisms designed to deal with DNA damage, collectively called the DNA damage response (DDR). There are three major options when dealing with DNA damage. First there can be repair of the damage, which results in restoration of the original DNA sequence. Second, there can be DNA damage tolerance. In this case, the lesions are bypassed to allow for continuation of replication, and then they can be repaired at a later time. Finally, if the damage is not processed it will lead to replication and/or transcription arrest and ultimately cell death. There can also be chromosomal rearrangements that occur when these processes are not operating correctly, which can result in mutation and cancer.

important excision repair pathway for removing predominantly mismatched normal bases, but under special conditions it can also remove modified bases such as 8-oxo-G or uracil in DNA [14-16].

Base excision repair (BER) is responsible for removing the major endogenous damage that results from oxidative stress, hydrolysis of bases, alkylation, and deamination (reviewed in [7, 8, 17, 18]). This includes repair of subtle modifications of DNA such as oxidative lesions, small alkylation products, and single strand breaks (SSBs). During the first step of BER, damaged bases are removed by DNA glycosylases resulting in formation of an AP site. Different DNA glycosylases recognize different types of damage. The next step depends on which type of glycosylase created the AP site. If it was a monofunctional glycosylase, then subsequent cleavage of the backbone will create a nick with a 3'OH and a 5'-dRP terminus. If the glycosylase was bifunctional (containing intrinsic AP-lyase activity), then cleavage will result in a 3'OH and a 5'phosphate terminus. In both cases, an AP endonuclease then nicks the DNA backbone and a 3'- or 5'-phosphodiesterase removes the remaining deoxyribose phosphate. Finally, a DNA polymerase fills the gap that is created (Pol β lyase removes 5'dRP) and DNA ligase seals the remaining nick. There are two branches of BER, termed short patch and long patch depending on how much DNA re-synthesis occurs and which DNA polymerase is involved.

Nucleotide excision repair (NER) removes a variety of structurally unrelated, helix distorting lesions that impair replication and transcription (reviewed in [7, 8, 19]). Specifically, this pathway removes CPDs and 6-4PPs that arise from UV radiation as well as chemical carcinogen-induced bulky adducts. During NER, first there is damage

recognition and opening of the DNA duplex. Then dual incisions are made flanking the damage to initiate repair, which results in excision of a patch of single stranded DNA containing the lesion. The remaining gap is filled by a DNA polymerase and the nick is sealed by DNA ligase. There are two classes of NER, global genome NER (GG-NER) and transcription-coupled NER (TC-NER). The latter specifically corrects damage that stalls transcription in the transcribed strand of actively transcribed regions. The mechanisms for the two classes differ in the recognition step. Patients with defects in NER develop sun-sensitive diseases such as xeroderma pigmentosum, Cockayne's Syndrome, and Trichothiodystrophy. These diseases confer severe predispositions to skin cancer, increasing the risk of cancer up 1000 fold compared to the risk in NER-proficient humans [4, 20].

Mismatch repair (MMR) corrects replication errors made by DNA polymerases and when non-identical duplexes exchange strands during homologous recombination (reviewed in [8], [21]). The mechanism of MMR is best characterized in bacteria and yeast, but many of the homologs of MMR repair proteins operate in mammalian cells. First, the MMR machinery binds to the mismatch and coordinates excision of a patch of DNA, including the mismatch, from the newly synthesized DNA strand. This allows for insertion of the correct base by a DNA polymerase. The strand discrimination mechanisms differ between bacteria and eukaryotes [22]. Loss of MMR has been shown to predispose patients to colon cancer [23].

Some mutagens create adducts that covalently attach DNA bases on two opposite strands at the same time, called interstrand crosslinks (ICL). These can also be caused by lipid peroxidation in the body. They pose a special challenge to DNA repair systems

because they block replication by preventing separation of the two strands of DNA, leading to the formation of DSBs (reviewed in [24]). The repair of ICLs occurs by complex mechanisms utilizing NER, recombination repair, and translesion synthesis [10]. Briefly, NER machinery makes incisions on both sides of the ICL on one strand and this fragment is displaced, resulting in an "unhooked" ICL and a gap in the other strand. Homologous recombination (HR) or translesion DNA synthesis (TLS) fills the gap and the "unhooked" ICL adduct is repaired by a subsequent round of NER.

Most DNA repair processes generate nicks or gaps in DNA as intermediates. The replication fork collapses when it reaches these sites and DSBs are formed. These are most often repaired by homologous recombination in bacteria and yeast and a process called non-homologous end joining (NHEJ) in mammalian cells. Defects in DSB repair caused by mutations in *BRCA1* and *BRCA2* can lead to breast and ovarian cancers [25].

1.4 DNA Damage Tolerance Mechanisms

A special challenge arises for cells if unrepaired damage is encountered during DNA replication and stalls the replicative polymerase (reviewed in [4, 7, 8]). A response called DNA damage tolerance promotes replication through and past an aberrant template, leaving the damage to be repaired at a later time point.

Cells have multiple strategies for tolerating damage to avoid the lethal effects of replication arrest (reviewed in [2, 4]). DNA damage tolerance contains two major branches: error-free recombinational damage avoidance (template switching) and translesion DNA synthesis (TLS). Post translational modification of the processivity clamp PCNA (proliferating cell nuclear antigen) plays a critical role in regulating which branch of DNA damage tolerance will be used (more extensive background on PCNA in

chapter 4.1.1). Monoubiquitylation of PCNA at Lys 164 promotes direct lesion bypass by recruiting specialized TLS polymerases to stalled forks. Polyubiquitylation of the same residue promotes damage avoidance through an unclear mechanism [4]. Sumoylation of PCNA at Lys 164 and Lys 127 inhibits recombination by recruiting Srs2 helicase, which disrupts Rad51 nucleoprotein filaments [26]. Though PCNA modification is important, it is likely that there are other regulatory factors as well.

Recombinational damage avoidance plays a major role in promoting restart when regression of the replication fork is blocked (reviewed in [2, 8, 27]). This process is defined as error-free because the damaged strand is not used as a template for DNA synthesis. Genetic studies suggest that there are three pathways of replication-associated recombination: template switching to the sister chromatid, fork regression, and a gap filling reaction.

In the first pathway, a switch of templates can occur in which the blocked nascent strand temporarily uses the undamaged sister chromatid as a replication template (reviewed in [27, 28]). There is also data to suggest that stalled or arrested forks can undergo a structural rearrangement known as fork regression. During this process the original template strands re-anneal, thereby extruding the newly synthesized strands as a short duplex. The resulting structure is referred to as a “chicken foot.” Through this, conservative DNA synthesis occurs on an undamaged, newly synthesized template strand. Then there is resolution of the chicken foot structure. Finally, when lesions are encountered there can be replication restart downstream of the lesion. This leaves gaps behind, and it is thought that recombination with homologous DNA is one of the ways in which these gaps can be filled.

DNA repair mechanisms and the damage avoidance pathway of DNA damage tolerance are called error-free mechanisms, reducing the mutagenic effect of DNA damage. However, under certain conditions it is critical for cells to be able to deal with excessive DNA damage, and they will do this even at the cost of mutagenesis. The second branch of DNA damage tolerance is TLS.

1.5 Translesion DNA Synthesis

During TLS, replicative DNA polymerases yield the damaged template to specialized polymerases which incorporate nucleotides across from the altered base(s) (insertion step) (Figure 1.2) ([7, 29, 30]). Most prominent in TLS are the low fidelity Y-family polymerases η, κ, ι, and Rev1 ([31, 32]), but in some cases insertion is accomplished by X-family, A-family, or B-family DNA polymerases ([33, 34]). Then there is extension of the aberrant primer terminus, achieved by the inserter or another polymerase (extension step). Most frequently this extension is accomplished by the error-prone B-family Polymerase ζ (Pol ζ) [9, 34-36]. Once the lesion is bypassed, it has been suggested that there could be a return to synthesis by replicative polymerases. Evidence also suggests that there could be post-replicative filling of the gap between the bypassed lesion and a downstream restart site, most likely by Pol ζ [9, 33-38].

TLS events can have opposing effects on mutagenesis. Some TLS polymerases are tailored to bypass specific types of lesions and incorporate predominantly the correct base, i.e. the base that should have been incorporated by the replicative polymerase in the absence of damage. Historically, this is called error-free bypass because the action of these polymerases suppresses induced mutagenesis. Each of the TLS polymerases has different substrate specificities for different types of lesions. However, the number of

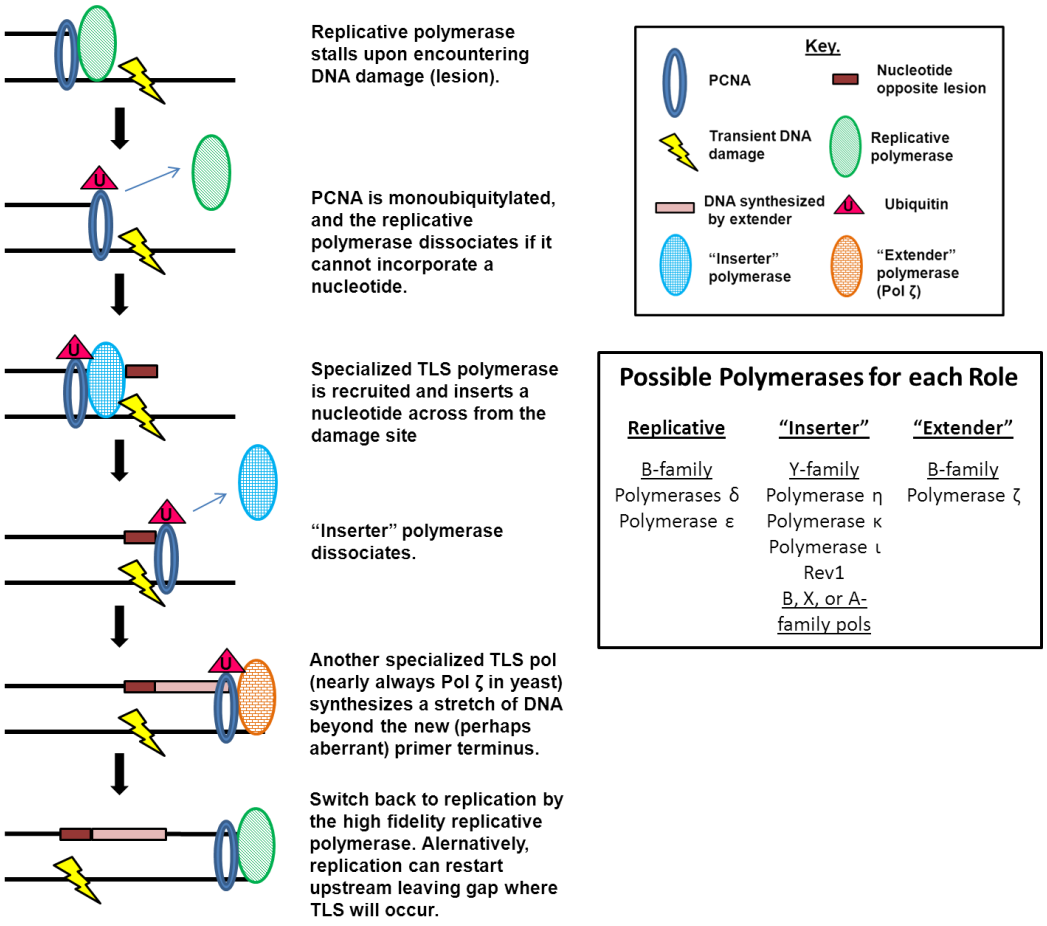

Figure 1.2 General Model of Translesion DNA Synthesis

During TLS, specialized polymerases put a "patch" on DNA damage to allow for its repair at a later time. This is done via a two-step mechanism: first there is insertion of a nucleotide across from the damage site, and then there is extension of the resulting primer terminus. A critical step in this process is the switching of DNA polymerases. This figure depicts a scenario where the insertion and extension step of TLS are performed by two different polymerases that are not in one complex. However, it is important to note that in some cases insertion can be performed by Rev1 (bound to Pol ζ) or by Pol ζ itself (see box).

lesions greatly exceeds the number of polymerases. Therefore most lesions are primarily bypassed by the addition of an incorrect base. This so called error-prone TLS is highly mutagenic. This process is carried out by a complex of proteins comprised of replicative polymerases, TLS Pol ζ, Rev1, and monoubiquitylated PCNA ([7, 9, 39, 40].

One critical event during TLS in eukaryotes is the physical switch between the polymerases. Details of how it actually occurs *in vivo* are not clear. Currently it is thought that it occurs via the two-step insertion-extension mechanism, proposed on the basis of experiments in yeast (Figure 1.2) [32, 34, 41]. Upon damage, PCNA is monoubiquitylated at K164 [42] and there is a switch from replicative Pol δ (or Pol ε) to another polymerase (predominantly Y-family polymerase), which inserts a nucleotide across from the lesion. Rev1 acts as an indispensable scaffold protein and, when necessary, a deoxycytidyl transferase inserting "C" opposite the lesion. Then there is a switch to Pol ζ which performs extension from this potentially aberrant terminus. If an error was made during bypass, the action of Pol ζ allows the altered sequence to remain in the nascent DNA strand sequence, leading to a mutation. Malfunction of this pathway abolishes induced mutagenesis. Many of the signals involved, aside from ubiquitylation of PCNA and RPA signaling, are unknown [43, 44]. One of the central enzymes involved in error-prone TLS is Pol ζ, and this enzyme will be the focus of this dissertation.

1.6 DNA Polymerase ζ

The main role of Pol ζ is as the "universal extender." It specializes in extension past distorted primer termini, such as those caused by mismatched bases inserted by another polymerase or a base across from a bulky lesion [9]. It can also act as both the inserter and extender polymerase across some types of lesions, such as thymine glycol

[9]. Pol ζ is responsible for most induced point mutations (96 % of UV-induced mutations) and roughly half of spontaneous mutations ([7, 45]). It synthesizes DNA *in vitro* with low fidelity and produces a characteristic mutational signature [46], found in mutation spectra *in vivo* [8, 47, 48]. Part of this signature is attributed to template switches [49]. Pol ζ is the only TLS polymerase essential for viability in mice, suggesting it is required for tolerance of endogenous DNA damage during development. In yeast, deletion of *REV3* encoding the catalytic subunit of Pol ζ is not lethal but causes growth retardation in strains with elevated levels of abasic sites [50]. Pol ζ is required for ICL repair and has been implicated in somatic hypermutation [10, 51].

1.7 Pol ζ and Cancer

Pol ζ plays a dual role in both the promotion and prevention of genomic instability that can lead to tumorigenesis. The effect of Pol ζ at the cellular level is very pronounced [35, 52, 53]). Mouse embryonic fibroblasts (MEFs) lacking Pol ζ exhibited sensitivity to various damaging agents and striking chromosomal instability: increased chromosome number (near tetraploid), increased chromosome fusions and fragmentation, and increased translocations [54]. This suggests that Pol ζ protects from cancer originating from large genomic rearrangements, though it causes point mutations that can contribute to cancer (Figure 1.3). Pol ζ can also contribute to resistance to chemotherapeutic cisplatin in human cells due to its ability to bypass intrastrand crosslinks [55]. Conditional knockout in mice enhanced spontaneous tumorigenesis, but reduction of Pol ζ levels has been associated with colon carcinomas (reviewed in [51]).

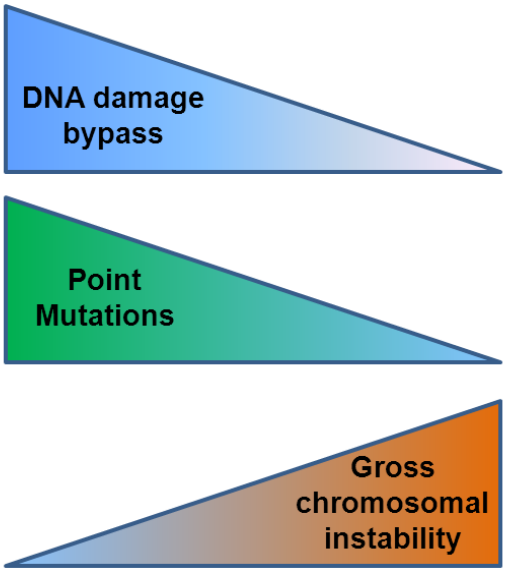

Figure 1.3 Dual roles of TLS in the prevention and promotion of carcinogenesis

Mutations induced by error-prone TLS are etiologic in most environmentally induced cancers, but it is clear that simply blocking TLS is not sufficient to reduce cancer risk. This can sometimes accelerate carcinogenesis through chromosomal instability. Modified from [52].

1.8 Thesis work

Understanding the molecular processes underlying TLS and its associated mutagenesis is likely to provide important insights into carcinogenesis and other genetic diseases caused predominately by genetic mutations. The purpose of the work presented here is to finely study the regulation and recruitment of Pol ζ to sites of DNA damage, focusing on the role of the C-terminal domain (CTD) of catalytic subunit Rev3. A novel mutant which lacks the CTD, *rev3ΔC*, is described and used to probe various aspects of mechanisms of UV-induced mutagenesis.

2 Materials and Methods

2.1 Materials

Most mutagenesis studies were done in the *Saccharomyces cerevisiae* strain 8C-YUNI101 (*MAT***a** *his7-2 leu2-3,112 ura3-Δ bik1*::*ura3-29RL trp1-1*$_{UAG}$ *ade2-1*$_{UAA}$) [56] and its derivatives. Studies of the effects of the deletion of *MGS1* on mutagenesis were done in a derivative of the strain BY4742 (*MATα his3Δ1 leu2Δ0 lys2Δ0; ura3Δ0*) (Life Technologies, U.S.A.). Extracts for western blotting were prepared from transformants of the protease-deficient strain BJ2168 (*MATa prc1-407 prb1-1122 pep4-3 leu2 trp1 ura3-52 gal2*) [57]. Plasmids used are described in the next section.

Mouse anti-GST, goat HRP-conjugated anti-mouse, and donkey HRP-conjugated anti-goat antibodies were from Genscript (Piscataway, NJ). Goat anti-human actin antibody (cross-reacts with yeast actin) was from Santa Cruz Biotechnology (Santa Cruz, CA). Super Signal West Femto Chemiluminescent Substrate detection kit and DreamTaq Green DNA Polymerase were from Thermo Scientific (Dubuque, IA). The 1X cOmplete EDTA-free protease inhibitor cocktail was from Roche (Indianapolis, IN). The Immobilon PVDF membrane was from Millipore (Billerica, MA). QuikChange Site Directed Mutagenesis kit was from Agilent Technologies (U.S.A.) All other chemicals were reagent grade and were purchased from Sigma Aldrich (St. Louis, MO) or Fisher Scientific (Atlanta, GA).

2.2 Creation of Mutant Strains

All mutant strains used in this dissertation are listed in Table 2.1.

Table 2.1: Description of mutant *Saccharomyces cerevisiae* strains

Mutant Category	Abbreviated Strain Name[a]	Genotype
rev3 mutants	*rev3-dd*	*rev3-D1142A,D1144A*
	rev3-ZnF	*rev3-C1398A,C1401A,C1414A,C1417A*
	rev3-FeS	*rev3-C1446A,C1449A,C1468A,C1473A*
	rev3ΔC	*rev3-Δ(1381-1505)*
	rev3-ZnF,FeS	*rev3-C1398A,C1401A,C1414A,C1417A C1446A,C1449A,C1468A,C1473A*
Other mutants	*pol30-K164R*	*pol30-K164R*
	pol32Δ	*pol32Δ::kanMX*
	rev1Δ	*rev1Δ::kanMX*
	mgs1Δ	*mgs1Δ::kanMX*
	MGS1↑	*LEU2::GAL1-MGS1*
Double mutants	*rev3ΔC-dd*	*rev3-Δ(1381-1505),D1142A,D1144A*
	rev3ΔC pol32Δ	*rev3-Δ(1381-1505) pol32Δ*
	rev3ΔC rev1Δ	*rev3-Δ(1381-1505) rev1Δ*
	rev3ΔC mgs1Δ	*rev3-Δ(1381-1505) mgs1Δ*
	rev3ΔC MGS1↑	*rev3-Δ(1381-1505) LEU2::GAL1-MGS1*
	rev3ΔC pol30-K164R	*rev3-Δ(1381-1505) pol30-K164R*
Strains with plasmids[b]	WT + vector	*[pRS425-GAL1-GST]*
	WT + *REV1↑*	*[GAL1-GST-REV1]*
	WT + *rev3-dd↑*	*[GAL1-GST-rev3-D1142A,D1144A]*
	WT + *rev3ΔC↑*	*[GAL1-GST-rev3-Δ(1381-1505)]*
	WT + *rev3-FeS↑*	*[GAL1-GST-rev3-C1446A,C1449A,C1468A,C1473A]*
	rev3Δ + vector	*rev3Δ [pRS425-GAL1-GST]*

rev3Δ + *rev3ΔC*↑	*rev3Δ [GAL1-GST-rev3-Δ(1381-1505)]*
rev3ΔC + vector	*rev3-Δ(1381-1505) [pRS425-GAL1-GST]*
rev3ΔC + *REV1*↑	*rev3-Δ(1381-1505)[GAL1-GST-REV1]*
rev3-FeS + vector	*rev3-C1446A,C1449A,C1468A,C1473A [pRS425-GAL1-GST]*
rev3-FeS + *REV1*↑	*rev3-C1446A,C1449A,C1468A,C1473A [GAL1-GST-REV1]*
rev1Δ + vector	*rev1Δ [pRS425-GAL1-GST]*
rev1Δ + *REV1*↑	*rev1Δ [GAL1-GST-REV1]*

[a]All mutants except *mgs1Δ* were created in the 8C-YUNI101 background (Materials and Methods)
[b]Description of plasmids is in 2.2

2.2.1 *rev3-ZnF* and *rev3-FeS*

Mutations in the regions encoding the yeast Rev3 C-terminal domain (CTD) were first introduced into yeast integrative plasmid pRevLCav2 [56] by Dr. Artem Lada. This plasmid contains the *Saccharomyces cerevisiae REV3* ORF region coding for 647 C-terminal amino acids, 335 bp of downstream noncoding sequence, and the *URA3* gene. A multiple-site plasmid mutagenesis protocol was used to create alleles coding for changes of cysteines 1398, 1401, 1414, and 1417 at MBS1 (ZnF) and cysteines 1446, 1449, 1468, and 1473 at MBS2 (FeS) to alanines [58]. The resulting plasmids encoding mutant *REV3* ORF ends were digested with SnaBI, and the yeast strain 8C-YUNI101 was transformed with the linear fragment to create the *rev3-ZnF* and *rev3-FeS* mutant strains [56].

2.2.2 *rev3ΔC* and *rev3ΔC-dd* alleles

The plasmid pRevLCav2-rev3ΔC is a deletion derivative of integrative plasmid pRevLCav2 [56], created by PCR of the plasmid region flanking the deletion and ligation by Dr. Artem Lada. *rev3ΔC* encodes for Rev3 lacking the C-terminus (amino acids 1381-1504). Site directed mutagenesis using the QuikChange kit was performed on pRevLCav2-rev3ΔC to create pRevLCAV2-rev3ΔC-DD, encoding for a catalytically dead Rev3. We used the same protocol as in 2.2.1 to integrate the mutant alleles into the genome and replace endogenous *REV3* [56], creating the *rev3ΔC* and *rev3ΔC-dd* mutant stains, respectively (Table 2.1).

2.2.3 Strains with additional mutations outside of Rev3

Wild type (WT) and *rev3ΔC* strains were transformed with the *Bst*EII-linearized plasmid YIp128-GAL-MGS1 (kindly provided by H. Ulrich) to create *WT + MGS1*↑ and

rev3ΔC + MGS1↑ strains, respectively, with integration of the *GAL-MGS1* cassette into the endogenous *LEU2* locus [59]. *rev3ΔC pol32Δ* and *rev3ΔC rev1Δ* strains were created by replacing *POL32* and *REV1*, respectively, with KanMX cassettes in the *rev3ΔC* strain.

2.2.4 Strains for overexpression of *REV* genes

Strains for overexpression of *rev3ΔC, rev3-dd, rev3-FeS* and *REV1* (Table 2.1) were obtained by transformation of 8C-YUNI101 *rev3Δ* (for *rev3* mutants) and 8C YUNI101 (for *REV1* overexpression) with derivatives of the multicopy plasmid pRS425-GALGST [60] containing the appropriate *GST-REV3* or *GST-REV1* allele under the control of a galactose-inducible promoter. The derivatives of the pRS425-GALGST-REV3 plasmid with mutations affecting the metal binding sites of Rev3, including *rev3ΔC,* were created by gap repair in yeast *in vivo,* described below (and in [61]). Site-directed mutagenesis primer sequences are shown in Appendix B.

2.2.5 Creation of p425-GALGST-REV3 derivatives using Gap Repair

For overexpression studies and western blot analysis, we constructed expression vectors encoding a fusion of full-length Rev3 with GST. The basic plasmid with a *LEU2* marker and a galactose-inducible promoter upstream of *REV3* was constructed by N. Sharma in the Dr. P. Shcherbakova laboratory. We used an *in vivo* gap repair method to transfer the mutant alleles of *REV3* from pRevLCav2 to the expression plasmid (Figure 2.1) [62]. Briefly, a yeast strain with deletion of the entire *REV3* gene was transformed by a mixture of two PCR fragments: the section of the expression plasmid pRS425-GALGST-REV3 without the region corresponding to the C-terminal part of *REV3,* and the section of the *REV3* gene corresponding to the mutated region from pRevLCav2 (plasmids were isolated, amplified in *E. coli*, and verified by sequencing). Yeast were

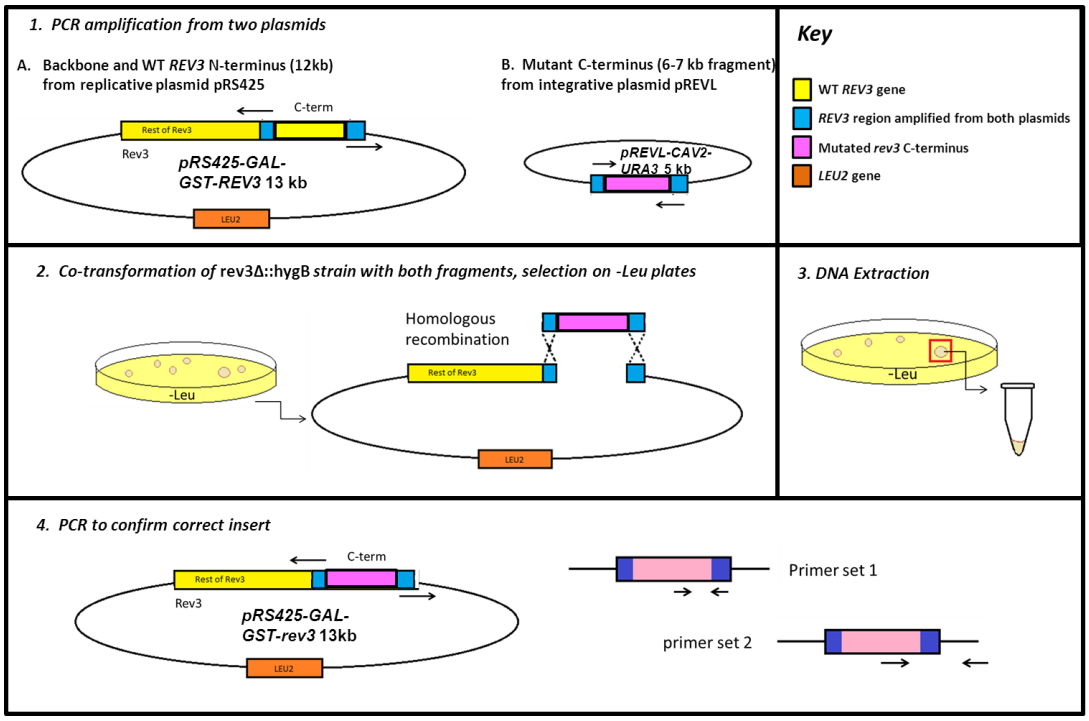

Figure 2.1: Creation of mutant pRS425 vectors using Gap Repair in Yeast

transformed with both fragments and the fragments were combined via homologous recombination.

2.3 Determination of Survival and Induced Mutation Frequencies

Yeast strains were typically grown for two days at 30 °C in 5 mL of yeast extract peptone dextrose medium with 60 mg/L adenine and uracil (YPDAU) with shaking. Cells were pelleted at 1000 x g in a Beckman Model TJ-6 centrifuge for 2 min and re-suspended in 1 mL of sterile water. Cells were diluted 200,000-fold and 100 µl aliquots plated on synthetic complete (SC) medium; 50-100 µl of undiluted cells were plated on SC-arg medium supplemented with 60 mg/L of L-canavanine (Can). Plates were irradiated with 0, 20, 40, or 60 J/m^2 of UV light. After three days of growth at 30 °C, colonies on SC plates were counted and survival was calculated by dividing the number of colonies at each UV treatment by the number of colonies without exposure (independently for each strain). After five days of growth, colonies on SC+Can plates were counted and the mutant frequency was calculated by dividing the number of colonies on SC+Can plates at each UV dose by the number of colonies on the SC plate at the same dose (SC colony count was first multiplied by dilution factor) as described in [63]. The induced Can^r mutant frequency was calculated by subtracting the spontaneous frequency (without treatment) from the mutant frequency for each UV dose [63]. All data points are averages of at least three independent trials (except one experiment of two trials), with duplicates of each sample in each trial. Error bars represent standard deviation.

Strains for overexpression studies of *MGS1* contained a *GAL1* promoter upstream of *MGS1* integrated at the *LEU2* locus. Mutagenesis studies in these strains were

performed as described above with the following modifications. These strains were grown for two days in 4.5 mL SC-raffinose medium (no glucose, 3% raffinose) and were induced with 0.5 mL sterile 20% galactose for 2.5 h prior to plating.

Experiments with overexpression of *rev3ΔC, rev3-FeS, rev3-dd,* and *REV1* (Table 2.1) were done as described above except the transformants were grown in SC-raffinose lacking leucine (-leu) to select for the presence of a plasmid, induced for 2.5 hr with 0.5 mL sterile 20% galactose, and plated with appropriate dilutions on SC-leu and SC-leu-Can plates. Yeast extract peptone dextrose and SC media were prepared as previously described [64].

2.4 Patch Test for Qualitative Evaluation of the Differences in Mutagenesis

For patch test analysis, all strains were plated on one YPDAU plate in rectangular patches. This plate was incubated at 30 ºC overnight until robust patch growth could be seen. These patches were replica plated onto plates in the following order: SC (to make sure subsequent plates would not get too much transfer), SC, SC+Can1, SC+Can2, SC+Can3, and SC+Can4. Can plates 1-4 were irradiated with 0, 20, 40, or 60 J/m^2 of UV, respectively. These plates were examined after five days of growth at 30 ºC.

2.5 Preparation of Yeast Extracts and Western blot

For the analysis of levels of soluble Rev3 variants, we used overexpression conditions because natural endogenous levels of Rev3 are very low. Protease-deficient BJ2168 strains were transformed with the appropriate variants of pRS425-GALGST-REV3 plasmids (sections 2.1 and 2.2) and grown in 12.5 mL synthetic complete glucose

lactic acid (SCGL) medium lacking leucine (-leu) overnight. The following day, 62.5 mL of SCGL-leu were added and growth continued. The third day, 62.5 mL of yeast extract peptone glycerol lactic acid adenine (YPGLA) medium were added and cells were grown for an additional 2.5 hr. Finally, cells were induced with 2.5 g galactose for 4 hr, collected, and flash frozen. Yeast extracts were prepared in buffer containing 50 mM Tris-HCl (pH 7.5), 300 mM NaCl, 1 mM EDTA, 10% sucrose, 10 mM β-mercaptoethanol, 1 mM PMSF, and 1X cOmplete EDTA-free protease inhibitor cocktail. The volume of buffer (in μL) equals the milligrams of wet cells multiplied by 2.68. Yeast cells overproducing Rev3 were thawed, mixed with 500 μL of 0.5-mm glass beads, and lysed with a Disruptor Genie™ (six cycles, two min each) at 4 °C. The lysates were cleared by centrifugation using a MIKRO 200R centrifuge at 8,000 x g for 15 min and then 10,000 x g for 10 min, all at 0 °C.

For Western blot analysis, proteins were separated on an 8% SDS-PAGE Laemmli gel at 200 V, followed by a 1 hr, 20V transfer to an Immobilon PVDF membrane at 4 °C. Mouse anti-GST and goat HRP-conjugated anti-mouse secondary antibodies were used to detect the GST-Rev3 fusion protein. Goat anti-human actin antibodies, which cross-react with yeast actin, and donkey anti-goat HRP-conjugated secondary antibodies were used to detect actin as the loading control. The blot was developed using the Super Signal West Femto Chemiluminescent Substrate detection kit.

2.6 Measurement of Spontaneous Mutation Rate using Fluctuation Analysis

Spontaneous mutation rates for WT and *rev3ΔC* strains were determined using the fluctuation test. Nine independent clones of each strain were grown overnight in 5 mL of

YPDAU. Fifty µL of this culture were plated on solid SC+Can medium to measure mutations in the *CAN1* gene, 50 µL were plated on medium lacking histidine (SC-His) to measure *his7-2* reversions, and 50 µL of 300,000 fold diluted culture were plated on complete medium to measure viability. Plates were incubated at 30 °C. Colonies on complete plates were counted after three days and colonies on selective plates were counted after five days.

The Can^r mutant frequency was calculated by dividing the mutant counts on SC+Can media by the counts on SC media (multiplied by the dilution factor). The frequency of *his7-2* reversions were calculated by dividing the mutant counts on SC-His media by the counts on SC media (multiplied by the dilution factor). The mutant frequency was then used to determine the mutation rate using the Drake equation [65]. Spontaneous mutation rates were compared between strains using the median value with 95% confidence limits [66].

2.7 Analysis of Mutational Spectra

Cells were plated and irradiated as described in section 2.3. Then, 45-50 independent colonies were collected from each strain (WT and *rev3*Δ*C*) at each dose and were colony purified by streaking them out on SC+Can plates (one colony per quarter plate). One colony was picked from each quarter, genomic DNA was isolated, and the *CAN1* was gene was amplified by PCR using DreamTaq Green DNA Polymerase (Thermo Scientific) and the primers CAN1ext-F2 and CAN1ext-R2 (see Appendix B for primer sequences). The PCR products were purified using the QIAquick PCR Purification kit and sent to Genescript for sequencing using the primers CAN1seq520F, CAN1seq699R, and CAN1seq2094R. DNA sequences were then analyzed using

Geneious Pro 5.4.6 software. Mutation frequencies were compared between strains using the paired Student's t-test. Proportions of mutations between strains were compared using the Z test (two sample t-test determining proportions). Where samples sizes were small, proportions were compared using Fisher's exact test instead of the Z test.

3 Genetic Analysis of Yeast Strains containing Different Variants of Catalytic Subunit (Rev3) of DNA Polymerase ζ

3.1 Introduction

3.1.1 The B-family of DNA polymerases

Eukaryotes have at least 15 DNA-dependent polymerases, divided into several families (reviewed in [7, 18, 67-69]). These polymerases differ in the structure of their polymerase active site, and have an assortment of additional domains to facilitate their specific biological function. One of the most important groups of polymerases is the B-family. They are defined by homology to *E. coli* Pol II and include replicative Pols α, δ, ε, and TLS Pol ζ (Figure 3.1). These polymerases function in chromosomal DNA replication, DNA repair, TLS, and homologous recombination.

Chromosomal DNA in eukaryotes is replicated through the concerted action of Pol α, Pol δ, and Pol ε (reviewed in [7, 18, 70, 71]). Because DNA synthesis occurs only in the 5' to 3' direction, the two antiparallel strands must be replicated differently using somewhat different machinery (Figure 3.2). The "leading strand" is synthesized continuously, and the "lagging strand" is synthesized discontinuously in 120-250 nucleotide fragments called Okazaki fragments. First, a complex of proteins unwinds the DNA at bidirectional replication origins and it is coated with the single-stranded binding protein RPA. Next there is loading of Pol α, which is associated with a primase subunit that synthesizes RNA primers at replication origins on the leading strand and at the start of each Okazaki fragment on the lagging strand. Then Pol α synthesizes short stretches of DNA, and turns over synthesis to Pol δ and Pol ε. The current model is that Pol δ

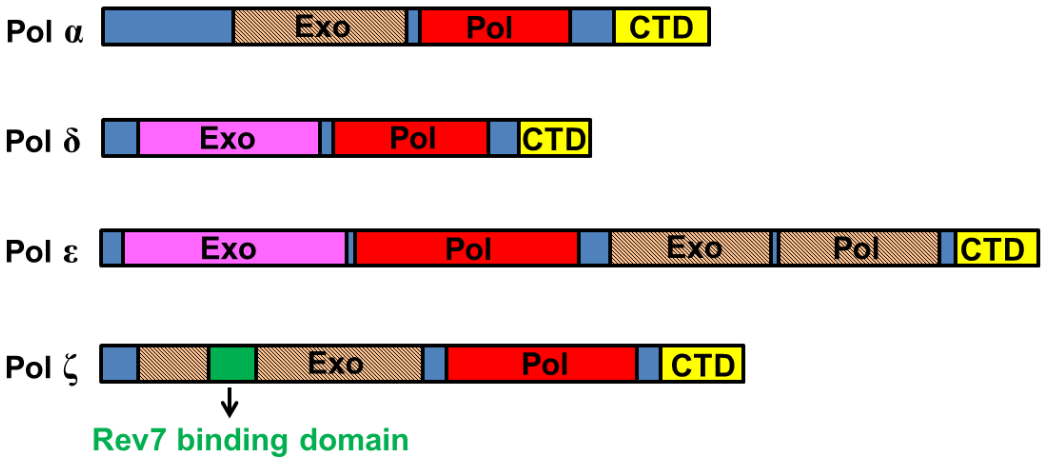

Figure 3.1: Simple schematic of the catalytic subunits of B-family DNA polymerases

Exo (pink boxes) – exonuclease domain for proofreading, Pol (red boxes) – polymerase domain for DNA synthesis, CTD (yellow boxes) – C-terminal domain involved in regulation and protein-protein interactions. Brown domains indicate that the respective domains are inactive.

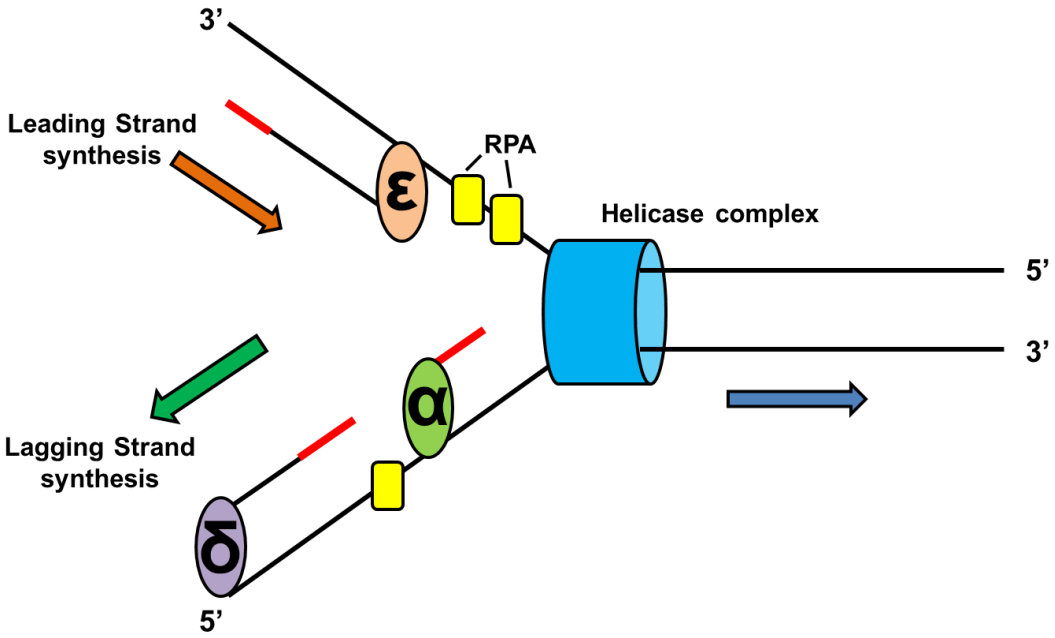

Figure 3.2: Simplified scheme of the eukaryotic replication fork

The double stranded DNA is first unwound by a helicase complex (blue cylinder). The leading strand is synthesized continuously in the direction of the moving replication fork (blue and orange arrows). Pol α/primase complex (green oval) lays down an RNA primer (red line) and a short stretch of DNA is synthesized by Pol α. The rest of the strand is completed by Pol ε (light orange oval). The lagging strand is synthesized discontinuously in the opposite direction to the overall fork progression (green arrow). Pol α/primase lays RNA primers and short DNA stretches at the beginning of each Okazaki fragment, then synthesis is completed by Pol δ (purple oval). Single stranded DNA is coated with RPA (yellow rectangles) for protection.

takes over synthesis of the lagging strand and Pol ε synthesizes the leading strand [72]. However, there is some debate whether or not Pol δ may also synthesize part of the leading strand (reviewed in [70]).

The fourth B-family member, Pol ζ, was introduced in section 1.6. Briefly, Pol ζ has limited capacity to bypass several types of DNA lesions, but its main biological role appears to be its capacity to extend from mismatched DNA termini ending with nucleotides incorporated opposite lesions by other polymerases. Pol ζ is also critical to restart synthesis at difficult template sites, such as hairpins, or when replicative polymerases are compromised [73].

The high fidelity of eukaryotic replication is due to three features: correct base selection and exonucleolytic proofreading by Pol δ and Pol ε, and the action of MMR (reviewed in [7]). Base selectivity is largely due to the structure of the polymerase active site, which allows for accommodation of only base pairs with the correct geometry (reviewed in [74]). Complementary base pairs have different free energies than non-complementary base pairs, and the error rate based on this alone is in the range of the low fidelity seen in TLS polymerases. Therefore, TLS polymerases are thought to have relaxed geometric selectivity, and so rely only on base-base hydrogen bonding for fidelity. Pol ζ has much lower fidelity that the other B-family polymerases *in vitro*, even when copying undamaged templates. All B-family members have exonuclease proofreading domains, but they are inactivated in Pol α and Pol ζ (Figure 3.1).

The work in this dissertation will focus on two of these B-family polymerases, Pol δ and Pol ζ.

3.1.2 Subunit structure of DNA Polymerases δ and ζ

Pol δ is a complex of four subunits in humans, and three in budding yeast (Table 3.1) (reviewed in [7, 75]). In yeast, the largest subunit, Pol3, is the catalytic subunit containing the polymerase and exonuclease active sites and a binding motif for the processivity clamp PCNA. The essential second subunit, Pol31, serves as a stabilizer for Pol3 and tethers it to the third subunit, Pol32. Pol32 contains a PCNA binding motif and a motif that mediates interaction with Pol α. Yeast or chicken cells with deletion of Pol32 show no severe growth defects, but yeast are UV-immutable and chicken cells show decreased mutagenesis in response to deaminase (AID) overexpression; this suggests a role for this protein in damage-induced mutagenesis [76, 77].

Pol ζ was long thought to be comprised of only two subunits: Rev3 and Rev7 [61]. However, it was recently discovered that the C-terminal domain (CTD) of the human catalytic subunit of Pol ζ binds two accessory subunits of Pol δ, p50/p66, and this predicted that human Pol ζ is a four-subunit complex (See Table 3.1 for nomenclature of human and yeast subunits) [78]. Four-subunit human Pol ζ was later purified from human cells and possessed polymerase activity superior to the two-subunit enzyme [79]. Yeast Pol ζ can also stably exist as a four-subunit enzyme, containing the catalytic subunit Rev3, accessory subunit Rev7, and Pol31/Pol32 (Figure 3.3) [80-82]. In this complex, Pol32 binds to Pol31, and Pol31 binds to the CTD of catalytic subunit Rev3 [51, 83-85]. During DNA damage bypass, Pol ζ is bound to the Y-family polymerase Rev1. Rev1 can act as an inserter, but its main role is thought to be as a scaffold for polymerase switches.

It is believed, based on the structure of another B-family member, Pol α, and a low resolution EM structure of Pol ζ, that the CTDs of both Pol3 and Rev3 are connected

Table 3.1: Nomenclature for yeast and human Pol δ and Pol ζ.

Organism	Subunit	Gene	Protein
		Polymerase δ	
Yeast	Catalytic	*POL3*	Pol3
	B	*POL31*	Pol31
	C	*POL32*	Pol32
Human	Catalytic	*POLD1*	p125
	B	*POLD2*	p50
	C	*POLD3*	p66
	Small 4th	*POLD4*	p12
		Polymerase ζ	
Yeast	Catalytic	*REV3*	Rev3
	Accessory	*REV7*	Rev7
	B, C	*POL31, POL32*	Pol31, Pol32
Human	Catalytic	*REV3L*	p353
	Accessory	*REV7*	p30
	B, C	*POLD2, POLD3*	p50, p66

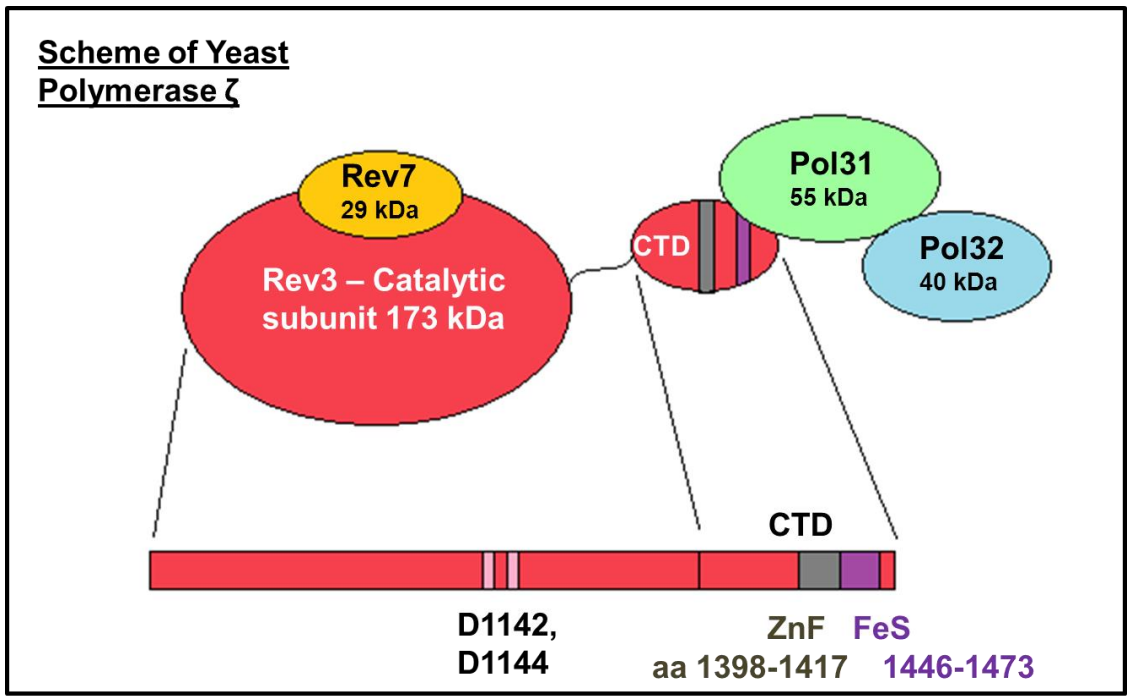

Figure 3.3: Scheme of four-subunit yeast DNA Polymerase ζ, highlighting the CTD

The catalytic subunit of DNA Polymerase ζ, Rev3, is thought to have a C-terminal domain which is attached by a flexible linker (no structure is available). This C-terminal domain contains a ZnF and an FeS cluster, the latter which is necessary for binding to Pol31. There are three accessory subunits: Rev7, Pol31, and Pol32. Pol31 and Pol32 are also subunits of replicative DNA Pol δ.

to the main catalytic domains by a flexible linker (Figure 3.3) [85, 86]. Both polymerases contain an FeS cluster in this domain [87], which is required for binding to Pol31/Pol32 (Figure 3.3) [78, 80, 81]. In addition, the region downstream of the cluster is also important for this binding [80].

3.1.3 Biological functions and regulatory roles of FeS clusters

The discovery that Pol δ and Pol ζ contained FeS clusters opened a vast window to new regulatory options for these polymerases. FeS clusters are ubiquitous cofactors present in many proteins that have been shown to control diverse processes including DNA replication, photosynthesis, respiration, and gene regulation (reviewed in [12, 88]). They exist in different structural classes, involving anywhere from a single Fe atom to multiple Fe and S atoms coordinated by Cys, His, Asp, or Arg residues (Figure 3.4). FeS clusters are some of the most versatile prosthetic groups due to their redox properties. These clusters can carry out redox as well as non-redox catalysis and confer redox sensitivity on many gene regulators.

FeS clusters perform many functions when present in proteins (reviewed in [12, 88, 89]). The ability to localize electron density over both the Fe and S atoms makes these clusters ideal for their primary role in transferring electrons in the electron transport chain. They can also help shape enzyme active sites, assisting in substrate binding and catalysis. Sometimes their role is to maintain the structural integrity of the protein (more functions listed in Table 3.2). These clusters are inserted via special biosynthetic pathways and the clusters can be both a source and target of ROS.

Relevant to this study, FeS clusters have been found to be essential components of diverse nucleic acid processing machinery including glycosylases, helicases, primases,

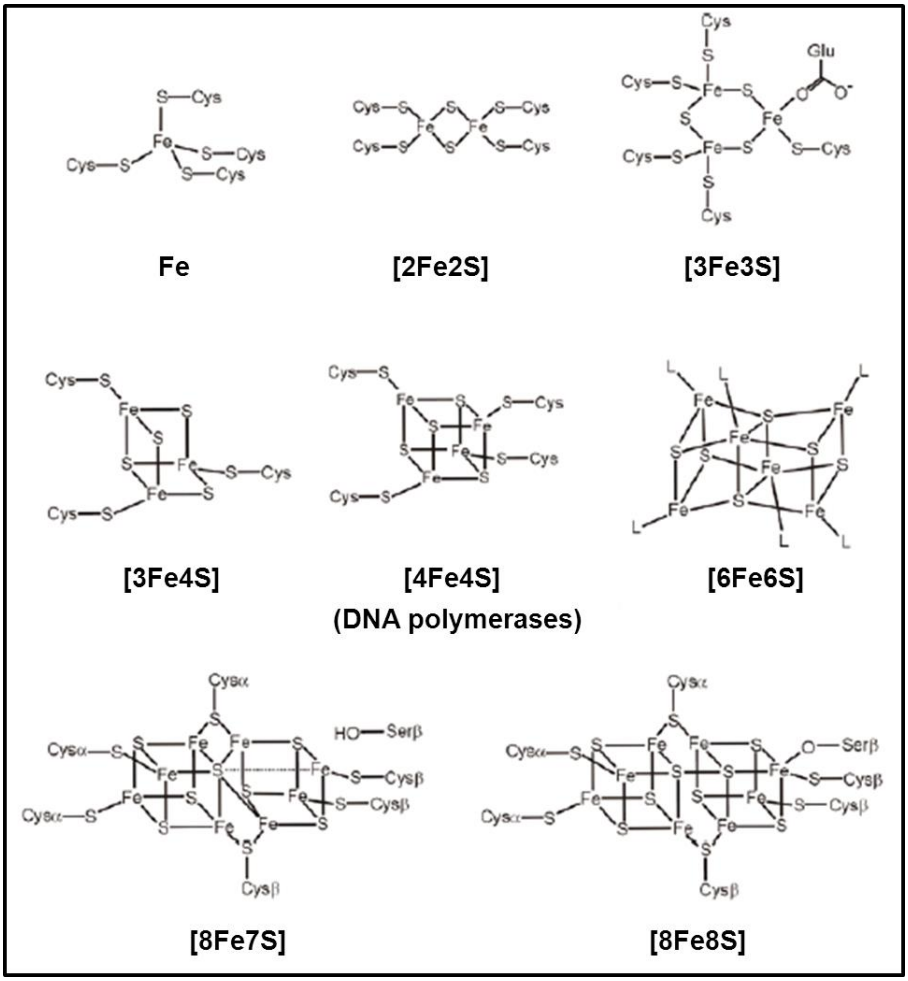

Figure 3.4: Types of FeS clusters

This figure shows structures of different types of FeS clusters, highlighting the fact that they range from simple to very complicated. Each of these clusters can also exist in a variety of oxidative states, increasing their versatility. The clusters discovered in B-family polymerases are of the [4Fe4S] type. Modified from [90].

Table 3.2 Biological Functions of FeS Clusters (modified from [89])

Function of FeS cluster	Examples of proteins
Electron transfer	Ferrodoxins; redox enzymes
Coupled electron/proton transfer	Rieske protein Nitrogenase
Substrate binding and activation	De-hydratases, radical SAM enzymes, Acetyl CoA synthase, Sulfite reductase
Fe or cluster storage	Ferrodoxins, Polyferrodoxins
Structural	Endonuclease III, MutY
Regulation of gene expression	SoxR, FNR, IRP, IscR
Regulation of enzyme activity	Glutamine PRPP amidotransferase, Ferrochelatase
Disulfide reduction	Ferrodoxin:thioredoxin reductase, Heterodisulfide reductase
Sulfur donor	Biotin synthase

transcription factors, nucleases, RNA polymerases, RNA methyltransferases, and recently DNA polymerases (reviewed in [12]). Roles of clusters in these proteins include structural roles, DNA binding, lesion detection, assembly, and helicase activity. One example is the FeS cluster present in the NER helicase XPD and its homologs: Chlr1, RTEL, and FancJ. Disease-causing mutations in these genes are often found to affect their FeS cluster. This cluster is thought to play a role in the structural integrity of these enzymes and in coupling of ATP hydrolysis to DNA translocation.

Another classical example of FeS clusters in DNA processing enzymes is DNA glycosylases (reviewed in [12]). Some (not all) classes of glycosylases contain clusters that sense damage via DNA-mediated charge transfer. The FeS clusters of EndoIII and MutY glycosylases become redox active upon binding DNA. This allows reduction of their [4Fe-4S] cluster to the +3 oxidative state, stabilizing the enzymes in the DNA-bound state and releasing an electron into the DNA base stacks. This electron can travel through the DNA to a distant FeS-containing glycosylase and promote its dissociation. This electron transfer is inhibited by the presence of intervening DNA lesions, thus targeting glycosylases to damage.

3.1.4 Goal of this chapter

Pol ζ is a central element in the DNA damage tolerance mechanism. To further understand the regulation and recruitment of Pol ζ to sites of DNA damage, we studied the function of the C-terminal domain (CTD) that contains the FeS cluster. In yeast and humans when the FeS cluster of Pol ζ is disrupted, there is loss of binding to the accessory subunit Pol31/p50 [78, 80]. It is possible that this cluster plays a structural role or that the switch is regulated by oxidation-reduction reactions [67]. To better understand

the mechanism of participation of Pol ζ in mutagenesis, we created several yeast strains with mutations affecting the CTD of Rev3 and measured their effects on UV-induced mutant frequency. We asked what role the FeS cluster of the catalytic subunit of Pol ζ, *REV3*, plays in UV-induced mutagenesis in yeast *in vivo*.

3.2 Results

3.2.1 Disruption of the FeS cluster in the C-terminus of Rev3 leads to a severe decrease in UV-induced mutagenesis

UV-induced mutagenesis is an effective readout for TLS in yeast. Deletion of *REV3*, *REV7*, or *POL32* results in complete loss of UV-induced mutagenesis. To better understand the role of Rev3, its subunits, and accessory proteins in TLS, we examined parameters of UV-induced mutagenesis in several strains with mutations affecting different parts of the protein (Figure 3.5A). A strain with the mutation *rev3-dd*, encoding catalytically inactive Pol ζ, served as a positive control. In this control strain two aspartates in the invariant DTD motif in region I of the active site (present in all B-family DNA polymerases) involved in catalysis were substituted to alanines, resulting in a catalytically inactive enzyme [7]. To measure mutagenesis, the popular canavanine-resistance forward mutation assay was used, where mutations of various types in the *CAN1* gene in yeast confer resistance to the toxic drug canavanine [91].

The CTD of Rev3 contains two cysteine-rich metal binding sites, CysA and CysB [92]. CysA forms a zinc finger (ZnF) and CysB coordinates an FeS cluster (Figure 3.3) [78, 86]. In this dissertation, CysA will be referred to as ZnF and CysB will be referred to as FeS. Each of these metal binding sites has four Cys residues that coordinate the four metal ions. To study the function of these sites, we created yeast strains that had the four

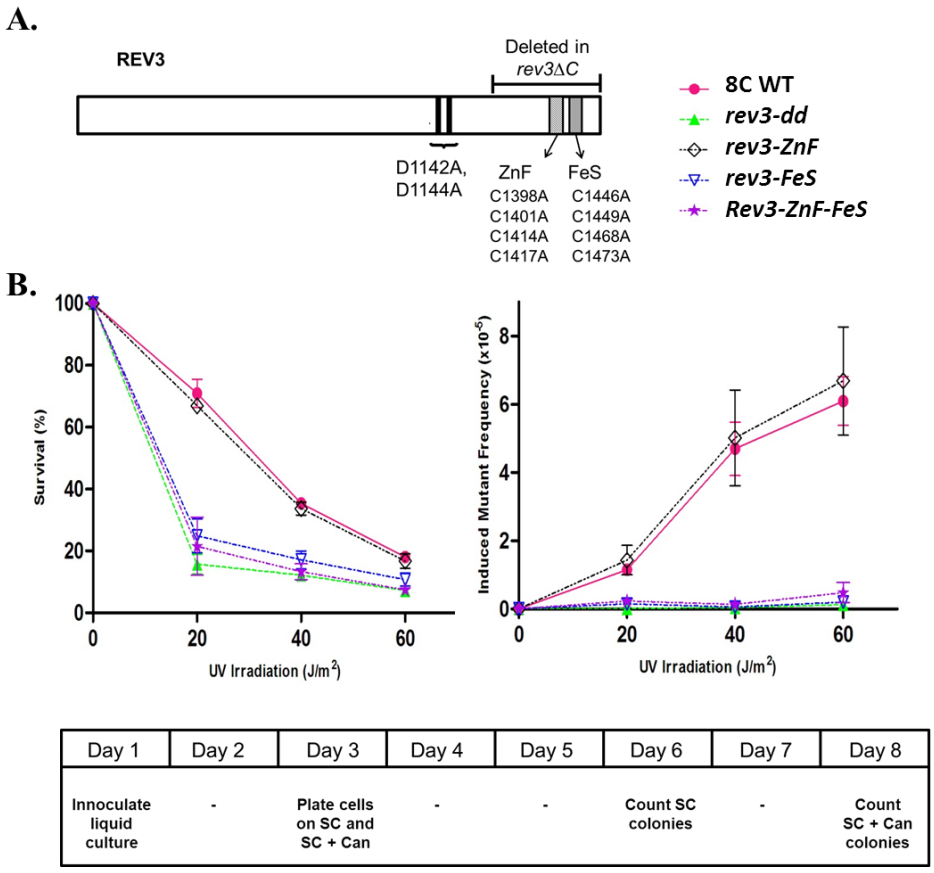

Figure 3.5: The FeS cluster of Rev3 is important for survival and mutagenesis in response to UV irradiation

A. Schematic view of Rev3 variants used in this study. **B.** Disruption of the FeS cluster, but not the ZnF, decreases survival and mutagenesis in response to UV damage. Experimental design for all mutagenesis experiments in this dissertation shown below graphs in B. WT (pink ●), *rev3-dd* (green ▲), *rev3-ZnF* (black ◇), *rev3-FeS* (blue ▽),), *rev3-ZnF-FeS* (purple ★). Data was collected and analyzed as described in Methods section 2.3 (three independent trials). All strains are described in Table 2.1.

Cys coordinating the ZnF or the Cys coordinating the FeS cluster replaced with Ala [78]. These strains were called *rev3-ZnF* and *rev3-FeS*. We also disrupted both clusters in a third strain (*rev3-ZnF,FeS*).

Mutagenesis was measured in various *rev3* mutants after exposure to increasing doses of UV radiation (UVR) (Figure 3.5B). Disruption of the ZnF motif of Rev3 had no effect on survival or mutagenesis. In contrast, disruption of the FeS cluster alone or both metal-binding sites resulted in severe reduction of mutagenesis and a drastic decrease in survival, similar to the catalytically inactive enzyme. Two other groups later confirmed these results [80, 81]. Therefore, the FeS cluster of the C-terminus of Pol ζ plays an important role in UV-induced mutagenesis.

3.2.2 Strains with the *rev3ΔC* mutation, lacking the entire C-terminus of Rev3, show robust mutagenesis at low UV doses and substantial, residual levels of mutagenesis at higher UV doses

Another variant of *REV3* was created that encoded a protein lacking the entire CTD, thus completely removing both metal binding sites and the platform for binding to Pol31/Pol32 (Figure 3.5A). It will be further referred to as *rev3ΔC*. Since the critical FeS cluster was missing, it was expected that this strain would display complete loss of UV-induced mutagenesis. Intriguingly, at low UV doses *rev3ΔC* showed robust induced mutagenesis levels, comparable to WT *REV3* (Figure 3.6). At higher UV doses, it retained residual mutagenesis. Residual mutagenesis was about 60% of WT levels at the intermediate dose of 40J/m^2 and only about 10% of WT levels at the highest dose of 60 J/m^2. The observed mutant frequencies in treated and untreated cultures are shown in Table 3.3 as an illustration of the magnitude of UV-induced mutagenesis.

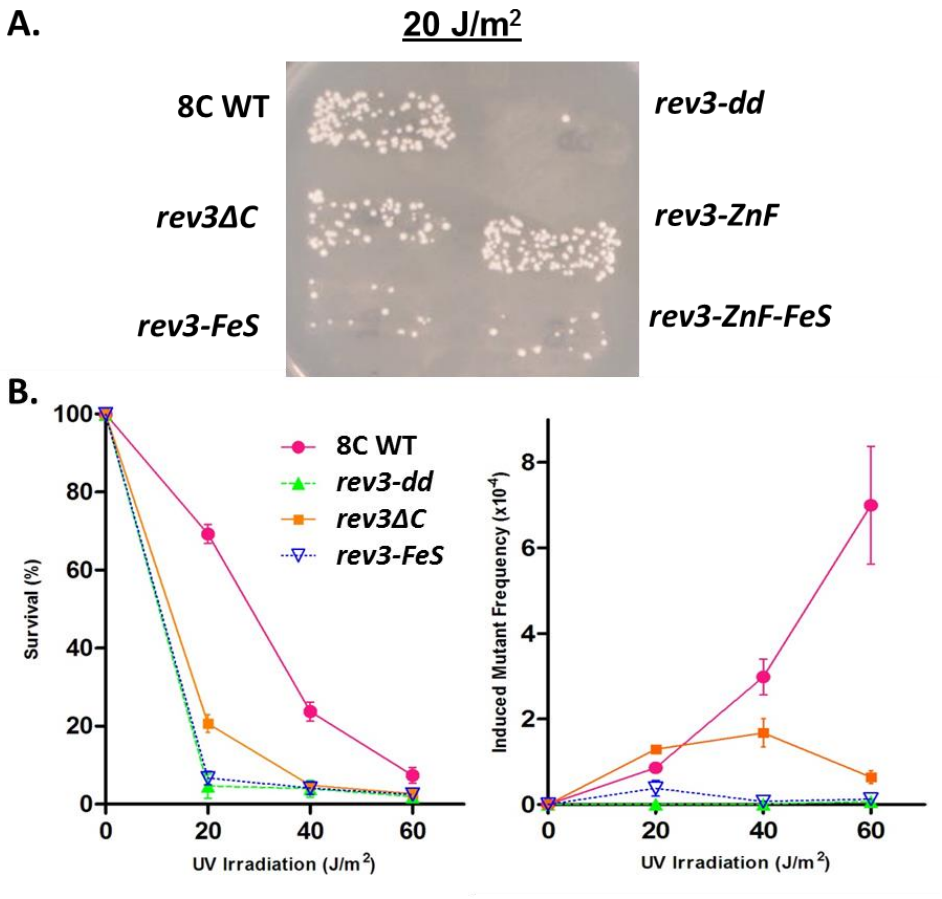

Figure 3.6: The *rev3ΔC* strain shows robust mutagenesis at low doses of UV irradiation and retains residual mutagenesis at high doses

A. Patch test illustrating the effect of *rev3* mutations on UV-induced mutagenesis (see section 2.4). Visible colonies represent Can resistant mutants induced by UV. **B.** WT (pink ●), *rev3ΔC* (orange ■), *rev3-dd* (green ▲), *rev3-FeS* (blue ▽). Data was collected and analyzed as described in Methods section 2.3 (three independent trials). All strains are described in Table 2.1.

Table 3.3 *rev3ΔC* strain shows robust mutagenesis at low doses of UV irradiation and retains residual mutagenesis at high doses.

Strain	UV Treatment (J/m^2)	Percent Survival[x]	Mutant Frequency ($x10^{-6}$)[y]	Induced Mutant Frequency ($x10^{-6}$)[y]
8C WT	0	100.0 ± 6.7	1 ± 0.4	-
	20	69.2 ± 0.9	87 ± 12	86 ± 12
	40	23.8 ± 3.0	299 ± 42	298 ± 42
	60	7.4 ± 7.0	701 ± 137	700 ± 137
rev3-dd	0	100.0 ± 8.8	0.8 ± 0.6	-
	20	4.6 ± 0.0	1.7 ± 1.7	1 ± 1
	40	3.9 ± 0.0	1.9 ± 1.2	1 ± 1
	60	2.0 ± 0.1	7.5 ± 5.4	7 ± 5
rev3ΔC	0	100.0 ± 8.6	0.8 ± 0.2	-
	20	20.6 ± 1.3	130 ± 9	129 ± 9
	40	4.8 ± 1.7	168 ± 33	167 ± 33
	60	2.7 ± 0.6	65 ± 15	64 ± 15
rev3-FeS	0	100.0 ± 15.8	0.8 ± 0.2	-
	20	6.7 ± 0.4	38.8 ± 18.5	38 ± 18
	40	4.1 ± 0.1	7.4 ± 3.6	7 ± 3
	60	2.5 ± 0.1	13.1 ± 11.0	12 ± 11

[x]values are mean ± SD in %
[y]values are mean ± standard deviation (SD)
Data are averages of 4 independent trials

3.2.3 Residual mutagenesis in *rev3ΔC* strains is dependent on the catalytic activity of Rev3

Disruption of the FeS cluster led to a severe loss of mutagenesis, but removal of the domain containing the cluster maintained decent mutagenesis levels. To rule out the possibility that another polymerase is recruited to assist Rev3ΔC and is responsible for the mutagenesis seen in the *rev3ΔC* strain, a mutant was created that was catalytically inactive and lacked the CTD of Rev3 (*rev3ΔC-dd)*. If another polymerase was responsible for the residual mutagenesis, this mutant strain would behave like *rev3ΔC*. However, the double mutant was hypersensitive and UV-immutable, similar to the catalytically inactive single mutant, *rev3-dd* (Figure 3.7). This demonstrates that the residual mutagenesis seen in *rev3ΔC* strains is dependent upon the catalytic activity of Rev3.

3.2.4 Rev3 variants with CTD alterations are not differentially degraded

It is formally possible that the Rev3ΔC protein is more stable than the other mutants or the WT holoenzyme, and thus being more abundant can participate in UV-induced mutagenesis despite missing subunits. However, we did not detect any substantial differences in Rev3 protein levels in the soluble fraction of extracts of the strains overexpressing *REV3* or various *rev3* mutant alleles by Western blot analysis (Figure 3.8A). Furthermore, artificial overexpression of *rev3ΔC* from a galactose-inducible promoter did not significantly increase survival or levels of mutagenesis in the *rev3ΔC* strain (Figure 3.8B).

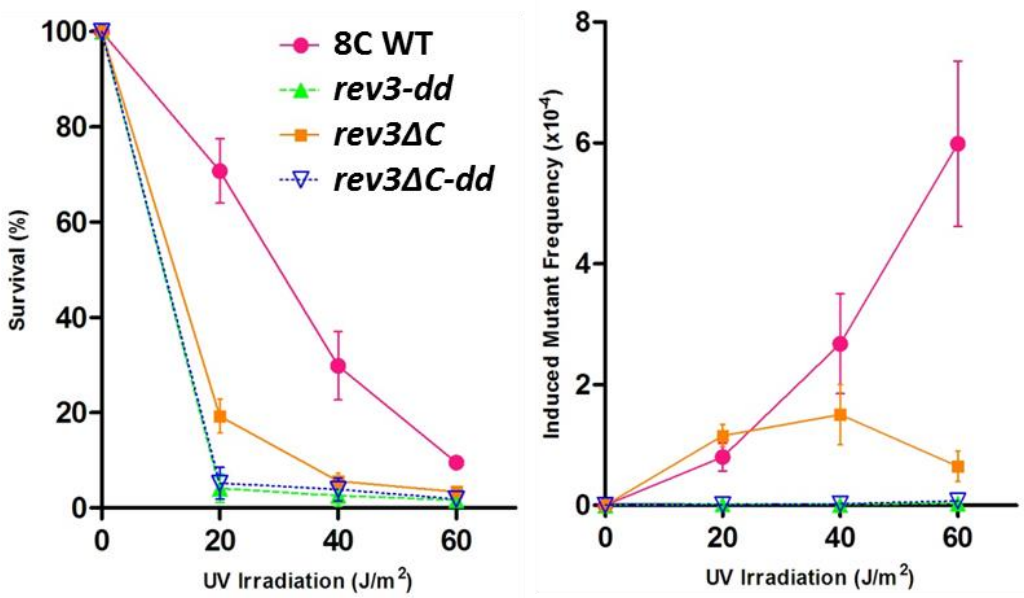

Figure 3.7: Induced mutagenesis in the *rev3ΔC* strain is dependent on the catalytic activity of Rev3

A. The *rev3ΔC-dd* mutant was hypersensitive and immutable; demonstrating that mutagenesis in *rev3ΔC* is dependent on the catalytic activity of Rev3**.** 8C WT (pink ●), *rev3-dd* (green ▲), *rev3ΔC* (orange ■), *rev3ΔC-dd* (blue ▽). Data was collected and analyzed as described in Methods section 2.3 (three independent trials). All strains are described in Table 2.1.

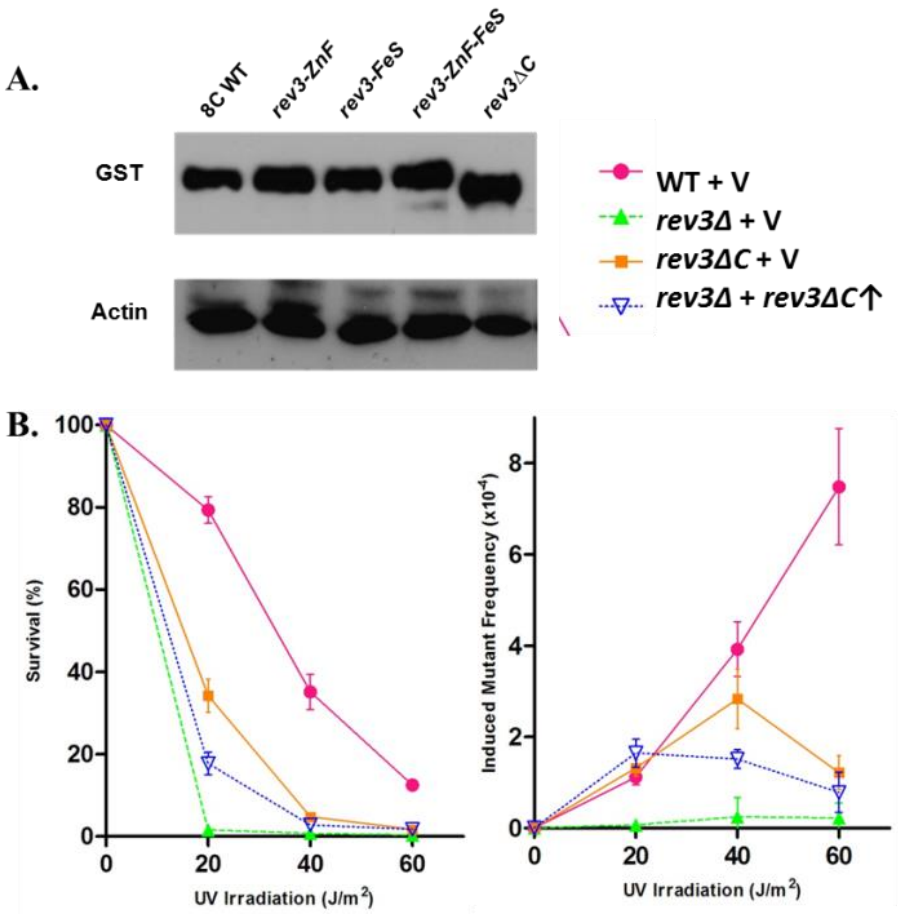

Figure 3.8: Rev3 protein in mutants is not differentially degraded, and mutagenesis levels are not increased by overproduction of Rev3ΔC

A. Western blot analysis of the overproduced CTD mutants of Rev3. There was only a slight increase in the levels of Rev3ΔC over WT Rev3. **B.** Artificial, robust overexpression of *rev3ΔC* over WT has no effect on mutagenesis**.** WT + vector (pink ●), *rev3Δ*+ vector (green ▲), *rev3ΔC* + vector (orange ■), *rev3Δ* + *rev3ΔC*↑ (blue ▽). Data was collected and analyzed as described in Methods section 2.3 (three independent trials). All strains are described in Table 2.1.

3.2.5 *rev3* mutations do not exert a dominant negative phenotype in UV-induced mutagenesis

To test whether the mutagenesis defects could be due to direct interference with damage bypass, we tested whether some *rev3* mutations lead to a dominant negative effect in strains with WT Rev3. We found that the presence of *rev3ΔC, rev3-FeS,* or *rev3-dd* on overexpression plasmids (see section 2.2) in the WT strain (8C-YUNI101, see Table 2.1 and 3.3 for description of *rev3-dd* mutant) did not affect UV-induced mutagenesis (Figure 3.9). Therefore, *rev3* mutants examined were not dominant negative and equally unable to compete with WT Pol ζ. It was verified that expression of GST tagged WT Rev3 was able to complement *rev3*Δ, thus the GST tag does not interfere with polymerase function (data not shown).

3.3 Discussion

In this chapter, we examined several mutations affecting the functionally significant CTD of Rev3. Mutation of the FeS cluster in the CTD of Rev3 severely decreases UV-induced mutagenesis (Figure 3.5) and has been shown to eliminate binding to Pol31 [78, 81]. These data suggests that the FeS cluster is essential for UV-induced mutagenesis, and that one of the functions of the cluster is to directly participate in binding with Pol31 or maintain the structural integrity of the CTD such that it can bind Pol31. Whether this cluster is redox active *in vivo* or not remains to be determined.

We discovered and further characterized a novel mutation affecting Pol ζ, *rev3ΔC*, which provides new insight into the regulation of Pol ζ during TLS. The *rev3ΔC* strain shows robust mutagenesis at low UV doses and substantial mutagenesis at higher doses. This mutagenesis is dependent upon the catalytic activity of Pol ζ (Figure

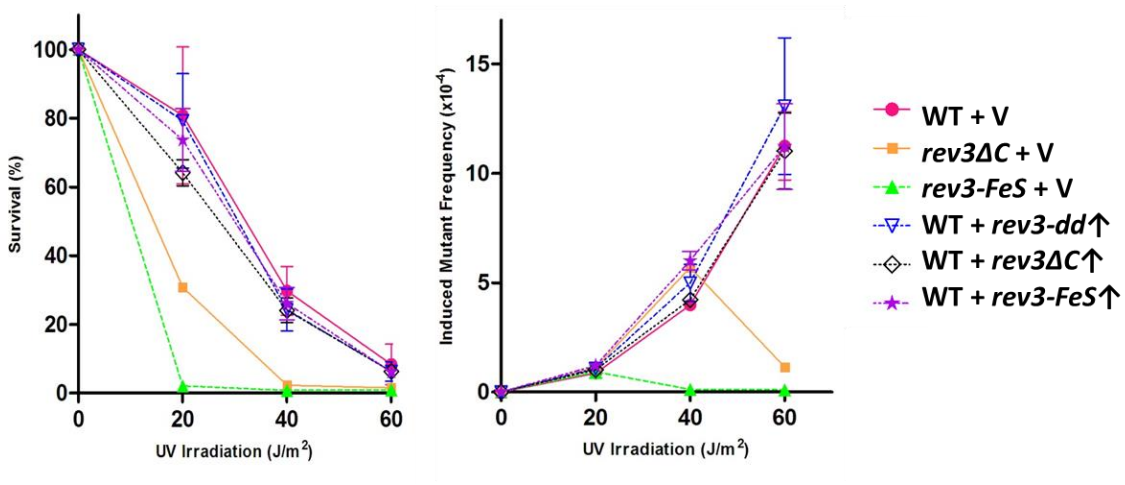

Figure 3.9: Effects of *rev3* mutations on UV mutagenesis alone and in the presence of WT *REV3*

WT strains additionally expressing mutant variants of Rev3 exhibit WT levels of survival and mutagenesis. Strains possess WT *REV3* in the chromosomal location and mutant *rev3* on an expression plasmid. WT + vector (pink ●), *rev3ΔC* + vector (orange ■), *rev3-FeS* + vector (green ▲), WT + *rev3-dd*↑ (blue ▽), WT + *rev3ΔC*↑ (black ◇), WT + *rev3-FeS*↑ (purple ★). Data was collected and analyzed as described in Methods section 2.3 (three independent trials). All strains are described in Table 2.1.

3.6). This intermediate effect on induced mutagenesis resembles effects of Rev3 truncation mutants that retained the FeS cluster, but lacked binding to Pol31/Pol32 due to loss of a downstream region required for that interaction [80, 81]. It has not been formally demonstrated that Rev3ΔC lacks binding to Pol31/Pol32, but it is very likely due to the facts presented previously (discussed more in section 4.3).

It is intriguing that the *rev3ΔC* mutant allele that encodes for a protein with a deletion of the entire CTD (Figure 3.5A) has a much milder effect than *rev3-FeS* (Table 3.3, Figure 3.6). Both mutants lack a functional FeS cluster and likely lack binding to Pol31/Pol32 (discussed in Chapter 4.3), so why are the phenotypes so different? The *rev3ΔC* strain clearly demonstrates that though the FeS of Rev3 cluster is important for UV-induced mutagenesis, it is far from essential.

We further investigated possible mechanisms to explain why *rev3-FeS* has a more severe phenotype than *rev3ΔC*. One hypothesis was that Rev3-FeS is degraded *in vivo*. We used western blot analysis to show that Rev3-FeS is not preferentially degraded compared to Rev3ΔC. It could also be that Rev3-FeS acts in a dominant negative fashion, actively decreasing mutagenesis by acting against other factors at the lesion site. However, we showed that neither Rev3-FeS nor Rev3ΔC exert a dominant negative effect in the presence of WT Rev3 (Figure 3.9). This directly shows that mutants are not acting against WT Rev3. It also strongly suggests that they are not acting against any other TLS factors, since there was no phenotype even though the mutants were present in high excess over WT Rev3. This indicates that the different phenotypes of the these two mutants cannot be explained by different effects of the two proteins on the TLS complex; in the presence of WT Pol ζ they are both excluded from any transactions.

There are two major mechanisms in which these mutations may affect Pol ζ: they may affect the catalytic function of the enzyme or recruitment to sites of damage. More data is necessary to further probe these mechanisms. The crystal structure of Rev3 has not yet been solved, so it is unknown where the FeS cluster lies in relation to the catalytic site in three dimensional space. It has been shown biochemically that two-subunit Pol ζ (Rev3/Rev7) and the Rev3-FeS mutant are catalytically active *in vitro* [81], though much less than the WT, four-subunit enzyme. It has not been formally shown yet whether Rev3ΔC is active. In terms of recruitment, Rev3ΔC is functioning so it is clearly recruited *in vivo* at least to some extent; it is unknown whether Rev3-FeS is ever recruited to the DNA. Further investigation of these possibilities will yield mechanistic insight into the function of the CTD of Pol ζ as a whole as well as the specific functions of the FeS cluster (see section 6.2).

3.3.1 Conclusions

We have demonstrated that the CTD of the catalytic subunit of Pol ζ, Rev3, plays an important role in UV-induced mutagenesis. The role of this domain is complex, and the presence of an FeS cluster is not obligatory for all transactions. We have also discovered a novel mutant of Pol ζ that may represent an alternative regulatory mechanism. This will be further investigated in Chapter 4.

***The data in this chapter were published in Siebler et al., 2014 [93].**

4 Genetic Regulation/Control of the Pol ζ Variant in Mutant *rev3ΔC* Strains

4.1 Introduction

As mentioned in Chapter 1, Pol ζ is responsible for 96% of UV-induced mutations and about half of all spontaneous mutations [7, 45]. Of course it does not act alone; many other proteins are also required for damage-induced mutagenesis. In order to understand how Pol ζ works, it is important to know what other proteins are involved in its regulation and recruitment.

4.1.1 Proliferating cell nuclear antigen (PCNA)

PCNA is central to many cellular processes and has been referred to as a master regulator (reviewed in [7, 26]). It interacts with more than 30 proteins, regulating a variety of DNA transactions: replication, DNA repair, DNA damage tolerance, MMR, BER, NER, chromatin assembly, epigenetic modification, and sister chromatid cohesion. PCNA exists as a homotrimer in yeast and humans, forming a ring structure with pseudohexameric symmetry. It can slide along DNA freely in both directions and is loaded to internal priming sites on DNA by the clamp loader replication factor C (RFC). One face of PCNA has sites for interaction with other proteins, and this face is always oriented toward the 3' growing end of the DNA. This allows PCNA to act as a discriminator between new and old strands (for example during MMR) [94].

Most important for our work are the roles of PCNA in DNA replication and DNA damage tolerance (reviewed in [7, 26, 39, 95]). During replication, PCNA tethers replicative Pol δ firmly to DNA and by doing so, drastically increases its processivity. It

has also been shown to enhance the bypass activity of four subunit Pol ζ. As discussed in section 1.4, PCNA plays a very important role in determining which branch of DNA damage tolerance will occur. Monoubiquitylation of PCNA at Lys 164 favors TLS, polyubiquitylation signals for error-free damage avoidance, and sumoylation inhibits *RAD52* dependent recombination pathways. Not only do these modifications help decide the pathway, they are also necessary for downstream transactions. In yeast, a mutation leading to a change of Lys 164 to Arg (K164R) eliminates ubiquitylation and Pol ζ-dependent UV-induced mutagenesis.

4.1.2 Y-family Polymerase Rev1

Rev1 is a DNA-dependent deoxycitidyltransferase belonging to the Y-family of DNA polymerases. This family in yeast includes low fidelity polymerases Pol η and Rev1 (reviewed in [7, 96]). The main role of these polymerases is in the bypass of damaged DNA. The active site of Y-family polymerases is much more open and solvent accessible, accounting for their low fidelity and ability to incorporate bases across from lesions. These polymerases have an extra domain called the "little finger" (or polymerase associated domain (PAD), or wrist), which plays a role in interaction with DNA.

Rev1 is required for damage-induced mutagenesis in yeast and human cells. Its deletion eliminates all mutagenesis. Rev1 can participate in this process through its enzymatic activity; Rev1 primarily catalyzes the incorporation of C opposite a template G (reviewed in [9, 97]). This is due to the fact that Rev1 has a strong structural preference for both a template G and incoming C. The "N-digit" of Rev1 is responsible for this selection: Arg324 selects an incoming C because it forms steric clashes with other bases. Leu 325 flips out the template G, and forms hydrogen bonds with it that cannot be made

with other bases. This “flipping out” allows for accommodation of some damaged G residues as well as AP sites (which provide no steric hindrance) in the template.

However the main role of Rev1 in TLS is not due to its catalytic function, but rather to its structural role (reviewed in [7, 9]). Rev1 is notable among TLS polymerases for its multiple binding partners and several protein-protein interaction modules. Mutations affecting the catalytic site of Rev1 have little effect on induced mutagenesis, whereas strains with a defective BRCT protein interaction domain of Rev1 are immutable. Rev1 can also stimulate the activity of Pol ζ *in vitro*. The current model is that Rev1 functions as scaffold for various DNA damage response proteins, helps localize TLS complexes to sites of DNA damage, and modulates polymerase switching at lesion sites through its ability to bind many TLS polymerases.

4.1.3 Pol32

Yeast strains with *pol32*Δ are cold sensitive, show defects in DNA replication, sensitivity to replication inhibitors and DNA damaging agents, and are defective for UV- and MMS-induced mutagenesis ([98]; reviewed in [51]). Due to its nature as a member of both replicative Pol δ and TLS Pol ζ, it plays important roles in ensuring genome stability and in mutagenesis. Work is currently being done in many groups to define roles of Pol32 associated with each polymerase.

4.1.4 Subunit sharing model of DNA polymerase switching during TLS

The existence of shared Pol31/Pol32 subunits was the basis for the proposal of a novel mechanism of switching between Pol δ and Pol ζ, through an exchange of the catalytic subunits on Pol31/Pol32 bound to PCNA (Figure 4.1) [78]. In the

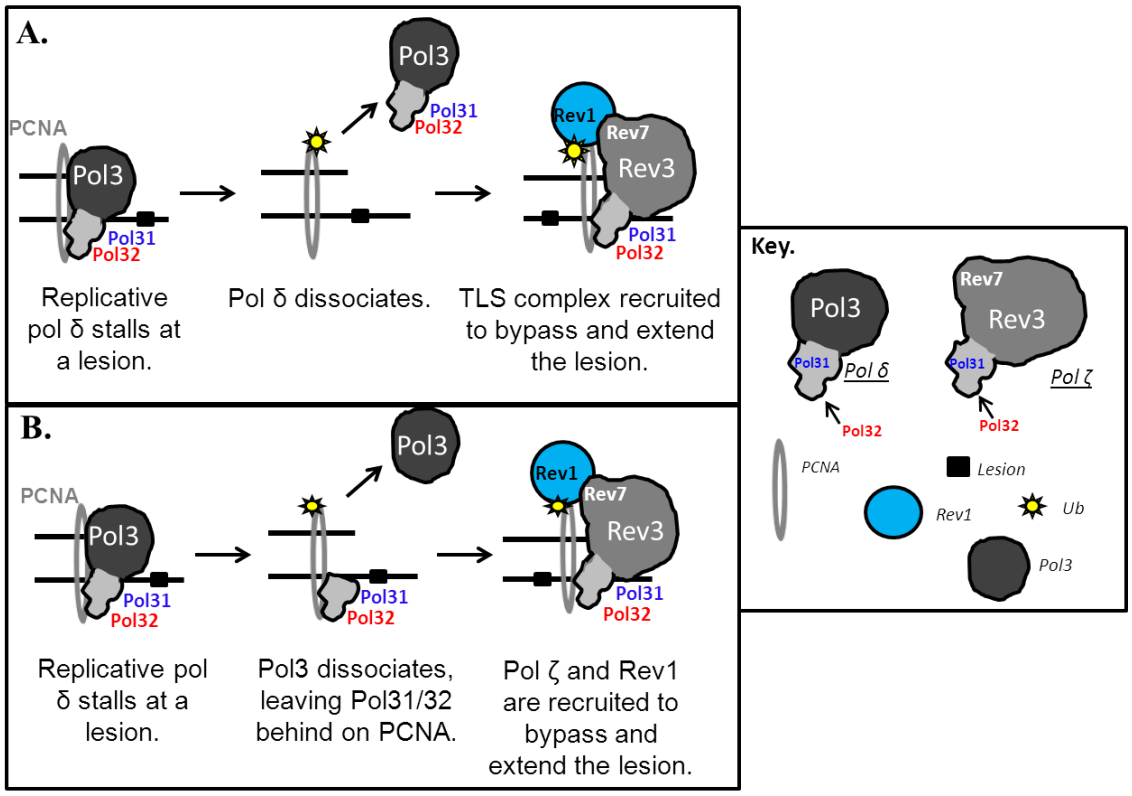

Figure 4.1: Models of polymerase switching during TLS

A. Classic two-event polymerase switch model. There is a switch from Pol δ to a TLS complex comprised of Rev1 and Pol ζ. After insertion of a nucleotide opposite the lesion by a member of this complex, Pol ζ extends the primer. Rev1 also acts as a scaffold. **B.** Illustration of the switch from Pol δ to Pol ζ in the new variant of polymerase switch model utilizing the exchange of Pol31/Pol32 subunits. The catalytic subunit of Pol δ (Pol3) dissociates from the DNA and Rev3/Rev7 binds to the Pol31/Pol32 still left on DNA. Other steps are the same as in A. **Note:** There is also a two-polymerase switch model, shown in general in Figure 1.2.

classical view, the whole polymerase complexes substitute for one another (Figure 4.1A). In this new scenario, Pol δ stalls at a lesion, which signals for PCNA monoubiquitylation by the Rad6/Rad18 complex. Then only the catalytic subunit of Pol δ, Pol3, dissociates (and/or is degraded [99]) and Rev3/Rev7 is recruited to Pol31/Pol32 left at the lesion site. This mechanism provides an easy, yet unproven, possibility for a switch back to Pol3 for processive synthesis if necessary (more in section 4.3). In this model, Pol δ plays a role in TLS by regulating the entire switch process. Indeed it has been shown that Pol32 plays a role in TLS independent of Pol ζ [76].

4.1.5 Maintenance of Genome Stability 1 (Mgs1)

Another important factor examined in this chapter is Mgs1. Mgs1 is an enigmatic regulator of TLS, an ATPase that plays a role in maintaining genomic stability in yeast by an unknown mechanism. Mgs1 has been shown to have both DNA-dependent ATPase and DNA annealing capabilities [100]. The human homolog of Mgs1, WRNIP1, interacts with the Werner helicase which is altered in the premature aging disease Werner's syndrome. Genetic evidence strongly suggests that Mgs1 plays roles in maintaining proper DNA topology and in error-free post-replication repair (PRR), both of which contribute to genomic stability [100].

In yeast, deletion of Mgs1 results in an increase in the spontaneous recombination rate (inter- and intrachromosomal) and increased rDNA instability [100]. Mgs1 is targeted to sites of replication stress through interactions with monoubiquitylated PCNA [59, 101]. Overproduction of Mgs1 severely reduces MMS-induced mutagenesis [59] and eliminates UV-induced mutagenesis in yeast, suggesting that it acts as a negative regulator of TLS. Mammalian WRNIP1 stimulates replicative Pol δ *in vitro* and binds the

catalytic subunit p125 and the accessory subunits p50, and p12 [102], providing further evidence of the connection between Mgs1 and replication/repair pathways. Using genetic means, yeast Mgs1 has been shown to interact with Pol δ subunits Pol3 and Pol31. Since Pol31 is known to also be a subunit of Pol ζ, it is logical to assume that Mgs1 can bind Pol ζ as well. There are several ideas as to the role that Mgs1 plays in genome stability; one involves its potential role in shuttling the damage to different branches of DNA damage tolerance [103, 104].

It has been suggested that Mgs1 shuttles toward error-free pathways, although it is unclear which ones specifically. Genetic evidence suggests that in addition to PRR and HR, there may be another alternative pathway to deal with DNA damage that is dependent on Mgs1. The *rad6 rad52* and *rad6 srs2 rad52* mutants, deficient in both HR and PRR, were still viable [103, 105, 106]. However, *MGS1* deletion was incompatible with inactivation of HR and PRR (synthetic lethality of *mgs1 rad18 srs2 rad51* and *mgs1 rad18 srs2 rad53* strains) [106]. The fact that the *rad6 mgs1* mutant is inviable also suggests that Mgs1 is essential in the absence of PRR [107]. Together this data suggests that Mgs1 participates in a novel error-free pathway which is essential for growth when PRR and HR pathways are impaired [106].

4.1.6 Goal of this chapter

In this chapter, we further characterize the C-terminal truncation mutant, *rev3ΔC*, using it as a tool to probe our understanding of polymerase switches *in vivo*. Since this mutant lacks the regulatory CTD of Rev3, its phenotypes can shed light on the function of that domain and on how it functionally interacts with other proteins that regulate TLS as a whole. It is known that TLS in yeast is dependent on the presence of several proteins;

here we examine if these factors are also required for TLS in *rev3ΔC* strains. We asked if Rev3ΔC is being recruited by a novel mechanism free of some of the regulatory partners of WT Rev3.

4.2 Results

4.2.1 Spontaneous mutagenesis is unaffected in the *rev3ΔC* strain

Yeast with *rev3ΔC* exhibit robust mutagenesis at low levels of UV irradiation, despite lacking the binding platform for Pol31/Pol32. Therefore, it could be free of some of the regulatory partners of WT Pol ζ. We wanted to test whether Rev3Δ*C* accessed DNA more frequently than WT Rev3 in the absence of DNA damage. We used fluctuation analysis to measure the spontaneous mutation rate in both strains. We found that *rev3ΔC* strains did not have increased levels of spontaneous mutagenesis compared to WT (Table 4.1).

4.2.2 Residual UV mutagenesis in the *rev3ΔC* strain is dependent on Pol32, monoubiquitylation of PCNA, and Rev1

As mentioned above, the presence of Pol32 and monoubiquitylation of the processivity clamp PCNA are known to be required for UV-induced mutagenesis in yeast [42, 77, 108]. Accordingly, in strains with the PCNA K164R variant that cannot be ubiquitylated, we observed decreased survival and suppressed UV-induced mutagenesis in both WT and *rev3ΔC* strains (Figure 4.2A). Deletion of *POL32* eliminated UV-induced mutagenesis and decreased survival in the WT strain. Interestingly, we found that although *rev3ΔC* lacks the domain needed for binding Pol31/Pol32, Pol32 is still required for mutagenesis in the *rev3ΔC* strain (Figure 4.2A).

Table 4.1: Spontaneous mutation rates at two reporters are unaffected in the *rev3ΔC* strain.

Strain	*CAN1* (x10^{-6})		His reversion (x10^{-8})	
	Median*	CL	Median	CL
8C WT	1.05	0.84-1.43	3.05	1.38-4.32
8C *rev3ΔC*	0.97	0.78-1.61	2.23	1.30-3.56

*eighteen independent cultures for each strain

** CL – confidence limits

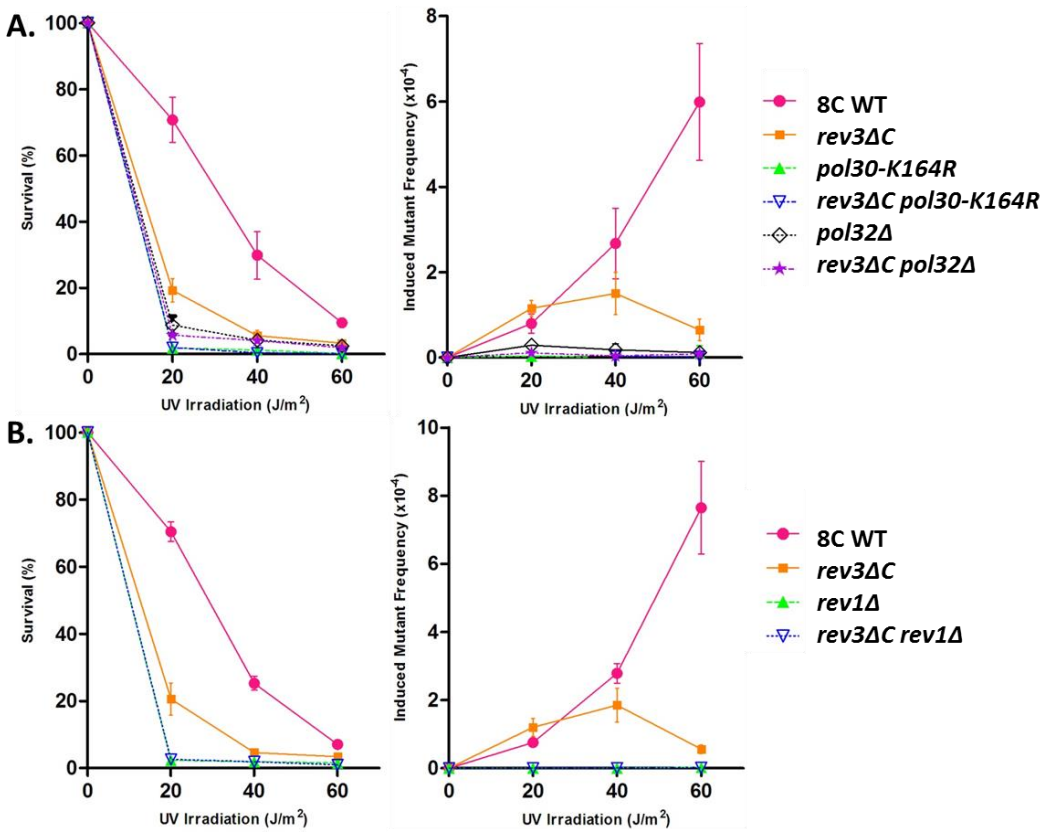

Figure 4.2: UV induced mutagenesis in the *rev3ΔC* and WT strains is under similar genetic control

A. Survival and mutagenesis of WT and *rev3ΔC* strains are both dependent upon monoubiquitylation of PCNA and the presence of Pol32**.** WT (pink ●), *rev3ΔC* (orange ■), *pol30-K164R* (green ▲), *rev3ΔC pol30-K164R* (blue ▽), *pol32Δ* (black ◇), *rev3ΔC pol32Δ* (purple ★). **B.** Survival and mutagenesis are dependent upon the presence of Rev1**.** 8C WT (pink ●), *rev3ΔC* (orange ■), *rev1Δ* (green ▲), *rev3ΔC rev1Δ* (blue ▽). Data was collected and analyzed as described in Methods section 2.3 (three independent trials). All strains are described in Table 2.1.

Rev1 binds to the Rev7 subunit of Pol ζ and to PCNA. These interactions could facilitate mismatch extension by Pol ζ during TLS [109]. Deletion of *REV1* reduced survival and eliminated UV-induced mutagenesis in both WT and *rev3ΔC* strains (Figure 4.2B).

4.2.3 Overexpression of *REV1* has little effect on UV-induced mutagenesis

It is possible that Rev1 is the only anchor holding Rev3ΔC to PCNA, since this variant of Rev3 has lost one major mode of interaction with PCNA through Pol31/Pol32. In this case, an increase in the concentration of Rev1 could elevate the chances of this backup interaction and increase mutagenesis. To test this, the effects of overproduction of Rev1 were investigated. Overexpression of *REV1* from a multicopy plasmid under the control of a galactose-inducible promoter did not affect survival and only slightly increased induced mutagenesis at high UV doses. It increased mutagenesis to the same degree in both WT and *rev3ΔC* strains (Figure 4.3).

4.2.4 Mgs1 is a negative regulator of Pol ζ in UV mutagenesis

It is known that overexpression of the ATPase *MGS1* lowers survival and severely decreases MMS-induced mutagenesis in cells with WT Rev3 [59]. We found the same effect for UV-induced mutagenesis (Figure 4.4A). Interestingly and unexpectedly, overproduction of Mgs1 had no effect on survival or the residual levels of mutagenesis seen in *rev3ΔC* (Figure 4.4A). *MGS1* deletion had no effect on UV sensitivity or induced mutagenesis in WT or *rev3ΔC* strains (Figure 4.4B). Deletion of *MGS1* was reported to abrogate the growth defect of *pol32*Δ cells. A preliminary experiment was done to test UV sensitivity and mutagenesis in *mgs1*Δ *pol32*Δ double mutants, but they behaved just like *pol32*Δ (data not shown). Therefore deletion of *MGS1* only rescues some *pol32*Δ

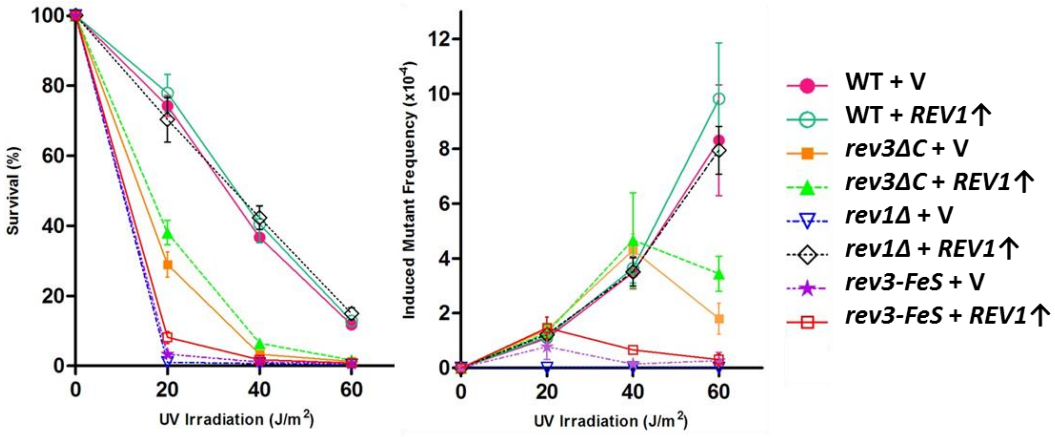

Figure 4.3: Overexpression of REV1 has little effect on UV-induced mutagenesis

Overexpression of exogenous Rev1 does not elevate mutagenesis at high doses of UV in WT and *rev3ΔC* strains**.** WT + vector (pink ●), WT + *REV1*↑ (light teal ○), *rev3ΔC* + vector (orange ■), *rev3ΔC* + *REV1*↑ (green ▲), *rev1Δ* + vector (blue ▽), *rev1Δ* + *REV1*↑ (black ◇), *rev3-FeS* + vector (purple ★), *rev3-FeS* + *REV1*↑ (red □). Data was collected and analyzed as described in Methods section 2.3 (three independent trials). All strains are described in Table 2.1.

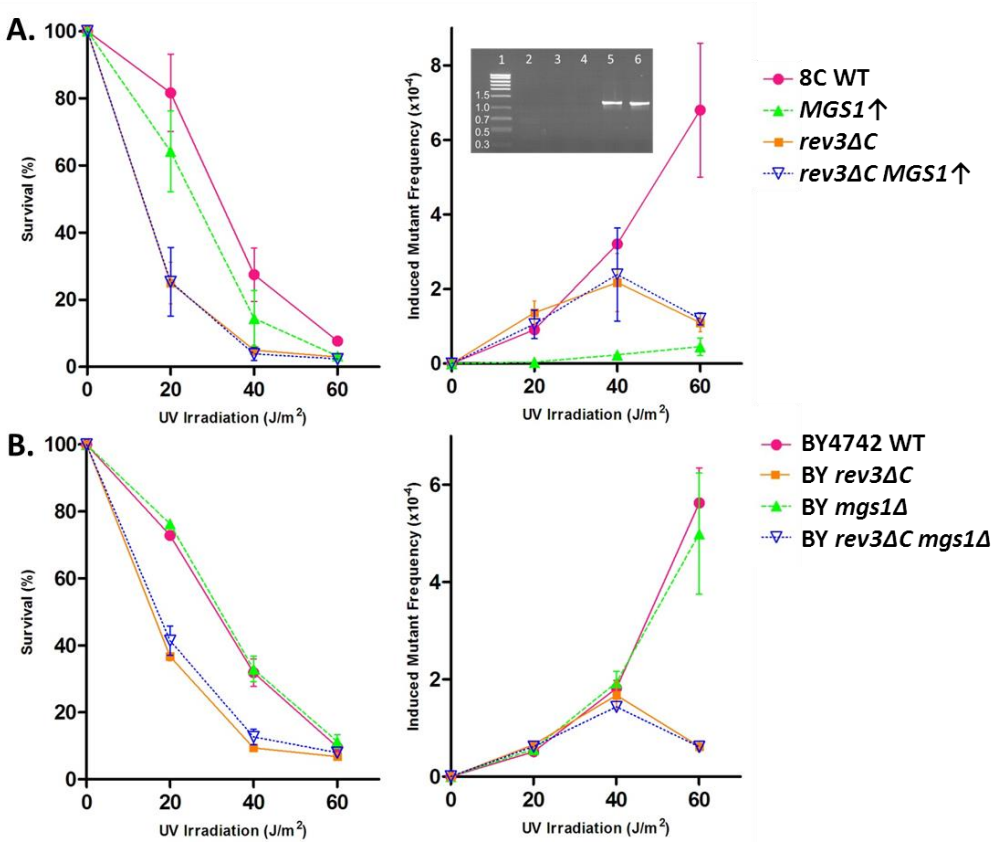

Figure 4.4: *rev3ΔC* truncation mutant is insensitive to suppression of UV-induced mutagenesis by overexpression of *MGS1*

A. Overexpression of *MGS1* suppresses mutagenesis only in the WT strain**.** 8C WT (pink ●), *rev3ΔC* (orange ■), *MGS1*↑ (green ▲), *rev3ΔC MGS1*↑ (blue ▽). **A. Insert**: PCR analysis confirms the correct integration of an *MGS1* expression cassette in WT and *rev3ΔC* strains. The forward primer had homology to the plasmid backbone sequence and the reverse primer had homology to the beginning of the *MGS1* gene; these primers amplify a region of about 1.3 kb. Lanes **1** – DNA ladder, **2** – blank PCR sample (no DNA added), **3** – 8C WT DNA, **4** – *rev3ΔC* DNA, **5** – WT + *MGS1*↑ DNA, **6** – *rev3ΔC* + *MGS1*↑ DNA. **B.** Deletion of Mgs1 has no effect on mutagenesis in WT and *rev3ΔC* strains**.** 8C WT (pink ●), *rev3ΔC* (orange ■), *mgs1Δ* (green ▲), *rev3ΔC mgs1Δ* (blue ▽). Data was collected and analyzed as described in Methods section 2.3 (three independent trials). All strains are described in Table 2.1.

defects.

4.2.5 Deletion of *MGS1* has no effect on spontaneous mutagenesis in *CAN1*

It has been shown that deletion of *MGS1* increased the spontaneous mutation rate in a stop codon reversion assay [110]. We re-examined this in two yeast strains, BY4742 and 8C, using the *CAN1* forward mutation reporter gene. There was no difference in the spontaneous mutation rate when *MGS1* was deleted alone or in combination with *rev3ΔC* (Table 4.2).

4.2.6 Mgs1 expression levels are modulated by DNA damage stimuli

Mgs1 negatively regulates the function of four-subunit WT Pol ζ, but only under conditions of overexpression. The *Saccharomyces* Genome Database (SGD) was mined to determine if overexpression of *MGS1* occurs under physiological conditions in yeast, particularly with respect to DNA damage. This database provides information from thousands of microarray datasets and pools them according to the level of expression change and how many conditions were found to elicit that response. The resulting figure was inconclusive. However, the database can identify genes that show expression profiles that are similar to Mgs1. Interestingly, it was found that Mgs1 shows a correlation with the expression pattern of the gene encoding the mismatch repair protein PMS1 in seventeen different datasets and a correlation with *RAD30*, encoding for DNA Pol η, in sixteen datasets (Figure 4.5). This is consistent with previous data suggesting that Mgs1 plays a role in promoting error-free damage bypass.

Table 4.2 Deletion of Mgs1 has no effect on spontaneous mutagenesis in *CAN1*

	***CAN1* (x10^{-7})**	
	CAN**	CL
BY WT	1.52	0.92-21.0
BY *rev3ΔC*	1.28	1.11-1.97
BY *mgs1Δ*	1.53	1.16-2.59
BY *rev3ΔCmgs1Δ*	3.47	2.34-11.6
8C WT	1.86	1.23-3.36
8C *rev3ΔC*	1.44	1.36-2.09
8C *mgs1Δ*	2.63	1.80-3.27
8C *rev3ΔCmgs1Δ*	2.65	2.09-3.37

*CL – confidence intervals

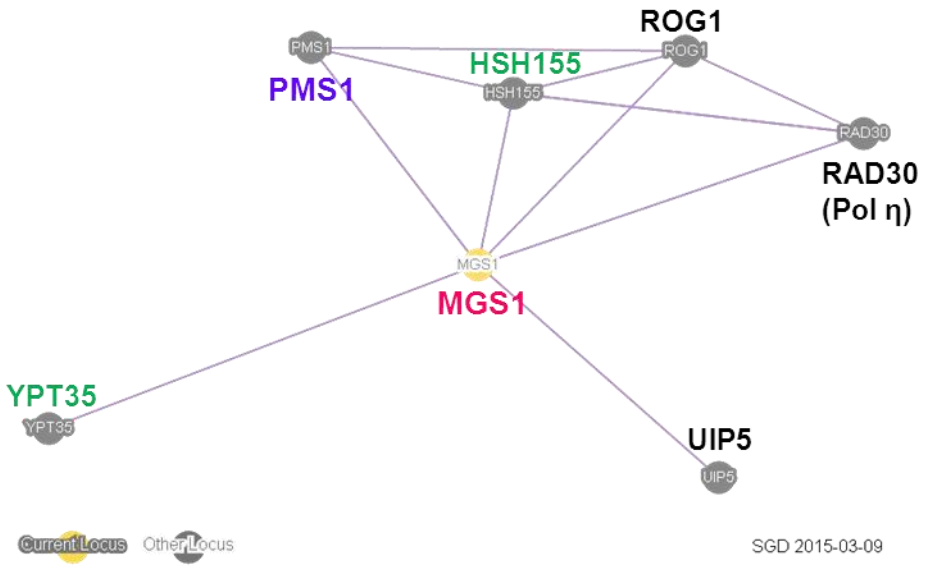

Figure 4.5: Mgs1 shows a similar expression pattern to DNA Polymerase η

Map showing genes with expression profiles most similar to Mgs1 (SGD), meaning the expression patterns of these two genes were induced/repressed in response to the same conditions. Color of the text indicates the number of studies that showed positive correlation between the specified gene and Mgs1. Green – 15, Black – 16, Blue – 17.

4.3 Discussion

4.3.1 Pol32 behaves differently as a subunit of Pol δ vs Pol ζ

For a long time it has not been well-understood why a subunit of Pol δ, Pol32, is required for TLS. Now it is clear that Pol31/Pol32 are also subunits of Pol ζ, though they appear to interact differently in comparison to the interaction with the catalytic subunit of Pol δ, as discussed in [80, 81]. This observation led to a simple explanation for why Pol32-deficient cells are immutable: because Pol32 is a subunit of Pol ζ. This is consistent with the fact that the FeS-less Pol ζ variant lacks binding to Pol31/Pol32 and confers immutability. However, the data presented here suggest that the scenarios of polymerase switches are more elaborate and complex.

We found that even though the protein in the *rev3ΔC* mutant lacks the region required for binding to Pol31/Pol32, the strain is still quite proficient in UV-induced mutagenesis. The effect of *rev3ΔC* is recessive, because it could be seen only when no WT *REV3* was present in the genome (Figure 3.8). This is consistent with observations that two subunit Pol ζ (Rev3/Rev7) is active *in vitro*, albeit less active than 4-subunit Pol ζ [81, 111]. Thus, Pol32 is not critical for elementary Pol ζ function.

Despite the fact that the *rev3ΔC* mutant most likely is not utilizing Pol32, we found that mutagenesis in the *rev3ΔC* strain is absolutely dependent on Pol32. This strongly suggests that the immutability of *pol32Δ* strains at least partly reflects an additional role of Pol32 in TLS related to Pol δ, because the loss of this subunit of Pol δ prevents UV-induced mutagenesis independent of its binding to Rev3. Indeed, in support of this idea it was recently shown in chicken cells that the Pol32 homolog can promote

TLS independent of Pol ζ [76]. This phenomenon of cross-talk between replicative and TLS polymerases better fits the initial step of the switch model depicted in Figure 4.1B. It appears that Pol32-less Pol δ is unsuitable for a proper switch to Pol ζ. This is consistent with the fact that the *pol3-13* mutation, leading to a change of one cysteine involved in FeS binding in the CTD of Pol δ, leads to suppression of UV mutability ([112] and (Stepchenkova, Siebler, and Pavlov, unpublished data)).

It is generally assumed that Pol δ is involved only in lagging DNA strand replication [72]. However, TLS events occur by the same mechanism on both DNA strands in a yeast system with a damaged plasmid [113]. In this context it is interesting that deletion of *POL32* eliminates all mutagenesis, suggesting that Pol32 is required for TLS events on both strands. Our data suggest that Pol ζ is active without Pol32 and that the effect of *pol32Δ* is partly due to it being part of Pol δ. If Pol ε is fully responsible for the whole leading strand, then it is difficult to explain why missing components of Pol δ attenuate mutagenesis on this strand. This supports the idea that Pol δ is also involved in leading strand replication [70] or that the polymerase switch involves a complex event: Pol ε switching to Pol δ and then to Pol ζ. Another possibility is that Pol δ is involved in mutagenesis by taking over synthesis from Pol ζ or filling the gaps resulting from re-initiation of DNA synthesis after TLS downstream of Pol ζ [33, 37].

A recent paper suggested that Rev7 of Pol ζ can bind to Pol32 *in vitro*, which would indicate that Rev3ΔC could hold on to this interaction [85]. This interaction appears to be weak, because Rev7 was not pulled down with Pol32 by tagged Pol31 [80]. Furthermore, mutations in *POL31* abolishing the interaction between Pol31 and Pol32 lead to UV-immutability, despite the fact that Pol32, *per se*, is untouched [83]. The fact

that we do not see substantial levels of mutagenesis in *rev3-FeS* suggests that this cluster has another function besides binding Pol31/Pol32 or that the interaction between Pol32 and Rev7 is insufficient for Pol ζ function.

4.3.2 Dependence of *rev3ΔC* on Rev1

Another important member of the TLS machinery is Rev1. It interacts with Rev3 via the Rev7 subunit [114]. Mutagenesis in *rev3ΔC* is dependent on Rev1 which indicates that Pol ζ with truncated Rev3 is recruited by Rev1, a scaffold protein during regular TLS. It is likely that the Rev1 interaction with Pol ζ is the reason that we see intermediate mutagenesis in *rev3ΔC* (Figure 4.6). WT Pol ζ can contact PCNA through both Rev1 and Pol31/Pol32, therefore there is robust TLS [115]. It is possible that *rev3-FeS* is unable to bind PCNA not only through Pol31/Pol32, but also through Rev1 due to steric hindrance caused by the absence of the FeS cluster in the CTD of Pol ζ. Rev3ΔC lacks sufficient binding to Pol31/Pol32, but can still maintain its contact with Rev1. This is sufficient for supporting some TLS functions and for mutagenesis at low doses, but confers a partial defect at higher doses. To explore this hypothesis, we tested whether overproduction of Rev1 would increase UV- induced mutagenesis in *rev3ΔC* strains, but found no such influence (Fig. 4.3C). Therefore, simple increase of Rev1 levels cannot compensate for the lack of subunits. It appears that chromosomal *REV1* is sufficient to fulfill the demand of the Rev1 protein after UV irradiation in both WT and *rev3ΔC* strains.

4.3.3 Novel, negative regulation of four-subunit Pol ζ by Mgs1

In most of our experiments, the genetic control of mutagenesis in the *rev3ΔC* strain was very similar to the WT strain. However we found one modulator of TLS,

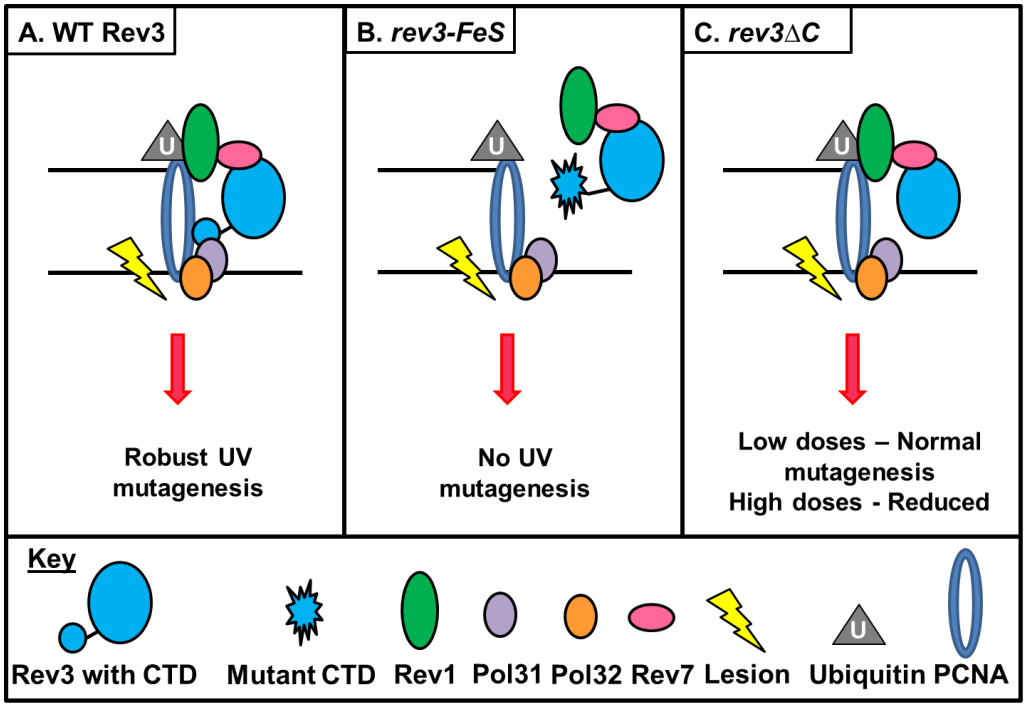

Figure 4.6 A model for differences between *rev3-FeS* and *rev3ΔC*

A. WT Pol ζ (light blue circles) is able to make two contacts with the processivity clamp PCNA (ring): one through Rev1 (green oval) which can bind monoubiquitylated PCNA and one through Pol31/Pol32 (purple and orange ovals, respectively). **B.** *rev3-FeS* cannot bind Pol31/Pol32, and perhaps the misfolded CTD (blue star) provides steric hindrance that also blocks the Rev1 interaction with PCNA, leaving no interaction and thus no mutagenesis. **C.** *rev3ΔC* cannot make the contact though Pol31/Pol32, but has no misshapen CTD so can hold on to the interaction with Rev1. This interaction alone is sufficient to support lower levels of mutagenesis, but cannot keep up at higher doses (giving residual mutagenesis phenotype).

encoded by the gene *MGS1*, that behaved differently. Overproduction of Mgs1 severely reduces MMS-induced mutagenesis [59] and eliminates UV-induced mutagenesis (Fig. 5A) in yeast, suggesting that it can act as a negative regulator of TLS. However we found that overproduction of Mgs1 had no effect on mutagenesis in the *rev3ΔC* strain.

Deletion of *MGS1* abrogates the growth defect of *pol32Δ, pol3Δct,* and *pol31* mutant cells, suggesting that in the context of damage sensitivity Mgs1 is an effector of Pol δ [59, 104]. It was also previously proposed that Mgs1 could compete with Pol32 for binding to PCNA, as overproduction of Mgs1 reduced the yeast two-hybrid interaction between Pol32 and Ub-PCNA [59]. Therefore it is possible that Pol32 could be knocked off of PCNA by Mgs1, resulting in lack of mutagenesis. However, we show here that overexpression of Mgs1 has no negative effect in the *rev3ΔC* strain. This result suggests that in the context of UV-induced mutagenesis, Mgs1 exerts its inhibitory effect by acting specifically on Pol32 bound to Pol ζ, not Pol δ (Figure 4.7). This is the first time that Mgs1 and Pol ζ have been implicated to functionally interact. It is well established that Mgs1 is a negative regulator of TLS, and we propose based on our data that one of the primary mechanisms could be through inhibition of Pol ζ.

If the inhibition by Mgs1 occurs through this proposed Pol32 competition mechanism, this result also argues against a strong interaction between Pol ζ and Pol32 through Rev7 binding to Pol32 (see above). If that were the case, Rev3ΔC would still be bound to Pol32 and Mgs1 would compete with it for binding, thus decreasing UV-induced mutagenesis in that strain. Consistent with the data in the literature [110], we found that deletion of *MGS1* had no effect on induced mutagenesis (Figure 4.4A). This was also true for the *rev3ΔC* strain (Fig. 5B).

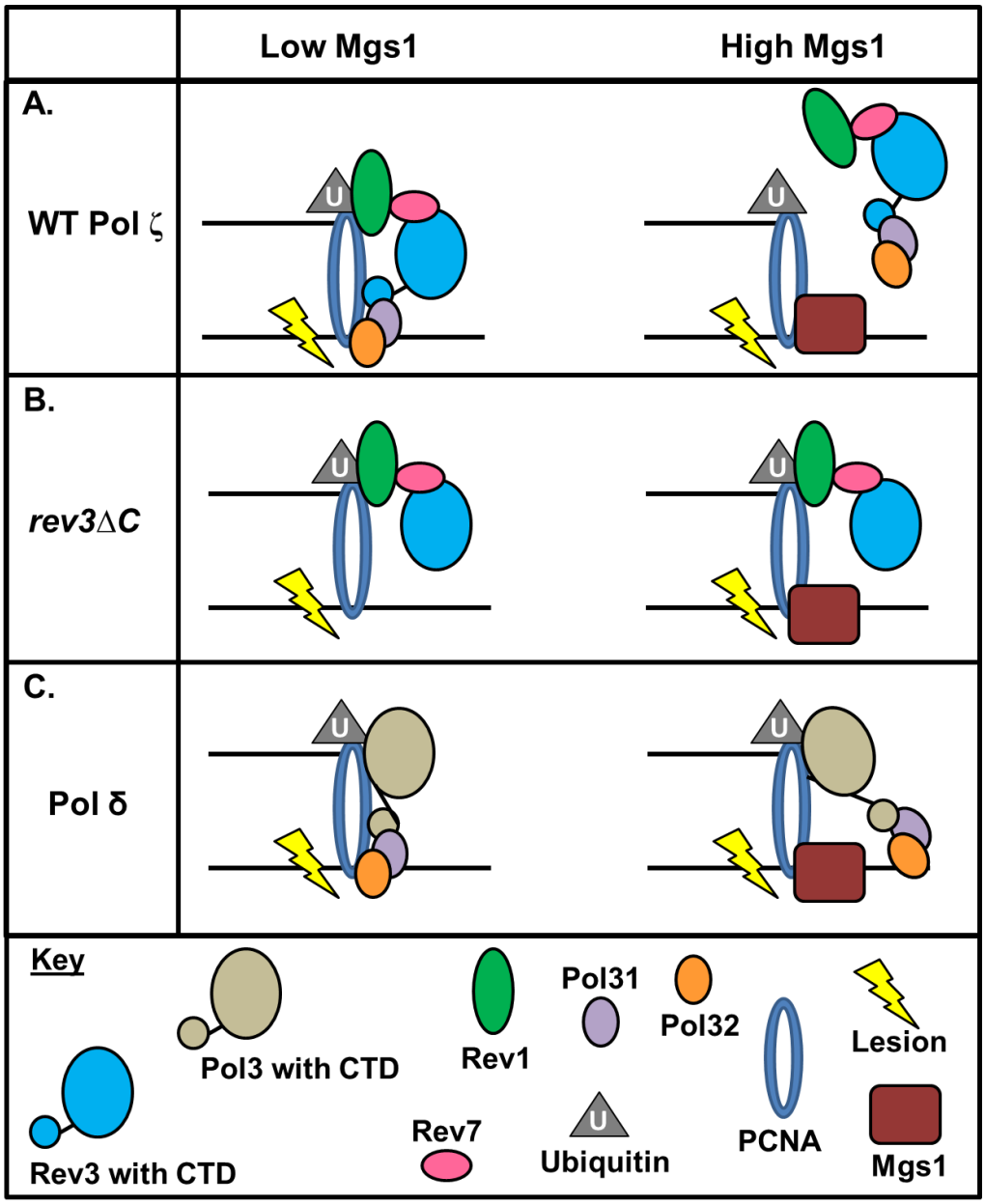

Figure 4.7 Model of Mgs1 inhibiting four-subunit Pol ζ through competition with Pol32

A. When Mgs1 is at high levels, it can compete with Pol32 for binding to PCNA. Because Pol ζ is rigid and comprised of all four subunits, this results in the entire enzyme being displaced and there is no mutagenesis. **B.** Rev3ΔC does not interact strongly with Pol31/Pol32, therefore Mgs1 competing with Pol32 has no effect on mutagenesis. **C.** When Mgs1 competes with binding of Pol32 that is bound to Pol δ, there is some innate flexibility that allows only Pol32 (and maybe Pol31) to be temporarily displaced.

If Mgs1 competes with Pol32 for binding to PCNA, this raises the question of why it preferentially affects involvement in mutagenesis of Pol ζ and not Pol δ, since both contain Pol32. As mentioned, the nature of these interactions is not identical. It was shown that Pol3 can form a stable complex with Pol31 alone, but Rev3 cannot [81]. A recent EM structure of Pol ζ may also give a clue to this differential binding nature [85]. Both Pol δ and Pol ζ contain catalytic and regulatory modules in their structures. However, there is flexibility between the two modules in Pol δ whereas four subunit Pol ζ appears to be more rigid. When Mgs1 displaces Pol32 of Pol δ, the flexibility may result in only Pol32 being temporarily displaced instead of the whole enzyme dissociating from PCNA (Figure 4.7). Because Pol ζ is rigid, Mgs1 competition with Pol32 may result in the whole polymerase being removed from PCNA. Another formal possibility is that during the polymerase switch, Pol31/Pol32 that are alone on the DNA are displaced, disrupting the switch. Since Rev3ΔC cannot be recruited by Pol31/Pol32, it is still able to come to the DNA through another mechanism.

It has also been suggested that Pols δ and ζ interact with PCNA differently. This was shown most clearly with a mutation affecting the monomer-monomer interface of PCNA, *pol30-113* [47]. Yeast strains with this mutation show no growth defects or sensitivity to the replication inhibitor HU, suggesting that this PCNA variant is sufficient for replication. However, these cells are UV-immutable indicating defective TLS. *In vitro*, *pol30-113* is an effective (albeit less than WT) processivity clamp for Pol δ, but not for Pol ζ [47].

Mgs1 at normal physiological levels may not play an active role in UV-induced mutagenesis, since *mgs1*Δ did not affect mutation frequency. In order to determine if this

inhibition of Pol ζ by Mgs1 occurs *in vivo*, data on Mgs1 expression under different conditions was mined from the *Saccharomyces* Genome Database (http://www.yeastgenome.org/). Mgs1 did not show a striking increase in expression in response to the various DNA damaging conditions examined, although UVR was not listed. However, in the data shown here Mgs1 overexpression eliminated mutagenesis in WT strains even in the absence of induction with galactose, suggesting that small increases may be sufficient for Mgs1 inhibition of TLS. Therefore it is possible that Mgs1 may be slightly overproduced and inhibit Pol ζ *in vivo* in response to some damaging conditions other than UVR in order to promote an error-free mechanism, such as DNA damage avoidance by template switching or a novel pathway involving Mgs1.

Expression profiles of Mgs1 correlated with profiles of *RAD30*, encoding the error-free TLS Pol η, and MMR protein *IPMS1* in numerous studies. In chicken cells, it has been suggested that the homolog of Mgs1, WRNIP1, acts upstream of Pol η to promote its error-free bypass of UV-induced lesions. Deletion of WRNIP1 in this study rescued the phenotypes of Pol η deletion such as UV sensitivity, trouble eliminating CPDs, and slow progression of replication forks in response to damage [116]. This could provide an explanation for the expression correlation and suggests that one of the error-free mechanisms driven by Mgs1 could be error-free TLS. The expression correlation data itself is interesting because it connects Mgs1 further to DNA damage and repair, but the significance of these similarities cannot be fully evaluated from the limited information available in the database. It is unclear what the connection between Mgs1 and *IPMS1*/MMR are.

Another possibility is that Mgs1 at endogenous levels inhibits Pol ζ-dependent damage tolerance in the absence of damage, rather than in its presence since Pol ζ is so mutagenic. Indeed deletion of Mgs1 has been shown to increase spontaneous mutagenesis [110]; however, we were unable to confirm that result (Table 4.2). This could be because the action of Mgs1 could be site-specific. We utilized the *CAN1* gene, which can detect a wide variety of mutations, but some weak effects in certain sites can remain undetected. The reversion system used in Shinagawa et al. detects only a narrow spectrum of changes [110].

4.3.4 Conclusions

This study shows that Pol ζ can function in TLS *in vivo* despite the absence of its CTD, which serves as a platform for binding to Pol31/Pol32. The necessity of Pol32 in this mutant strain highlights the importance of Pol δ integrity in TLS since Pol32 is required even when not a member of Pol ζ. Furthermore, we have shown a novel inhibitory effect of the ATPase Mgs1 specifically on the four-subunit Pol ζ. Both Pol δ and Pol ζ have Pol32 as a subunit, but use it for somewhat different transactions. It is possible that Mgs1 can directly compete with Pol32 bound to Pol ζ for binding to PCNA and decrease induced mutagenesis, but does not compete with Pol32 of Pol δ.

***Most of the data in this chapter were published in Siebler et al., 2014 [93].**

5 Spectra of UV-induced *can1* Mutations in the *rev3ΔC* Strain

5.1 Introduction

5.1.1 UV-induced DNA damage

DNA damage induced by UVR is one of the best characterized DNA damage/repair systems (reviewed in [2, 20, 117, 118]). It is well known that UVR-induced damage is a major cause of skin cancer [119]. The major source of UVR for living organisms is solar irradiation, which is divided into three wavelength groups. UVA (315-400 nm) is the most prevalent and is least efficient at inducing DNA damage because it is not absorbed by DNA. However, it can produce secondary photoreactions and generate ROS such as singlet oxygen [120, 121]. The majority of solar UVB (280-315 nm) radiation is filtered by atmospheric ozone, but because it is absorbed by cellular DNA it is the major contributor to DNA damage [122, 123].

All UVC (< 280 nm) radiation is blocked by ozone and is not normally dangerous, but the ozone layer is being depleted in some areas [124]. UVC could be generated by artificial sources, and thus lead to human exposure. Most mutation research has been done using UVC with an emission maximum at 254, close to the absorption peak for DNA (260) and not efficiently absorbed by proteins. UVC is an appropriate, though not ideal, experimental system to study UVR-induced mutagenesis because the major lesions induced by UVC are the same as those induced by UVA/UVB (but are induced more efficiently). One difference is that simulated sunlight (UVA/UVB) converts most 6-4PPs into Dewar isomers (see below) and additionally induces 8-oxoG lesions into DNA [63].

UVR is one of the most effective and carcinogenic exogenous agents that interacts with DNA and affects genome integrity (reviewed in [2, 20, 117]). The two most abundant mutagenic and cytotoxic DNA lesions induced by UVR are 1) cyclobutane-pyrimidine dimers (CPDs) and 2) 6,4 photoproducts (6-4PPs) and their Dewar (valence) isomers (Figure 5.1). Both CPDs and 6-4PPs distort the DNA helix, which can be an impediment to replication and transcription. Damage caused by UVR can lead to mutagenesis, tumorigenesis, and cell death.

CPDs are the most abundant and cytotoxic (apoptotic) lesions induced by UVR [125], making up close to 75% of UV lesions (reviewed in [2, 20, 117, 118]). CPDs are a four-carbon ring structure involving positions C5 and C6 of neighboring pyrimidines (Figure 5.1). CPDs remain roughly parallel but they lose their planar π electrons, lose aromaticity, and exhibit a 36º relative rotation [126]. DNA with a CPD is underwound and bent by about 30º at the lesion (buckled) [127]. Only the *cis-syn* conformation is allowed in the DNA duplex and it is the most common. Where CPDs occur in DNA depends on which dipyrimidine is involved, but also the surrounding sequence context.

6-4PPs may be less cytotoxic than CPDs, but are more mutagenic and this mutagenesis can be lethal; they make up close to 25% of UV lesions (reviewed in [2, 20, 117, 118]). 6-4PPs are formed by a noncyclic bond between C6 of the 5’ end and C4 of the 3’ end of involved pyrimidines (Figure 5.1) [128]. They introduce prominent distortion in the double helical structure because the crosslinked pyrimidine bases are almost perpendicular to each other. This can cause segmentation of DNA (B-form regions of DNA separated by kinks) which is exacerbated when a mismatched base is inserted opposite the lesion. UV sources bordering UVA/UVB, such as sunlight, tend

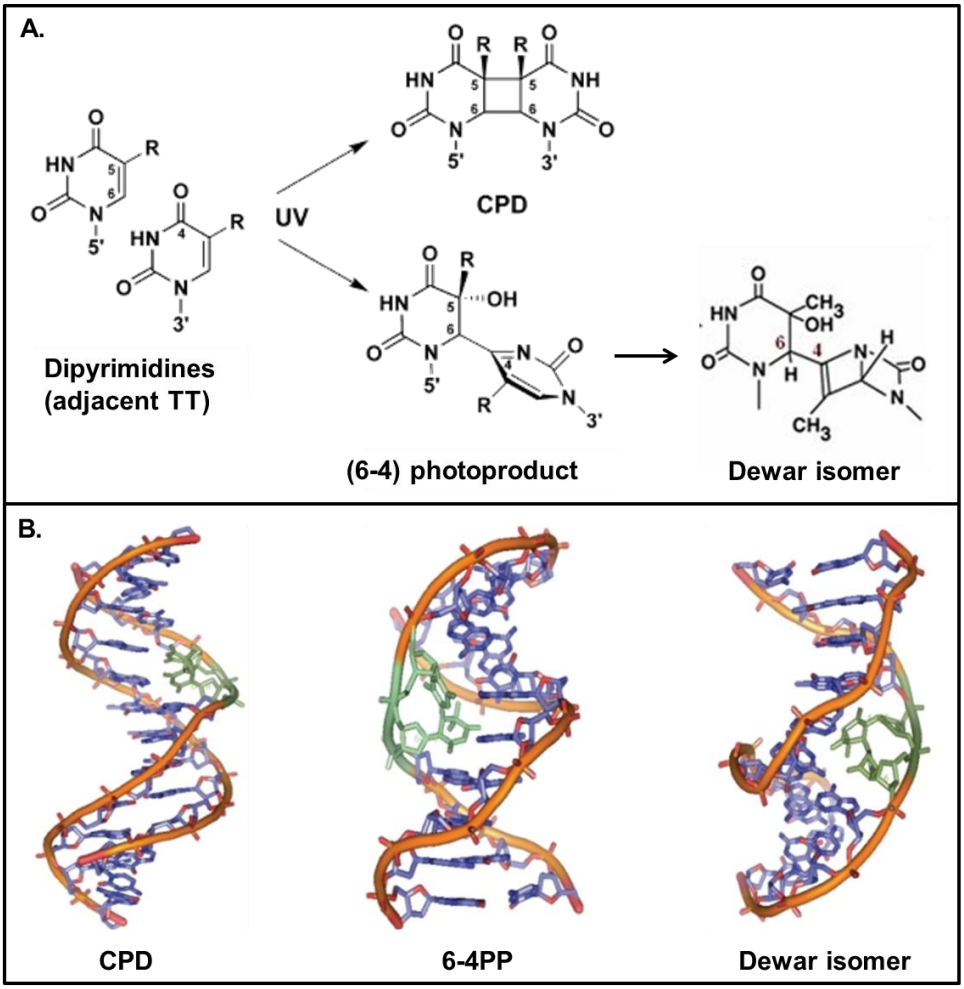

Figure 5.1 UV-induced DNA lesions distort the DNA

A. Scheme showing the major lesions induced by UVR: cyclobutane pyrimidine dimer (CPD), (6-4) photoproduct and its Dewar isomer. **B.** Scheme showing the distortion/bending of DNA by various types of UV lesions. Modified from [117, 129] and http://cosmobiousa.com/uvantibodies.html.

to convert 6-4PPs to Dewar isomers [130-132]. 6-4PPs and their Dewar isomers cause helical bending of 44 º and 21 º, respectively [133]. Not surprisingly, 6-4PPs have been shown to correlate with mutational hotspots [134].

Although CPDs and 6-4PPs are by far the most prominent lesions (especially from UVC), UVR has been shown to induce many other types of damage as well (reviewed in [2, 117]). UVR induced ROS (such as singlet oxygen and free radicals) can act as powerful oxidants leading to formation of a variety of oxidative lesions including 8-oxo-7,8-dihydroguanyl (8-oxoG), 8-oxo-A, 2,6-diamino-4-hydroxy-5-formamidoguanine (FapyGua), FapyAde, and oxazolone [122, 135] and can contribute to apoptosis [136]. UV-induced modifications of purines have also been observed, though less frequently [122, 137]. These are primarily AA dimers and TA photoproducts. Pyrimidine hydrates and thymine glycol can also be formed.

DNA strand breaks are observed extensively under treatment with UVB and UVC (reviewed in [2, 117]). DSBs can affect both strands of DNA and lead to loss of genetic material; therefore they are the most deleterious form of DNA damage. It is believed that UVR does not directly create DSBs, but rather it creates other types of lesions that lead to replication fork collapse and subsequent formation of DSBs (reviewed in [138]). Simulated sunlight yields SSBs and alkali sensitive lesions, 8-oxoG, though CPD and 6-4PP are still the predominant lesions.

5.1.2 DNA Repair of UV lesions

There are several repair pathways in cells that can deal specifically with damage induced by UVR. Photoreactivation by the enzyme photolyase is one of the most important and frequently used mechanisms (reviewed in [20, 117, 139]). Photolyases are

present in bacteria, fungi, plants, invertebrates, and many vertebrates but seem to be absent or nonfunctional in humans [140]. Photolyases bind specifically to CPDs, then directly monomerize the cyclobutane ring using the energy of visible/blue light. It is thought that some organisms also have 6-4PP photolyases. Efficiency of photoreactivation under proper conditions is extremely high.

Dark repair pathways are more complex and replace the damaged DNA with new undamaged DNA, rather than reversing the damage. The major pathway in many organisms, including humans, that repairs UV-induced lesions and other helix distorting lesions is NER (introduced in section 1.3 and references therein, reviewed in [20, 117, 118]). This pathway is widely conserved from prokaryotes to humans and is one of the most versatile and flexible repair systems. It has been hypothesized that changes in DNA rigidity due to lesions is the key factor in NER lesion recognition [141]. The severity of DNA distortion caused by UV lesions correlates with repair efficiency: 6-4PPs are more destabilizing than CPDs, and are more efficiently repaired ([142], reviewed in [118]). Both CPDs and 6-4PPs lose base stacking and thus reduce the persistence length (rigidity) of DNA (Figure 5.1).

Some proteins may sense specific DNA lesions, but others conduct a “stress test” to see where the DNA is too flexible [118]. Briefly, ATP binding causes stress and bends DNA, and when ATP hydrolysis relieves the stress the damaged DNA responds by strand separation whereas undamaged DNA returns to B-form. Some other repair enzymes such as yeast photolyase and bacterial T4 endonuclease recognize distorted DNA using a concave surface at the active site, which approaches the minor groove only of DNA bent by a lesion. The lesion (CPD or 6-4PP) or the A’s opposite are flipped out from the

duplex into the active site for cleavage [131, 143, 144].

Other repair pathways can act on UV-induced damage other than CPDs and 6-4PPs (reviewed in [117]). As mentioned, UVA can also induce oxidative damage through the production of ROS, and these lesions can be repaired by BER (introduced in section 1.3). HR and NHEJ can act to repair the DSBs that occur as secondary effects of UVR. HR is considered more accurate because it uses a homologous region of DNA, whereas NHEJ is error-prone because it joins broken chromosomal ends independent of sequence homology. It is also important to note that when damage occurs in cells, there can be activation of cell cycle checkpoints which can stop the progression of the cell cycle in order to provide more time for DNA repair. Cell cycle checkpoints can also induce apoptosis to eliminate damaged cells, avoiding carcinogenic potential.

5.1.3 Error-free and error-prone bypass of UV-induced lesions

In situations where repair does not occur before UV-induced damage is encountered by replication machinery, CPDs and 6-4PPs can cause replication fork arrest and ultimately cell death. Under these conditions, bypass of these lesions can be the only choice for cell survival and TLS is one of the major bypass mechanisms. The two main TLS polymerases that act upon damage induced by UVR in yeast are Pol η and Pol ζ (in complex with Rev1).

Pol η is a member of the Y-family of DNA polymerases and is primarily involved in TLS events that lower the probability of mutations (frequently referred to as error-free) (reviewed in [9, 20, 118]). It is able to facilitate efficient and accurate bypass of CPDs, especially inserting A across from CPDs at TT sites [145, 146]. Most polymerases can only accommodate one template base in their active site; however Pol η can readily

accommodate two normal pyrimidine bases simultaneously, or a CPD for bypass. Efficiency of Pol η is increased on CPDs compared to normal T residues, so polymerase switching from Pol η to another polymerase like Pol ζ may occur as a transition from the preferential use of the damaged template to disfavored use of the undamaged downstream template [145]. The role of Pol η in bypass of 6-4PPs is more controversial. Most studies have shown that Pol η plays a minor role in bypass of these lesions (discussed in [63, 147]) and it was shown that deletion of Pol η only decreased bypass of a plasmid 6-4PP by 7.5% [148]. However, one study found that strains lacking Pol η showed a 10-fold decrease in mutagenic bypass of a plasmid 6-4PP [149]. In yeast, Pol η transcripts are induced three- to four-fold in response to UV damage, although this was not seen in mice. Loss of Pol η results in the variant form of the cancer predisposition disease xeroderma pigmentosum (XPV).

Even though Pol η can help avoid mutations when bypassing some lesions such as UVR photoproducts or 8-oxoG, it is one of the lowest fidelity polymerases on undamaged DNA. This property is exploited during somatic hypermutation in immunoglobulin genes (reviewed in [9, 20]). Pol η can synthesize DNA with low efficiency across other types of damage such as abasic sites, AAF, guanine adducts, benzo[a]pyrene adducts, and some cisplatin adducts. Pol η binds preferentially to monoubiquitylated PCNA, which can explain its recruitment. It can itself be ubiquitylated, but the functional significance of this is not well understood.

Pol ζ plays a key role in error-prone bypass of UV-induced lesions (Pol ζ is reviewed in Chapters 1 and 3, and references therein). It has been suggested that *in vivo* Pol ζ plays a major role in bypassing 6-4PPs, but a minimal role in bypassing CPDs even

though it can inaccurately bypass a CPD lesion *in vitro* ([148, 150], discussed in [147]). This trend is opposite that of Pol η. As mentioned, Pol ζ is most efficient at extending from distorted termini that result from nucleotides inserted by other polymerases. Pol η and Pol ζ can act together on these lesions, with Pol η acting as the inserter and Pol ζ acting as the extender. This can result in the correct nucleotides being inserted across from the lesion, but Pol ζ may make errors during extension of the downstream region which can lead to mutations [38]. When Pol η is absent in yeast cells, mutagenesis induced by UVR is elevated, suggesting that Pol ζ can take over bypass of these lesions. Ninety six percent of UV-induced mutations are dependent on Pol ζ [45, 51]. However, to the credit of Pol ζ it should be mentioned that across some lesions, such as thymine glycol, Pol ζ can perform both insertion and extension in a way that prevents mutations (error-free) [9].

5.1.4 UV-induced mutational spectra

Measuring mutational spectra can provide a wealth of information that cannot be discerned by simply measuring rates of mutagenesis in cells [147, 151, 152]. These spectra represent different types of mutations: base pair substitutions, frameshift mutations, and large gene rearrangements. Frameshifts include single or multiple base pair insertions and deletions that change the reading frame for transcription. Base pair substitutions are categorized as transitions or transversions. Transitions are changes from a purine to a purine or a pyrimidine to a pyrimidine, and there are two classes of these. Transversions are changes between purines and pyrimidines, and there are four classes. Within each class, the exact nucleotide change can also be examined. For example, a

nucleotide change from C to T belongs to the CG to TA class of transversions, and is a base pair substitution.

Mutational spectra have been examined in the p53 gene in human skin cancers, which are primarily caused by UVR ([153], reviewed in [152, 154]). The gene encoding p53 is mutated in over 50% of human cancers and 50% of all skin cancer; there are 300 potential detectable sites available for mutational analysis. Upon UVR, p53 levels are increased to block cells in the G1 phase of the cell cycle and allow for repair of DNA damage. Most mutations in p53 in skin cancers are CG to TA transitions (mainly C to T) and 90-96% of all base substitutions occur in dipyrimidine sites (TT, CT, TC, CC). This well-known UV signature is consistent with the fact that UVR primarily induces CPDs and 6-4PPs, occurring at these sites. Patients with XP have a very high percentage of the UV signature CC to TT tandem mutations as well.

In this dissertation, mutational spectra in response to UVR were studied in a yeast model system. It has been shown that mutational spectra from skin tumors are very similar to spectra observed in UVR targets in model systems, but are different from spectra described in other cancers (discussed in [155]). When yeast were transformed by an irradiated vector containing human p53 cDNA, the UV spectrum was not significantly different from that found in patient non-melanoma skin tumors [155], highlighting the fact that yeast is a suitable model to study cancer-relevant UVR mutagenesis.

In yeast, the *CAN1* gene is often used to study such mutational spectra (discussed in [63, 147]). *CAN1* encodes an arginine permease that transports the toxic drug canavanine into cells. Therefore, mutations that disable the permease can be selected for on media supplemented with canavanine. This system is able to detect all types of base

pair substitutions, deletions, insertions, and complex mutations. UVC-induced spectra in *CAN1* consist predominantly of base pair substitutions and tandem and nontandem complex mutations ([63], discussed in [147]), these complex mutations being a signature of Pol ζ [8, 47, 48]. Frameshift mutations account for 5-20% of mutations (discussed in [147]). In UVC spectra, transversions were predominantly AT to TA, with GC to AT also present. Base substitutions in *CAN1* occur mainly at dipyrimidines (89-97%) (roughly equal at TT, CC, TC and slightly less at CT) and there is bias for -1 over +1 frameshift mutations. This is the system utilized in the studies described here.

5.1.5 Goal of this chapter

This chapter addresses more specifically the UVR-induced mutagenesis defect seen in the *rev3ΔC* strain. It known that Pol ζ creates point mutations that contribute to cancer, while preventing potentially tumorigenic chromosomal rearrangements (discussed in chapter 1). The goal of this chapter was to determine if the C-terminus of Rev3 might play a role in regulating different functions and mutational specificities of Pol ζ. We asked if *rev3ΔC* is deficient at making all types of mutations or only certain types in response to UVR to help further define the extent to which the CTD of Rev3 regulated TLS.

5.2 Results

5.2.1 Rev3ΔC is most proficient at participating in the formation of transitions

As shown in Figure 3.6, the *rev3ΔC* strain had a lower induced mutant frequency than the strain with WT Pol ζ at intermediate to high doses of UVR. To determine which specific types of mutations occur at a lower frequency in *rev3ΔC* strains, an additional set

of mutagenesis data was collected. From this trial, 45-50 independent WT and *rev3*Δ*C* clones were selected from SC+Can plates at each UV dose. The *CAN1* gene was amplified from the DNA of these clones and sequenced (Figure 5.2). The frequencies of each type of mutation were compared between the two strains at three different UV doses. Figure 5.3 shows the average induced mutant frequency curves for WT and *rev3*Δ*C* (average of new trial for sequencing and all trials from Figure 3.3). The inset shows just the individual trial used to collect clones for sequencing analysis to show the exact fold differences in total mutagenesis between the two strains.

Low UV dose, 20 J/m^2- At this dose, there was a significantly higher frequency of transition mutations in *rev3*Δ*C* than in WT (Figure 5.4A). When mutations were further divided into the six major classes of base substitutions, plus deletions and insertions, both classes of transitions were significantly increased in *rev3*Δ*C* (Figure 5.4A). *rev3*Δ*C* also had significantly lower frequencies of two types of tranversions: GC to TA and TA to GC. Mutations are shown mapped to *CAN1* in Appendix C, Figure C.1.

Intermediate dose, 40 J/m^2- At this dose, there was no difference in the frequency of transitions between WT and *rev3*Δ*C,* but *rev3*Δ*C* displayed a lower frequency of transversions and frameshifts (Figure 5.4B). This decrease in transversion mutations was found to be due to significant decreases in all substitution classes except TA to GC. The decrease in frameshift mutations was due to a decrease in deletions; there was no difference for insertions (Figure 5.4B). Mutations are shown mapped to *CAN1* in Appendix C, Figure C.2.

High dose, 60 J/m^2- At the highest dose of 60 J/m^2, the *rev3*Δ*C* spectrum exhibited lower frequencies of all types of mutations compared to WT (Figure 5.4C).

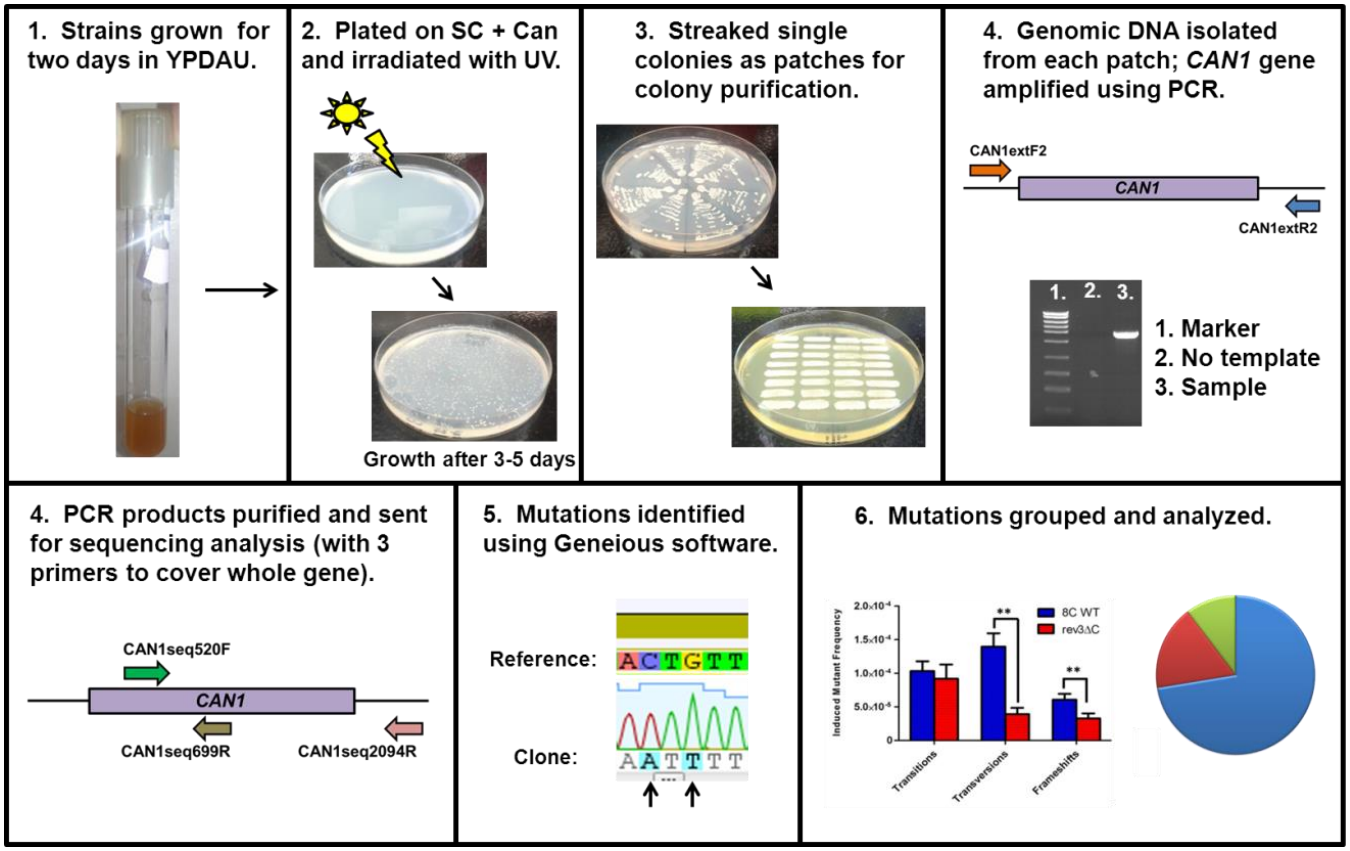

Figure 5.2 Scheme of experiments to determine mutational spectra

This procedure is described in section 2.7.

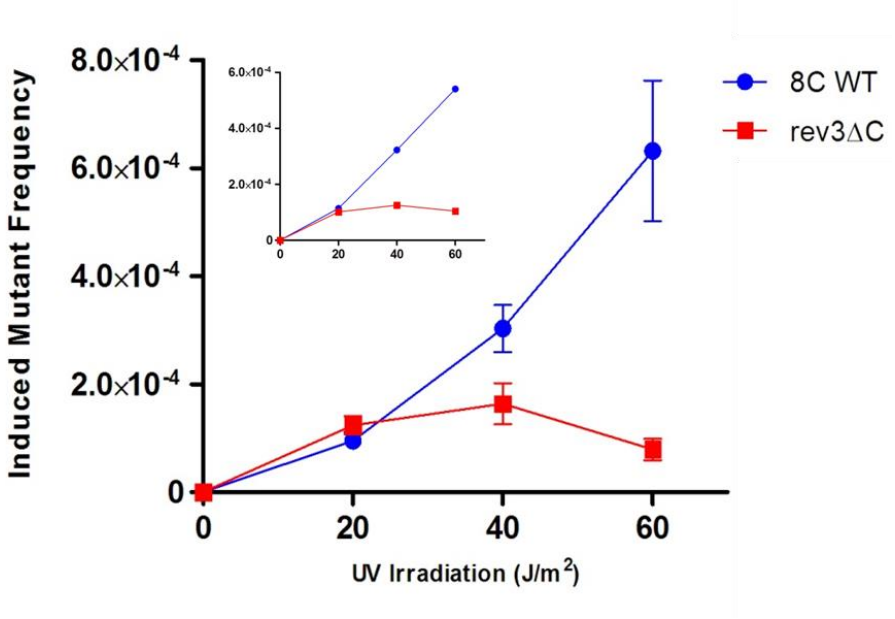

Figure 5.3 Mutagenesis levels in WT and *rev3ΔC* strains used for mutational spectra analysis

Average mutagenesis levels including all trials from Chapter 3 and the trial used for mutational spectra. These averages were used for all subsequent statistical analysis. 8C WT (blue ●), *rev3ΔC* (red ■). **Inset:** Mutagenesis levels in WT and *rev3ΔC* strains in the individual trial used to collect clones for sequencing. Data was collected and analyzed as described in Methods section 2.3 (four independent trials). All strains are described in Table 2.1.

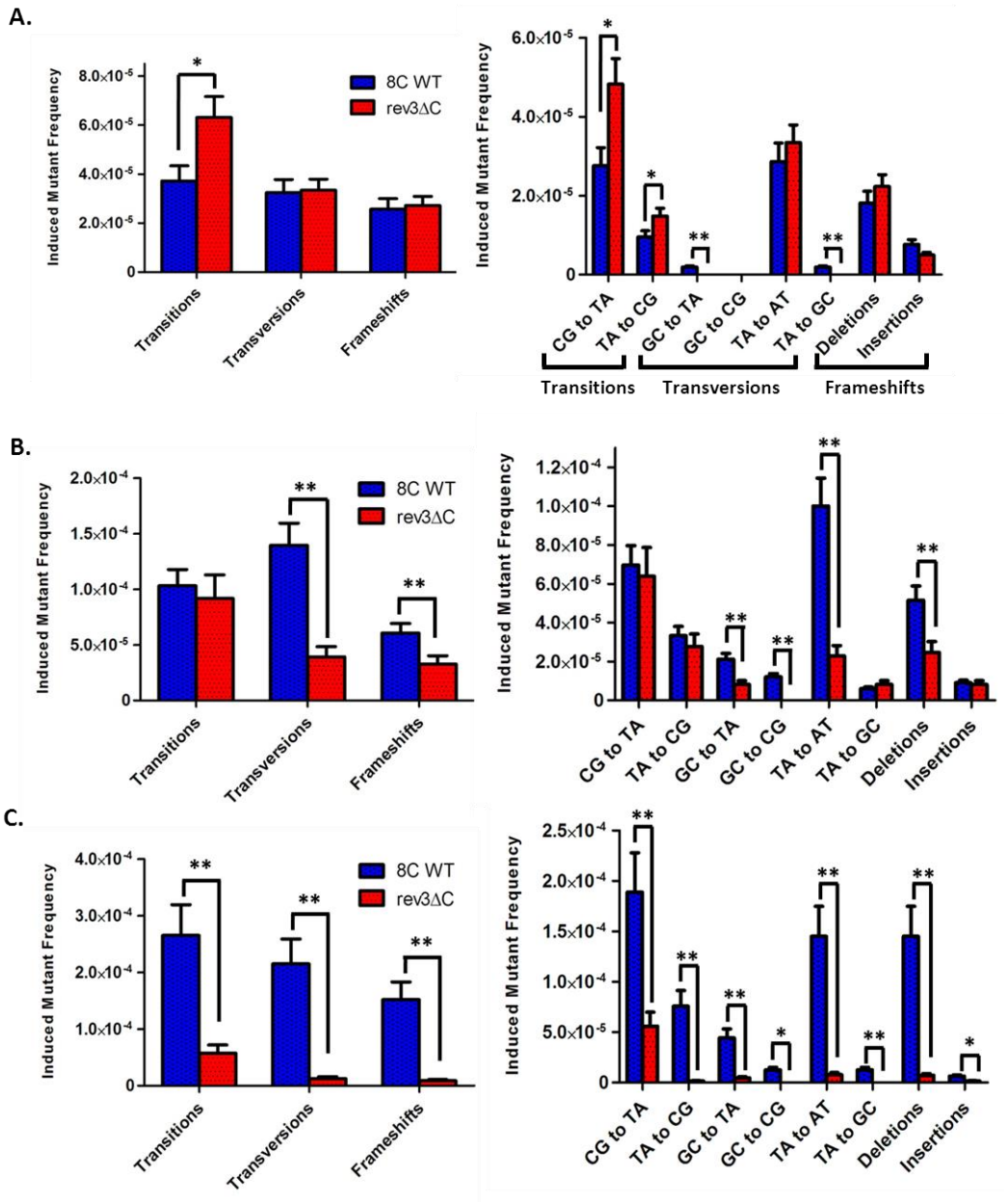

Figure 5.4 *rev3ΔC* has an altered mutational spectrum compared to WT, especially at an intermediate UV dose of 40 J/m^2

A. At 20 J/m^2, *rev3ΔC* spectra showed more transitions than WT but a deficiency in making three of the four types of transversions. **B.** At 40 J/m^2, *rev3ΔC* showed significantly fewer transversions (due to decreases in almost all classes) and frameshifts (due to deletions). **C.** At 60 J/m^2, *rev3ΔC* was highly deficient in all types of mutations compared to WT. All means are averages of four independent trials, Paired Student's t-test, *$p < 0.05$, **$p < 0.01$.

There were decreased frequencies of deletions, insertions, and all six classes of base substitutions (Figure 5.4C). At this high dose, almost exclusively CG to TA transition mutations were detected in *rev3ΔC*. Mutations are shown mapped to *CAN1* in Appendix C, Figure C.3.

5.2.2 Rev3ΔC creates Pol ζ specific complex mutations, albeit at a lower frequency than WT Rev3

Nearly all UV-induced mutations are dependent on Pol ζ, and its mutational signature has been studied *in vitro*. One of the signatures of Pol ζ is the formation of complex mutations. These are defined here as multiple mutations in the same clone within ten base pairs. We found that Rev3ΔC is capable of making complex mutations, but at a lower frequency than WT for all doses studied (Figure 5.5A).

Complex mutations can be broken down into two categories: those that occur in adjacent base pairs (tandem complex mutations) and those that have unchanged bases between the mutations (non-tandem complex mutations). It appears that *rev3ΔC* spectra exhibit a higher proportion of tandem complex mutations than WT, but this difference is only statistically significant at 60 J/m^2 (Fisher's exact test, $p = 0.0182$) (Figure 5.5B).

5.2.3 The majority of mutations in WT and *rev3ΔC* strains occur in dipyrimidine (DP) sites

It is known that UVR induces primarily CPDs and 6-4PPs, both of which occur at dipyrimidine (DP) sequences (TT, CT, TC, CC; discussed in introduction). Correspondingly, the majority of mutations induced by UVR occur in these DP sites. The percentage of mutations found in DPs versus non-DPs was compared between WT and *rev3ΔC* strains, excluding complex mutations from the analysis. In both strains, the

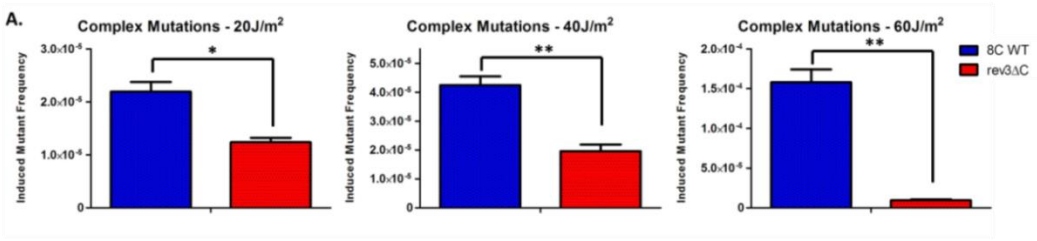

B. **Percentage of Complex Mutations that are Tandem in WT and *rev3ΔC***

	8C	*rev3ΔC*
20 J/m^2	25	44.4
40 J/m^2	28.5	57.1
60 J/m^2	65.5	100

Figure 5.5 *rev3ΔC* creates complex mutations at a lower frequency than WT

A. All means are averages of four independent trials, Paired Student's t-test, *$p < 0.05$, **$p < 0.01$. **B.** Only percentages at 60 J/m^2 were statistical significance at $p = 0.05$, two sample t-test for proportions (Z-test) and Fisher's Exact test.

majority of mutations occurred in DP sites and there was no statistical difference between the two strains (Table 5.1).

Then the proportion of total DP sites that were mutated was determined by taking the number of mutations at DP sites in each strain divided by the total number of DP sites in the *CAN1* gene. The transcribed and non-transcribed DNA strands were analyzed separately. In both strains, a statistically higher proportion of DP sites present in the non-transcribed strand were mutated compared to the transcribed strand at two doses (low and high for WT, intermediate and high for *rev3*Δ*C*) (Table 5.2). There was no significant difference in the proportion of sites mutated between the two strains.

5.2.4 At the highest UV dose, the *rev3*Δ*C* strain shows increased mutagenesis at CC sites compared to WT

For each strain, the different types of DPs (CC, TT, TC, CT) were also analyzed (strands not analyzed separately). First, the percentage of total mutations that were detected at each site was examined. The number of mutations found at each type of DP site were divided by the total number of mutations in the respective spectra. The *rev3*Δ*C* spectrum at 60 J/m^2 showed an increase in the proportion of mutations found at CC sites and a decrease in non-pyrimidine sites compared to WT (Figure 5.6A).

Then the percentage of total DP sites of each type that were mutated was examined. The number of mutations detected of each DP type were divided by the total number of sites of that type present in the *CAN1* gene. Mutations that were found in overlapping sites (example: CTC), where it could not be determined which dimer the affected base was involved in, were analyzed separately (data not shown). *rev3*Δ*C* showed a significant decrease in the proportion of TT sites mutated and an increase in the

Table 5.1 Percentage of mutations occurring in dipyrimidine (DP) sites

UVR Dose	WT	*rev3ΔC*
20 J/m^2	91.4	95.2
40 J/m^2	83.7	88.9
60 J/m^2	85.4	95.6

*complex mutations excluded

Table 5.2: Percent of PD sites mutated in the transcribed and non-transcribed strands

	WT			*rev3ΔC*		
	NTS	TS	p value	NTS	TS	p value
20 J/m^2	6.5	3.1	0.016	5.6	4.1	0.280
40 J/m^2	5.8	3.8	0.168	7.3	2.9	0.003
60 J/m^2	8.1	2.9	0.001	7.3	4.1	0.035

*p values are Z test, NTS – non-transcribed strand, TS – transcribed strand

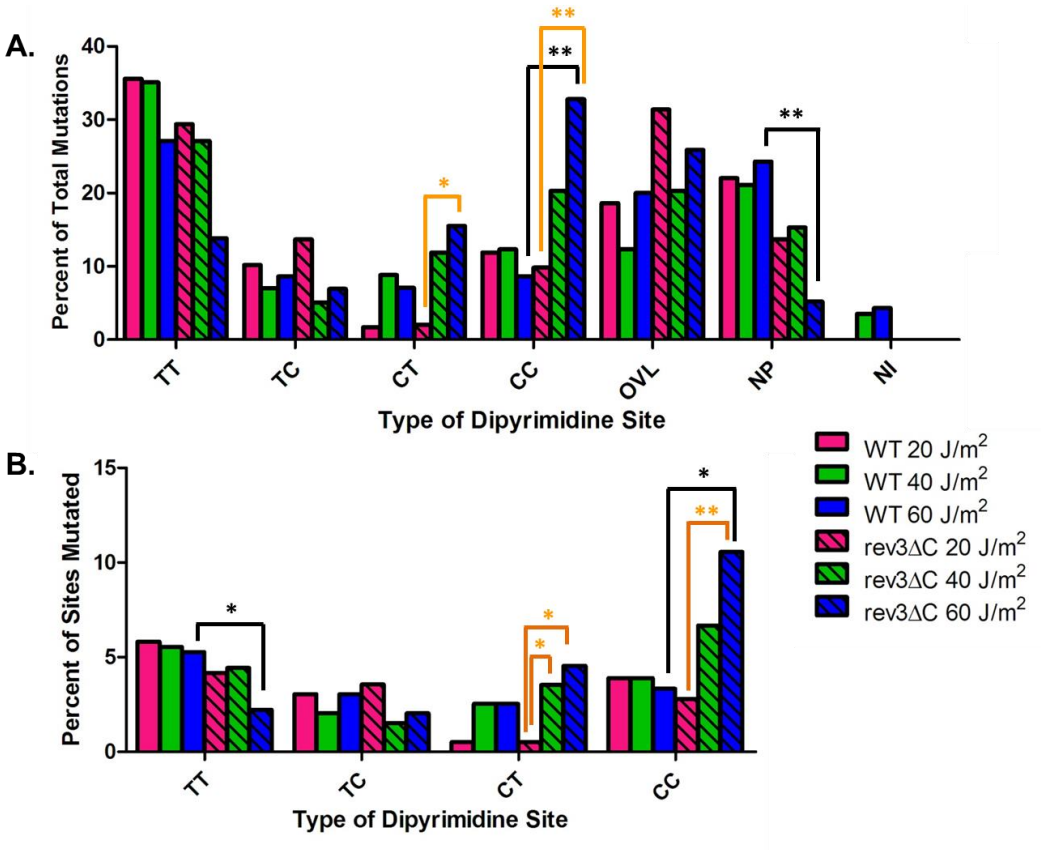

Figure 5.6 Mutations in different classes of DP sites mutated differ according to strain and UVR dose

A. Percent of total mutations found at each type of DP site. Percent = mutations found at each DP type/total number of mutations found in spectrum. The *rev3ΔC* spectrum at 60 J/m^2 showed a higher proportion of mutations in CC sites and a lower proportion in NP sites compared to WT. Within *rev3ΔC*, there was a higher proportion of mutations in CT and CC sites at 60 J/m^2 compared to 20 J/m^2. **B. Percent of total sites of each DP type mutated.** Percent = mutations found in each DP type/total number of sites of that DP type present in the *CAN1* gene. *rev3ΔC* shows a decreased proportion of total TT sites and increased proportion of total CC sites mutated compared to WT. Within *rev3ΔC,* a higher proportion of CT and CC sites were mutated at 60 J/m^2 compared to lower doses. **Key.** Black lines/asterisks - comparison of strains, Orange lines/asterisks - comparison of doses. Open bars - WT data, hashed bars - *rev3ΔC* data. Pink bars - 20 J/m^2, green bars - 40 J/m^2, blue bars - 60 J/m^2. OVL – overlapping DP sites (ex CTC), NP – non-pyrimidine sites, NI – non-identified DP sites. Z-test, * $p < 0.05$, **$p < 0.01$.

proportion of CC sites mutated at 60 J/m^2 compared to WT (Figure 5.6B). A table showing the number of each type of DP site present in *CAN1* is shown in Appendix D.

5.2.5 Different doses of UV irradiation alter the mutational spectra in the *rev3ΔC* strain

The proportions of mutations in different classes (transitions, etc.) and different types of DP sites (TT, etc.) were compared within each strain between the three UV doses used.

WT - There was no significant difference between the proportion of any class of mutation at 20, 40, or 60 J/m^2 (Figure 5.7). There was no significant difference in the percentage of mutations that occurred at DP sites versus non-DP sites between doses (complex mutations alone or all mutations (complex included or excluded); data not shown). There were also no significant differences in the proportion of total mutations that were found in each specific type of DP site (Figure 5.6A) or the proportion of total DP sites of any type that were mutated between the three doses (Figure 5.6B).

rev3ΔC - The *rev3ΔC* strain showed a significantly higher percentage of transition mutations at the highest dose (60 J/m^2) compared to the lowest dose (20 J/m^2) (Figure 5.8). The increase seen in transitions was due to a significant increase specifically in CG to TA transitions (Figure 5.8). There was a decrease in the percentage of TA to CG transitions. There was also a significant decrease in the percentage of TA to AT transversions at the 60 J/m^2 dose compared to 20 J/m^2.

There was no significant difference in the percentage of mutations that occurred at DP sites versus non-DP sites between doses (complex mutations alone or all mutations

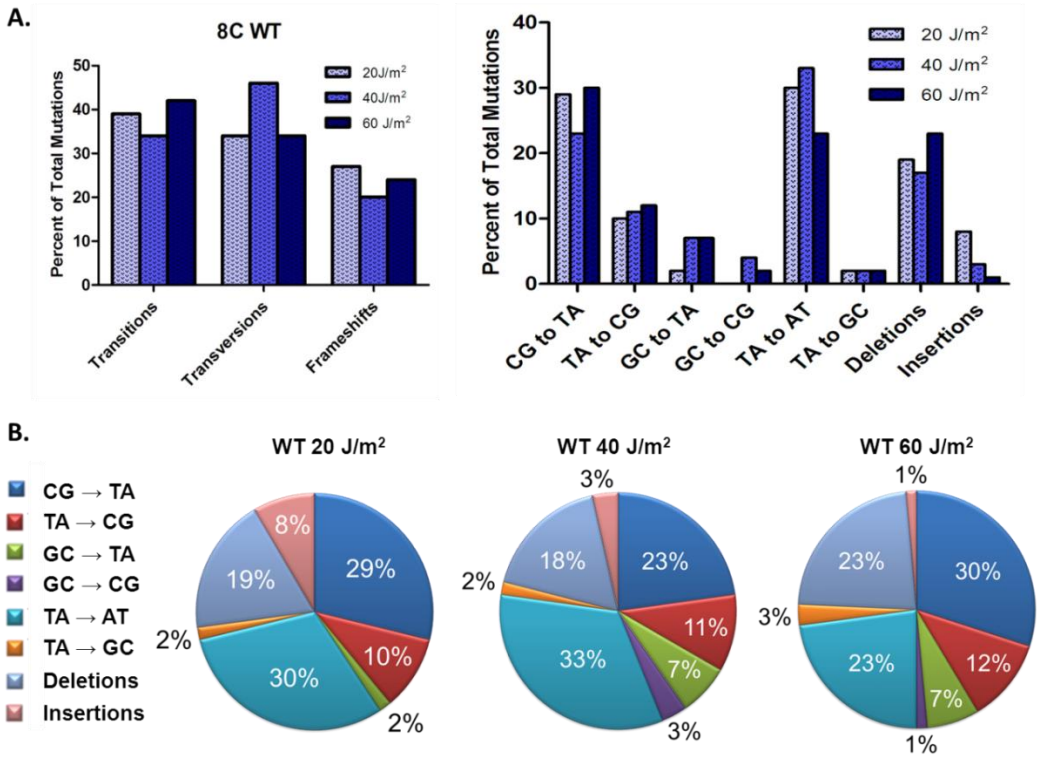

Figure 5.7 Increasing doses of UV irradiation do not alter the *CAN1* mutational spectra in WT yeast cells

Z test and Fisher's Exact test, *p < 0.05, **p < 0.01.

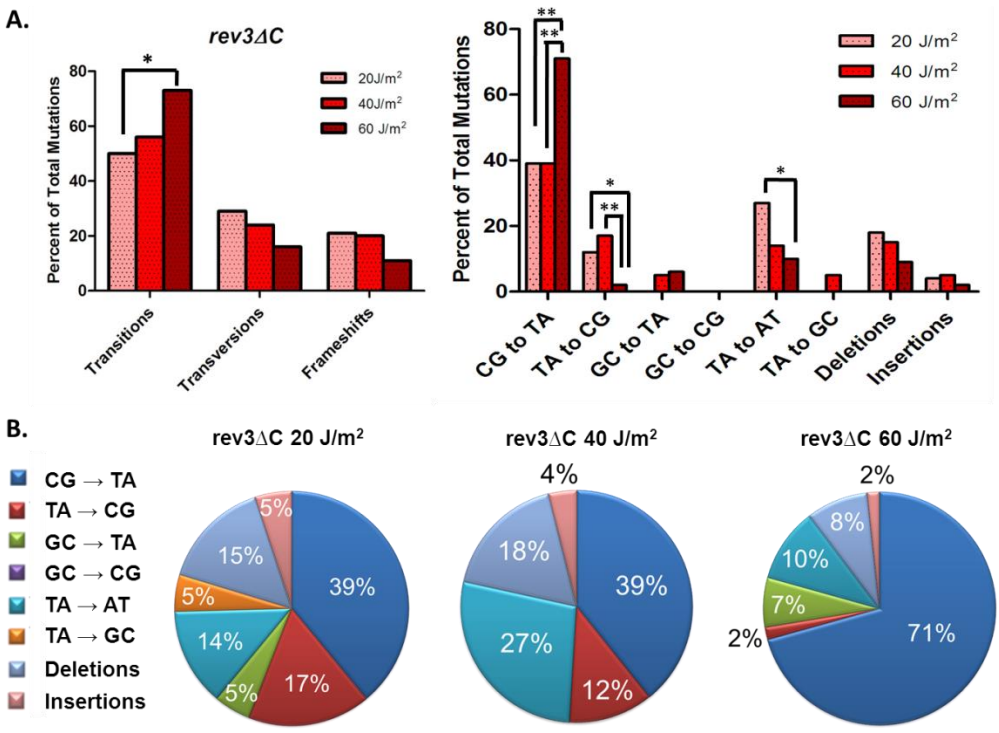

Figure 5.8 Increasing doses of UV irradiation increase the proportion of transitions in *rev3ΔC*

Z test and Fisher's Exact test, *p < 0.05, **p < 0.01.

(complex included or excluded); data not shown), as seen in WT strains. When the specific types of DP sites were compared in *rev3*Δ*C,* there was a significant increase in the proportion of total mutations that occurred in CT and CC sites at 60 J/m^2 (Figure 5.6A). Also, a significantly higher proportion of the total CT and CC sites were mutated at 60 J/m^2 compared to the lower doses (Figure 5.6B).

5.3 Discussion

In this chapter, we asked if the Pol ζ variant present in the *rev3*Δ*C* mutant strain is deficient at participating in all types of mutations, or only certain types in response to UVR. Comparing UV-induced mutational spectra between WT and *rev3*Δ*C* strains can further define the regulatory role of the CTD of Rev3 during TLS. We found that *rev3*Δ*C* shows a strong bias toward making transitions. There is a milder defect with respect to transitions than transversions/frameshifts, and a higher UV dose is needed to elicit this effect. The CTD of Rev3 may normally be involved directly or indirectly in making certain types of mutations (depending on if the CTD modulates the active site of the catalytic polypeptide) or it may allow Pol ζ to be recruited more efficiently to some types of lesions.

5.3.1 Altered mutational spectra in *rev3*Δ*C* compared to WT strains at all doses

Spectra were examined at three different doses to accurately reflect the fact that the severity of the mutagenesis defect of *rev3*Δ*C* strains is dose dependent. At the lowest dose used, 20 J/m^2, *rev3*Δ*C* showed an increase in both classes of transitions (CG to TA and TA to CG) and a decrease in two classes of transversions (GC to TA and TA to GC) compared to WT (Figure 5.4). As a result of these two opposing trends, there was no

difference in the overall mutation frequency between *rev3ΔC* and WT strains at this dose (Figure 5.3).

At the intermediate dose of 40 J/m^2, *rev3ΔC* strains showed about a 50% reduction in total induced mutant frequency (Figure 5.3). This dose was the most discriminatory between the two strains in terms of mutational spectra. The *rev3ΔC* spectrum displayed significantly lower frequencies of all classes of transversions except TA to GC, and had a lower frequency of deletions (Figure 5.4).

At the highest dose, 60 J/m^2, *rev3ΔC* exhibited a six fold reduction in overall induced mutant frequency and was significantly impaired in making/extending from all types of mutations compared to WT (Figures 5.3, 5.4). The defect in transitions was much less severe, and was only apparent at this dose. In fact, 71% of mutations seen in *rev3ΔC* at this dose were CG to TA transitions.

5.3.2 The transition bias of Rev3ΔC

If the spectra between WT and *rev3ΔC* did not differ, it would suggest a general defect in induced mutagenesis, such as a simply less active Pol ζ or a general recruitment defect. However, the differing spectra suggest that the CTD of Rev3 is involved in regulation of TLS in a more specific manner. The decrease seen in overall induced mutant frequencies in *rev3ΔC* strains could be due to the fact that lesions or sequence contexts where transversions usually arise may not be efficiently bypassed by Rev3ΔC. Perhaps Rev3ΔC has more difficulty inserting bases resulting in transversions compared WT and/or Rev3ΔC may be less efficient at extending transversions inserted by other polymerases such as Pol η. Rev3ΔC may be recruited less efficiently to lesions where transversions usually arise.

Structurally speaking, it is reasonable that Rev3ΔC should have less difficulty with transitions because these involve substitution of a two-ring base for a two-ring base, or a one ringed base for a one ringed base. These should be easier to form than transversions which substitute a two-ring structure for a one-ring structure or vice versa. The latter would be more distorting to the double helix of DNA, posing difficulty for both insertion and extension. It is formally possible that Rev3ΔC is an inferior enzyme, so only the simplest mutations to make/extend remain (transitions).

Another possibility is that Rev3ΔC is more proficient at bypassing one of the two major types of UV lesions (discussed in 5.3.4). It will be very important in the future to determine whether the regulatory role of the CTD is in recruitment to DNA or whether it actually affects catalysis. Without a solved structure showing Rev3 with the CTD in the Pol ζ complex, it is not known where the domain lies in relation to the catalytic residues or DNA binding site. Deamination of Cs in 6-4PPs could also be playing a role in this process. If it takes more time for mutations to be addressed by Rev3ΔC, this could allow time for involved C residues to be deaminated to U, resulting in an A incorporation.

5.3.3 Rev3ΔC forms complex mutations at a lower frequency than WT

One of the signatures of Pol ζ is the formation of complex mutations, which are not seen in *rev3*Δ strains [63]. These can occur by a template switching mechanism, or when Pol ζ makes errors/mutations during extension of sequences downstream of the lesion site. They are defined here as multiple mutations in the same clone within ten base pairs, although it has been shown recently that stretches synthesized by Pol ζ can be much longer, up to several hundred nucleotides [38]. In our strains, Rev3ΔC was able to participate in formation of these complex mutations, both tandem and non-tandem, but at

a lower overall frequency than WT (Figure 5.5). It is most likely that Rev3ΔC is equally as proficient at participating in the formation of complex mutations as WT and a lower frequency of them just reflects the lower total induced frequency. This is supported by the fact that the proportion of complex mutations in the strains is not significantly different, even though the total frequencies are.

Sequences of some clones examined in this study had distant mutations separated by 20-1500 bp. These distant mutations were detected in 7 WT and 5 *rev3ΔC* clones total, occurring at all three doses. The distance ranges were similar for both strains: 20-1498 bp for WT and 15-1151 bp for *rev3ΔC*. This could mean that Rev3ΔC can potentially synthesize long stretches of DNA. However this cannot be determined definitively because these events are rare, and at present it is not possible to tell whether these mutations were independent events of long patches or error-prone synthesis after the initial extension.

5.3.4 Comparing spectra at low, intermediate, and high doses of UVR

The differential effects of the *rev3ΔC* mutation at different doses indicate that the mechanisms of TLS might be somewhat different at low and high doses of mutagen exposure. Indeed, it has been shown using bioinformatic approaches that NER proteins, responsible for repair of most UVR-induced lesions, form dose specific interactions/networks in response to different doses of UVR [156]. Another study showed that there was a reversal in the relative sensitivities of yeast cells lacking Pol η or Pol ζ at 40 J/m^2 [147]. Cells lacking Pol ζ were more sensitive at low doses, whereas cells lacking Pol η were more sensitive at higher doses. This role for Pol η in survival at higher doses may reflect the fact that its transcription is induced in response to UVR. There may be a

greater dependence on Pol ζ for tolerating lesions produced by low UV doses. Cells lacking both TLS polymerases had similar mutagenesis levels to *rev3*Δ alone up to 40 J/m^2, then at higher doses the double mutant was more sensitive than either single mutant. This suggests that Pols η and ζ may act together to bypass some UV lesions at lower doses, but in addition Pol ζ can promote UV survival independent of Pol η at higher doses.

This could imply that Rev3ΔC specifically has difficulty efficiently bypassing lesions by itself or with Pol δ (highest dose), but can efficiently take over synthesis from Pol η (lower doses). These data, together with our observations, support the fact that different UVR doses may trigger slightly different repair/tolerance mechanisms in addition to just inducing different levels of DNA damage. It is interesting to note that the dose where we saw the most bias in our spectra is the same dose at which Pol η and ζ contributions seem to shift (40 J/m^2). This dose may represent a certain threshold in cells.

Not all aspects differed depending on the UVR doses used. We compared the effects of the three doses used within each strain, and found that there were no significant differences in any analyses between the WT spectra obtained at each dose (Figure 5.6, Figure 5.7). However, there were some differences in the 60 J/m^2 spectra of *rev3*Δ*C* compared to the lower doses. Transitions were higher in *rev3*Δ*C* at the highest dose compared to the other two; this was due to an increase in CG to TA (Figure 5.8). It appears that Rev3ΔC is deficient in making/extending transversions at high doses, so it compensates through transitions instead.

Most mutations in both strains were found in DP sites, consistent with the fact that most lesions are CPDs or 6-4PPs. It has been shown that CPDs and 6-4PPs are

repaired by separate enzymes [147, 157, 158]. To date, only CPD photolyase has been identified in yeast. Photoreactivation was neither specifically induced nor controlled in our experiments, so it is not clear to what extent CPDs were repaired by this mechanism. 6-4PPs are usually formed preferentially at CC and CT dimers, whereas CPDs are formed at TT [153]. In the data presented here, a higher proportion of total mutations were found in CC sites and a higher proportion of total CC and lower proportion of total TT sites were mutated in *rev3ΔC* at 60 J/m^2 compared to WT (Figure 5.6). Additionally, there was an increase in the proportion of mutations found at CC and CT sites and the proportion of total CC/CT sites mutated at 60 J/m^2 in *rev3ΔC* compared to lower doses. These data may reflect a stronger role for Rev3ΔC in the bypass of 6-4PPs (and deficiency in CPD bypass), especially high doses of UVR.

5.3.5 Comparing spectra determined in this study to earlier studies

Mutation spectra presented here for both strains share many features with *CAN1* spectra reported in the literature. Studies showed that 5-20% of UV induced mutations are frameshifts (discussed in [147]), here the range was 12-17%. The majority of mutations described previously and in our study were base pair substitutions and complex mutations that increase with dose. The spectra were dominated by AT to TA transversions, most mutations were in DP sites, and deletions were more frequent than insertions. As in many spectra, both strains used here showed a higher proportion of mutated sites in the non-transcribed strand than the transcribed strand at multiple doses (Table 5.2). This can be due to differential repair, for example TC-NER increases repair efficiency on the transcribed strand so less mutations may arise on this strand.

Several, though not all, features of these spectra are also consistent with those observed in p53 in human skin cancers. Both spectra (skin tumors and spectra in this study) display a high proportion of CG to TA mutations, but yeast strains used here also have a high proportion of TA to AT which are absent in human cancers. Most CG to TA mutations were C to T and most mutations were present in DPs (83-95% when complex mutations are excluded) depending on the dose. Many of these similarities can be attributed to the fact that the nature of the damage is the same, they also reinforce the relevance of UV spectra measurement and analysis in yeast. Our study also shows that lack of the CTD does not make spectra more dissimilar to human cancers. It is important to note several reasons why the differences seen are present: 1) different genes are being considered (p53 vs. CAN1), 2) photoreactivation in yeast is known to correct CPDs and experiments here did not control for photoreactivation, and 3) skin cancers were exposed to sunlight, a mixture of different wavelengths (see section 5.1), whereas experiments here were done with UVC.

5.3.6 Conclusions

We have shown in this chapter that mutational spectra produced by Pol ζ lacking the CTD (strains with the *rev3*Δ*C* mutation) differ from those produced by WT. *rev3*Δ*C* strains show the strongest defects in making/extending transversions and frameshift mutations, while they are very proficient at transitions at low and intermediate doses. Mutational spectra in *rev3*Δ*C* strains, unlike WT, are altered by increased doses of UVR. Overall, data presented here highlight the fact that the function of the CTD in regulation of TLS may be very intricate, because the absence of CTD of Pol ζ alters specificity of TLS.

6 Conclusions, Discussion, and Future Directions

6.1 Overall Conclusions and Discussion

6.1.1 Functions of the CTD of Rev3

From the genetic studies of *rev3ΔC* presented here, several general functions of the CTD of Rev3 have been revealed. It was found that the CTD of Rev3 is required for efficient mutagenesis at intermediate to high doses of UVR (Figure 3.6). In the absence of the CTD, induced mutagenesis is drastically reduced at 60 J/m^2 and the mutagenesis that remains is dependent on Pol ζ (Figures 3.6, 3.7). At this dose, all classes of mutations were produced at a lower frequency in *rev3ΔC* (Figure 5.4). Despite this clear role of the CTD in regulating UV-induced mutagenesis, it appears not to play a role in the formation of spontaneous mutations by Pol ζ as there was no difference in spontaneous mutation rates between the strains (Table 4.1). Whether or not *rev3ΔC* produces an altered spontaneous mutation spectra has yet to be determined.

When examining UV-induced mutational spectra, it was found that most transversions and frameshifts were dependent on the CTD of Rev3 (Figure 5.4). These types of mutations were decreased at intermediate UV doses in *rev3ΔC* and were nearly lost at the high dose. This suggests that regulation of Pol ζ by the CTD is fine-tuned, as opposed to regulating all or no properties/functions of the enzyme. The CTD is not required for the formation of Pol ζ signature complex mutations, as these are formed at all doses used (Figure 5.5).

Several characteristics of Pol ζ were shown not to depend on the CTD. The CTD does not appear to alter the overall stability of Pol ζ. None of the CTD mutants were

preferentially degraded compared to WT (Figure 3.8). The CTD is not necessary for the TLS transactions dependent on Rev1 or Ub-PCNA, because these proteins are still required in *rev3ΔC* strains (Figure 4.2).

6.1.2 Speculation on specific roles of the CTD

It is clear that the Pol ζ complex containing the Rev3ΔC catalytic subunit (referred to as simply Rev3ΔC) is a functional, yet inferior enzyme. This could be due to many reasons. The CTD may play a role in the level of activity of Pol ζ, through its binding to Pol31/Pol32 or through another unknown regulatory mechanism. Therefore, Rev3ΔC could have lower activity than WT Pol ζ. Another possibility is that the CTD plays a role in recruitment, so in its absence Pol ζ is recruited by a novel mechanism that is less efficient. The mutational spectra analysis may suggest a more specific role of the CTD in the determination of what types of mutations are made. It could be that the CTD assists in bypass of some lesions, but not others. For example, it may be required for assisting in bypass of CPDs but not 6-4 PPs, due to the increase in mutated CT and CC sites in the *rev3ΔC* strain.

Although Pol ζ is required for almost all UV-induced mutations, it is important to keep in mind that Pol η plays a very important and active role in the bypass of UV-induced DNA damage. It was suggested that at low doses of UVR, Pol η and Pol ζ can act together to bypass lesions and at higher doses Pol ζ can do it alone if Pol η is absent [147]. The CTD of Pol ζ may be more critical for the insertion of nucleotides across from lesions, and less so in extension past nucleotides inserted by another polymerase.

6.1.3 Rev3ΔC could be recruited by a novel mechanism

Data presented here raise the possibility that in the absence of the CTD, Pol ζ is recruited by an alternative mechanism. Rev3ΔC lacks strong binding to Pol31/Pol32 similar to Rev3FeS, but has a less severe phenotype (Figure 3.6). Neither can be recruited by the subunit sharing model of polymerase switching (Figure 4.1). It is not clear at this point whether Rev3-FeS is recruited at all.

This potential novel mechanism used in strains with the *rev3ΔC* mutation still requires Pol δ for the switch, as Pol32 is required for mutagenesis in this strain. The mechanism is also dependent on the monoubiquitylation of PCNA and the presence of Rev1 (Figure 4.2). It was hypothesized that this mechanism might be free of some of the regulation that acts on WT Pol ζ. Indeed, Rev3ΔC escapes negative regulation by the ATPase Mgs1 (Figure 4.4). Mgs1 is thought to decrease induced mutagenesis by competing with Pol32 (of Pol ζ, Figure 4.7) at sites of TLS or by shuttling to different branches of the DNA damage tolerance pathway by an unknown mechanism. Regardless of the exact mechanism of negative regulation by Mgs1, Mgs1 does not regulate the Rev3ΔC variant of Pol ζ, highlighting a role for the CTD related to Mgs1. Rev3ΔC is not recruited too promiscuously to DNA, as there was no effect on the spontaneous mutation rate in *rev3ΔC* (Table 4.1). As mentioned, this new mechanism utilized by Rev3ΔC is regulated, though maybe not as harshly as the canonical pathway of WT Pol ζ.

6.1.4 Conclusions about the phenotypes of the *rev3ΔC* mutation

All mutagenesis in *rev3ΔC* strains was dependent on the catalytic activity of Pol ζ; therefore this Rev3ΔC variant is active and recruited to sites of DNA damage (Figure 3.7). The relative extent of activity and recruitment *in vivo* are difficult to estimate.

Despite the negative effect of CTD mutations on induced mutagenesis, none of the CTD mutants studied actively interfere with TLS or are dominant negative to WT Pol ζ (Figure 3.9). When the mutant alleles were grossly overexpressed in the presence of endogenous levels of WT Pol ζ, mutagenesis was present at WT levels. If they negatively impacted any proteins necessary for TLS, some decreased mutagenesis would be expected due to the sheer excess of the mutants over WT in these strains. Additionally, there was no difference in mutagenesis with endogenous levels of *rev3ΔC* vs. overexpression of *rev3ΔC* (Figure 3.8). If it was playing a dominant negative role, overexpression would have decreased mutagenesis even more. The decreased mutagenesis does not seem to be related to a problem with availability of Rev3ΔC, since its overproduction had no effect and there was no effect on spontaneous mutagenesis.

6.1.5 Broader Conclusions

The work detailed here allows for some conclusions affecting the DNA polymerase and TLS fields, outside of just delineating functions of the CTD. Studies of *rev3ΔC* revealed two broader implications, discussed in Chapter 4. The phenotype of *rev3ΔC* shows that Pol ζ activity is not dependent on Pol31/Pol32, though they may affect efficiency. The dependence of Rev3ΔC on Pol32, despite only a possible weak interaction with Pol32 through Rev1, highlights the importance of Pol δ in TLS (Figure 4.2). This role could be in insertion across some types of lesions such as abasic sites, mutation fixation, post-replicative gap filling, or in the regulation of the polymerase switch itself.

The fact that overexpression of Mgs1 eliminates mutagenesis in WT strains, but not *rev3ΔC*, suggests a novel role for Mgs1 as a direct inhibitor of DNA Pol ζ (Figure

4.5). This also argues against the fact that it inhibits Pol δ in TLS, although certainly other studies have shown well that Mgs1 does exhibit several other regulatory effects on Pol δ. This inhibition of Pol ζ suggests another mechanism by which Mgs1 can suppress mutagenic effects of DNA damage tolerance.

6.2 Future Directions Chapter 3

6.2.1 Redox reactivity of polymerase FeS clusters

The FeS cluster present in the CTD of Rev3 has been shown to be required for binding to Pol31, and disruption of this cluster eliminates UV-induced mutagenesis in yeast [78, 81]. This demonstrates that the FeS cluster is important for mutagenesis, though it is not essential because strains lacking the CTD still exhibit mutagenesis (Figure 3.6). One function of this cluster appears to be a structural role in binding to Pol31/Pol32, and this may play a role in polymerase switches if they occur by subunit sharing (Figure 4.1). We hypothesize that a change in the oxidative state of the cluster may trigger dissociation of the catalytic subunits [67]. To test this, aliquots of each purified polymerase could be oxidized and reduced *in vitro,* and binding of Pol3/Rev3 to Pol31/Pol32 could be assessed using native gel electrophoresis or pull-down followed by western blot analysis. This would determine whether redox regulation of the FeS can contribute to subunit switching.

6.2.2 EPR characterization of FeS clusters in human polymerases

There are several types of FeS clusters (Figure 3.4). It has been found using electron paramagnetic resonance (EPR) that yeast B-family polymerases contain [4Fe-4S] type clusters [87]. However, the human enzymes have not been examined as thoroughly,

which is very important for the validity of the yeast model. In preliminary experiments, we purified a complex of the CTD of human p125 (Pol3) with p50/p66 (Pol31/Pol32 in yeast). We confirmed a [4Fe-4S] type cluster using UV-visible spectroscopy and elemental analysis with Inductively Coupled Plasma Mass Spectrometry (ICP-MS); four Fe molecules per complex were present. The same analysis could be performed on the CTD of human Pol ζ and electron paramagnetic resonance (EPR) experiments would confirm biophysically that it behaves like a [4Fe-4S] cluster. EPR would also allow measurement of the redox potential of this cluster to determine if the conditions needed to oxidize/reduce the clusters match conditions present physiologically in cells.

6.2.3 Finding an explanation for the differing phenotypes of *rev3ΔC* and *rev3FeS*

The entire CTD, containing the FeS cluster, has a milder effect on UV-induced mutagenesis than the mutant with a disrupted FeS cluster. Delineating this difference will shed light on the functions of the CTD as a whole and the function of the FeS cluster. It also could reveal a novel recruitment mechanism only seen in the absence of the cluster. The differences in phenotype could be due to the activity levels of the polymerases encoded by *rev3ΔC* and *rev3-FeS*. To examine this, it would be of interest to purify these variants of Pol ζ from yeast. Western blot analysis could be used to confirm whether or not these variants can bind Pol32 through the weak, minor interaction with Rev7 that has been recently proposed. Then the activity of these proteins in *in vitro* primer extension assays on damaged and undamaged templates could be examined. In these assays, a labeled primer with a molecular bumper to prevent random sliding of PCNA is annealed to a template (with or without DNA adducts) and incubated with a polymerase and accessory factors. The products analyzed on a DNA sequencing gel will provide

information on how many nucleotides the polymerase variants added to the labeled primer on a normal or damaged template. The role of accessory factors could also be investigated.

The severity of the *rev3-FeS* phenotype may be due to a lack of recruitment to DNA. This could be assessed in yeast using ChIP assays to see if *rev3-FeS* is present on the DNA. This will be compared to *rev3*Δ*C*, which we know is recruited but to an unknown extent. Pol ζ is present at low levels in cells, so both variants would need to be overexpressed. If this approach would be unsuccessful, an alternative method could be to attempt pulldown of Rev3 variants with PCNA and probe for Pol ζ using western blot analysis. This approach would be informative because TLS polymerases are thought bind PCNA when it is present on DNA.

6.2.4 Studying the phenotypes of *rev3*Δ*C* with other mutagens

The intermediate trend of mutagenesis in *rev3*Δ*C* could be confirmed using other mutagens, such as MMS, to see whether its effect is UVR specific. Furthermore, it is known that absence of Pol ζ can lead to formation of chromosomal rearrangements [54], which could be in part be due to its role in the repair of DSBs caused by ICLs. Mutagenesis in *rev3*Δ*C* strains capable of detecting chromosomal rearrangements in response to agents that cause ICLs, such as cisplatin or mitomycin C, could be measured to determine if this mutant could represent a "happy medium": proficient at ICL bypass to help prevent chromosomal rearrangements while making fewer point mutations.

6.3 Future directions Chapter 4

6.3.1 The subunit sharing DNA polymerase switch model

A key step in the subunit sharing model of polymerase switching (from Pol δ to Pol ζ) during TLS is Pol31/Pol32 remaining on the DNA/PCNA once Pol3 has dissociated (Figure 4.1). To test this model, fluorescence resonance energy transfer (FRET) could be utilized (Figure 6.1). In this system, a donor fluorophore (e.g. Cy3) on one molecule is excited and emits a wavelength that excites an acceptor fluorophore (Cy5) on a second molecule (that is in very close proximity) (Figure 6.1A). Typically Cy3 emission is seen when the two partner molecules are unbound, and Cy5 emission is seen when they are bound.

The situation with Pol δ would be more complicated because FeS clusters like the one present in Pol3 are strong quenchers of fluorescence. In a hypothetical future experiment, Cy3 could be attached to a DNA template downstream from a damaged site and Cy5 could be attached to Pol31. Then DNA synthesis reactions would be monitored by FRET at the single molecule level. If the model is correct, a spectra resembling Figure 6.1B could be expected. When Pol δ is not bound to DNA, only Cy3 fluorescence could be seen (Figure 6.1C). When Pol δ binds DNA, the FeS cluster of Pol3 could be close enough to quench Cy3 and there would be no signal (Figure 6.1D). Finally, if only Pol31/Pol32 remain bound to DNA, Cy3 could excite Cy5 and only Cy5 emission would be seen (Figure 6.1E). This is only a general scheme, more fine details would need to be worked out before performing this complicated analysis. For example, one limitation could be that if Pol ζ is needed to displace the catalytic subunit of Pol δ, Pol ζ would also quench the signal.

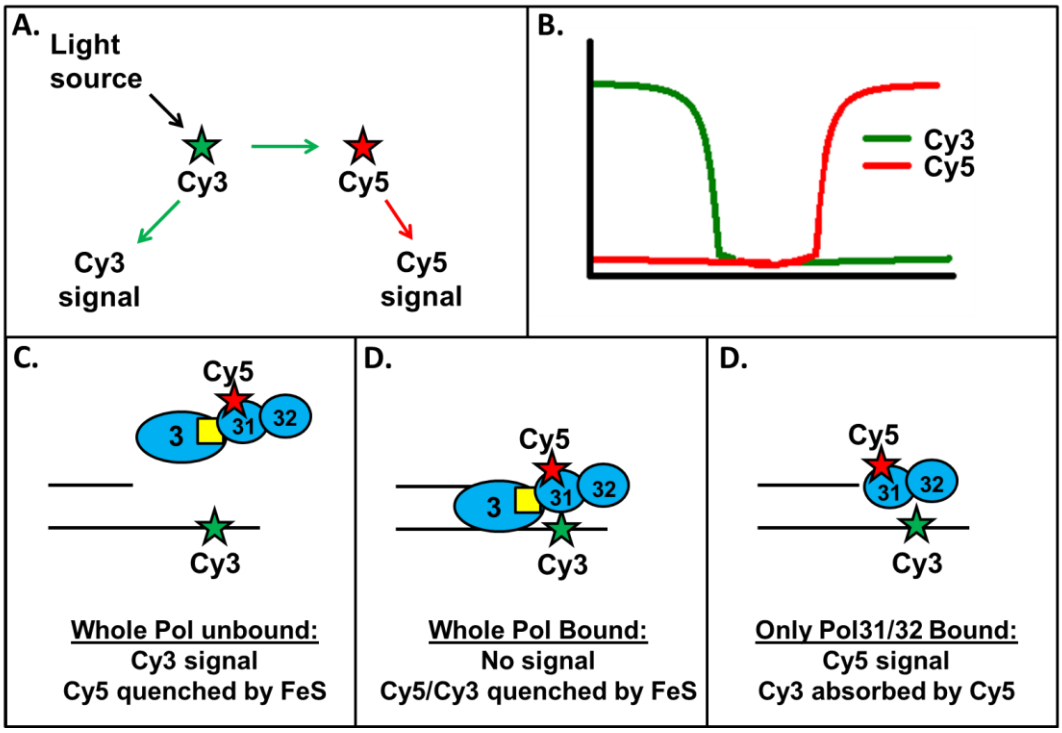

Figure 6.1 Scheme to test subunit sharing model of polymerase switch using FRET

Key: "3" indicates either Pol3 or Rev3, "31" indicates Pol31, and "32" indicates Pol32. **A.** Theory behind FRET. The light source activates a donor chromophore, which emits a wavelength that can activate an acceptor if they are in close proximity (such as two bound proteins). **B.** Theoretical FRET curves over time if Pol3/Rev3 can leave the DNA without Pol31/Pol32. **C-D.** Breakdown of each type of FRET signal in this experiment.

6.3.2 Direct inhibition of Pol ζ synthesis by Mgs1

Overexpression of Mgs1 in yeast inhibited induced mutagenesis only in strains with WT Pol ζ (Figure 4.5). To further investigate this inhibition, Mgs1 could be purified and it effect will be studied using primer extension assays *in vitro*. Reaction components could include Ub-PCNA, polymerase (Pol δ, Pol ζ WT, or Pol ζ Rev3ΔC), dNTPs, primed DNA template, and Mgs1. First all components could be added to the reaction simultaneously to see if Mgs1 will have an effect on primer elongation by the polymerase. Then in separate samples, Mgs1 could be pre-incubated with the other components prior to addition of the polymerase. We hypothesize that Pol δ activity would be unaffected or very slightly affected, but primer extension by WT Pol ζ would be inhibited because Mgs1 can outcompete Pol32 of Pol ζ for binding to Ub-PCNA. This would support our previous hypothesis that Mgs1 can only compete with Pol32 bound to Pol ζ and not Pol δ. We would expect to see no effect on Rev3ΔC, because it lacks a strong interaction with Pol31/Pol32 and there was no effect of *MGS1* overexpression *in vivo*.

6.3.3 Cellular context for Mgs1 inhibition of Pol ζ

It is unknown under what *in vivo* conditions this negative regulatory effect of Mgs1 on Pol ζ/TLS occurs. It has been shown that deletion of Mgs1 elevates spontaneous reversion mutations, while having no effect on induced mutagenesis [110]. Therefore Mgs1 may inhibit dangerous TLS in the absence of damage. We were unable to confirm this result using forward mutations in *CAN1*, so spontaneous mutagenesis rates in *mgs1*Δ mutant strains could be measured using the *ade2-1* nonsense reporter analogous to the reporter used in [105], which allow for detection of a small subset of mutations.

Furthermore, TLS is thought to occur by two non-mutually exclusive models. In one model, TLS occurs at the fork during S-phase and in the other it helps fill post-replicative gaps during the G2 phase. To determine if Mgs1 could play a larger role during one of these types of TLS, mRNA expression levels could be measured throughout the cell cycle in synchronized yeast cultures.

6.4 Future Directions Chapter 5

6.4.1 Effect of photoreactivation on mutagenesis in WT and *rev3*Δ*C* strains

UV light primarily induces CPDs and 6-4PPs. Differences in the roles of Pol η and Pol ζ were seen when yeast plates were incubated in the presence or absence of light [147], because CPDs are more readily corrected by photoreactivation than are 6-4PPs. The spectra presented here were collected from mutants grown uncovered, but in a somewhat shaded incubator. It appeared that *rev3*Δ*C* showed higher proportions of mutations at CC and CT sites as the dose was increased, which could indicate a more prominent role of 6-4PPs in mutagenesis in this strain. To compare the effect of these two separate types of damage between strains and between doses, additional spectra could be obtained with plates grown in the presence or absence of photoreactivation. Also, WT and *rev3*Δ*C* strains could be transformed with plasmids containing a CPD or a 6-4PP and then examined for bypass as was done in [148]. Substrates would be gapped double stranded plasmids designed as in [148].

6.4.2 Spontaneous mutational spectra in *rev3*Δ*C* during DRIM

Strains with *rev3*Δ*C* showed altered mutational spectra in response to UV damage, even at 20 J/m^2 where the total induced mutant frequency was equivalent to WT

(Figure 5.4). Therefore, spontaneous mutation spectra could be collected and analyzed to compare WT and *rev3*Δ*C*. This will help determine if the partial *rev3*Δ*C* deficiency is occurring only when recruited to damage sites, or also during replication stalling without damage such as during defective replisome induced mutagenesis (DRIM) [48]. The latter condition would be provoked by the addition of hydroxyurea (HU) or the use of replicative DNA polymerase mutants.

6.4.3 Ability of *rev3*Δ*C* to prevent chromosome rearrangements in mammalian cells

Eventually, this work should be continued in mammalian cells. It was shown in MEFs that the deletion of *REV3L* results in elevation of gross chromosomal rearrangements [54]. *rev3*Δ*C* yeast strains produce some types of mutations proficiently (transitions), but not others, and has a lower total frequency of induced mutagenesis than WT. Therefore, we want to investigate if a human variant of Rev3ΔC can accomplish bypass preventing chromosomal instability, while being more deficient at detrimental bypass such as the formation of point mutations. To test this, mouse *REV3L*Δ*C* would be expressed from a vector in Pol ζ-deficient MEFs and mutation frequency would be measured to see if it was decreased. Chromosome spreads would be examined to look at ploidy, translocations, double minutes, and other chromosomal anomalies.

7 References

[1] T. Lindahl, Instability and decay of the primary structure of DNA, Nature, 362 (1993) 709-715.

[2] E.C. Friedberg, G.C. Walker, W. Siede, R.D. Wood, R.A. Schultz, T. Ellenberger, DNA repair and mutagenesis, 2 ed., ASM Press, Washington D.C., 2006.

[3] J.H.J. Hoeijmakers, DNA damage, aging, and cancer, New England Journal of Medicine, 361 (2009) 1475-1485.

[4] G. Ghosal, J. Chen, DNA damage tolerance: A double-edged sword guarding the genome, Transl Cancer Res, 2 (2013) 107-129.

[5] D. Hanahan, R.A. Weinberg, Hallmarks of cancer: The next generation, Cell, 144 (2011) 646-674.

[6] H. Shiwaku, H. Okazawa, Impaired DNA damage repair as a common feature of neurodegenerative diseases and psychiatric disorders, Current Molecular Medicine, 15 (2015) 119-128.

[7] Y.I. Pavlov, P.V. Shcherbakova, I.B. Rogozin, Roles of DNA polymerases in replication, repair, and recombination in eukaryotes, International Review of Cytology, 255 (2006) 41-132.

[8] S. Boiteux, S. Jinks-Robertson, DNA repair mechanisms and the bypass of DNA damage in *Saccharomyces cerevisiae*, Genetics, 193 (2013) 1025-1064.

[9] L.S. Waters, B.K. Minesinger, M.E. Wiltrout, S. D'Souza, R.V. Woodruff, G.C. Walker, Eukaryotic translesion polymerases and their roles and regulation in DNA damage tolerance, Microbiol Mol Biol Rev, 73 (2009) 134-154.

[10] S. Sharma, C.E. Canman, Rev1 and DNA polymerase ζ in DNA intrastrand crosslink repair, Environ Mol Mutagen, 53 (2012) 725-740.

[11] M.J. Longley, M.A. Graziewiez, R.J. Bienstock, W.C. Copeland, Consequences of mutations in human DNA polymerase γ, Gene, 354 (2005) 125-131.

[12] M.F. White, M.S. Dillingham, Iron-sulphur clusters in nucleic acid processing enzymes, Curr Opin Struct Biol, 22 (2012) 94-100.

[13] A. Aguilera, B. Gomez-Gonzalez, Genome instability: A mechanistic view of its causes and consequences, Nat Rev Genet, 9 (2008) 204-217.

[14] C. Colussi, E. Parlanti, D. Degan, E. Aquilina, D. Barnes, P. Macpherson, P. Karran, M. Crescenzi, E. Dogliotti, The mammalian mismatch repair pathway removes DNA 8-oxodGMP incorporated from the oxidized dntp pool, Current Biology, 12 (2002) 912-918.

[15] S. Boiteux, L. Gellon, N. Guibourt, Repair of 8-oxoguanine in *Saccharomyces cerevisiae*: Interplay of DNA repair and replication mechanisms, Free Radical Biology and Medicine, 32 (2002) 1244-1253.

[16] H. Saribasak, D. Rajagopal, R.W. Maul, P.J. Gearhart, Hijacked DNA repair proteins and unchained DNA polymerases, Philos Trans R Soc Lond B Biol Sci, 364 (2009) 605-611.

[17] D.O. Zharkov, Base excision DNA repair, Cell Mol Life Sci, 65 (2008) 1544-1565.

[18] M. Garcia-Diaz, K. Bebenek, Multiple functions of DNA polymerases, CRC Crit Rev Plant Sci, 26 (2007) 105-122.

[19] O.D. Scharer, Nucleotide excision repair in eukaryotes, Cold Spring Harb Perspect Biol, 5 (2013) a012609.

[20] R.P. Sinha, D. Hader, UV-induced DNA damage and repair: A review, The Royal Society of Chemistry and Owner Societies, 1 (2002) 225-236.

[21] P. Modrich, Mechanisms in eukaryotic mismatch repair, J Biol Chem, 281 (2006) 30305-30309.

[22] B.D. Harfe, S. Jinks-Robertson, DNA mismatch repair and genetic instability, Annu. Rev. Genet., 34 (2000) 359-399.

[23] N. Papadopoulos, A. Lindblom, Molecular basis of HNPCC: Mutations of mmr genes, Human Mutation, 10 (1997) 89-99.

[24] C. Clauson, O.D. Scharer, L. Niedernhofer, Advances in understanding the complex mechanisms of DNA interstrand crosslink repair, Cold Spring Harb Perspect Med, 3 (2013) 1-32.

[25] C.S. Walsh, Two decades beyond BRCA1/2: Homologous recombination, hereditary cancer risk and a target for ovarian cancer therapy, Gynecol Oncol, 137 (2015) 343-350.

[26] G.L. Moldovan, B. Pfander, S. Jentsch, PCNA, the maestro of the replication fork, Cell, 129 (2007) 665-679.

[27] D. Branzei, Ubiquitin family modifications and template switching, FEBS Lett, 585 (2011) 2810-2817.

[28] E.C. Friedberg, Suffering in silence: The tolerance of DNA damage, Nat Rev Mol Cell Biol, 6 (2005) 943-953.

[29] H. Ohmori, E.C. Friedberg, R.P.P. Fuchs, M.F. Goodman, F. Hanaoka, D. Hinkle, T.A. Kunkel, C.W. Lawrence, Z. Livneh, T. Nohmi, L. Prakash, S. Prakash, T.

Todo, G.C. Walker, Z. Wang, R. Woodgate, The Y-family of DNA polymerases, Molecular Cell, 8 (2001) 7-8.

[30] V. Pages, R.P.P. Fuchs, How DNA lesions are turned into mutations within cells?, Oncogene, 21 (2002) 8957-8966.

[31] W. Yang, Portraits of a Y-family DNA polymerase, FEBS Lett, 579 (2005) 868-872.

[32] S. Prakash, R.E. Johnson, L. Prakash, Eukaryotic translesion synthesis DNA polymerases: Specificity of structure and function, Annu Rev Biochem, 74 (2005) 317-353.

[33] J.E. Sale, Translesion DNA synthesis and mutagenesis in eukaryotes, Cold Spring Harb Perspect Biol, 5 (2013) a012708.

[34] Z. Livneh, O. Z, S. Shachar, Multiple two-polymerase mechanisms in mammalian translesion DNA synthesis, Cell Cycle, 9 (2014) 729-735.

[35] G.N. Gan, J.P. Wittschieben, B.O. Wittschieben, R.D. Wood, DNA polymerase ζ (pol ζ) in higher eukaryotes, Cell Res, 18 (2008) 174-183.

[36] J.E. Stone, D. Kumar, S.K. Binz, A. Inase, S. Iwai, A. Chabes, P.M. Burgers, T.A. Kunkel, Lesion bypass by *S. cerevisiae* pol ζ alone, DNA Repair (Amst), 10 (2011) 826-834.

[37] A.R. Lehmann, R.P. Fuchs, Gaps and forks in DNA replication: Rediscovering old models, DNA Repair (Amst), 5 (2006) 1495-1498.

[38] O.V. Kochenova, D.L. Daee, T.M. Mertz, P.V. Shcherbakova, DNA polymerase ζ-dependent lesion bypass in *Saccharomyces cerevisiae* is accompanied by error-prone copying of long stretches of adjacent DNA, PLOS Genetics, (2015) epub ahead of print.

[39] H.D. Ulrich, How to activate a damage-tolerant polymerase, Cell Cycle, 3 (2014) 14-17.

[40] V. Pages, A. Bresson, N. Acharya, S. Prakash, R.P. Fuchs, L. Prakash, Requirement of Rad5 for DNA polymerase ζ-dependent translesion synthesis in *Saccharomyces cerevisiae*, Genetics, 180 (2008) 73-82.

[41] S. Prakash, L. Prakash, Translesion DNA synthesis in eukaryotes: A one- or two-polymerase affair, Genes & Development, 16 (2002) 1872-1883.

[42] P. Stelter, H.D. Ulrich, Control of spontaneous and damage-induced mutagenesis by SUMO and ubiquitin conjugation, Nature, 425 (2003) 188-191.

[43] H.D. Ulrich, Deubiquitinating PCNA: A downside to DNA damage tolerance, Nature Cell Biology, 8 (2006) 303-305.

[44] T.T. Huang, A.D. D'Andrea, Regulation of DNA repair by ubiquitylation, Nat Rev Mol Cell Biol, 7 (2006) 323-334.

[45] C.W. Lawrence, V.M. Maher, Mutagenesis in eukaryotes dependent on DNA polymerase ζ and Rev1p, Phil. Trans. R. Soc. Lond., 356 (2001) 41-46.

[46] X. Zhong, P. Garg, C.M. Stith, S.A. Nick McElhinny, G.E. Kissling, P.M. Burgers, T.A. Kunkel, The fidelity of DNA synthesis by yeast DNA polymerase ζ alone and with accessory proteins, Nucleic Acids Res, 34 (2006) 4731-4742.

[47] M.R. Northam, P. Garg, D.M. Baitin, P.M. Burgers, P.V. Shcherbakova, A novel function of DNA polymerase ζ regulated by PCNA, The EMBO Journal, 25 (2006) 4316-4325.

[48] M.R. Northam, H.A. Robinson, O.V. Kochenova, P.V. Shcherbakova, Participation of DNA polymerase ζ in replication of undamaged DNA in *Saccharomyces cerevisiae*, Genetics, 184 (2010) 27-42.

[49] M.R. Northam, E.A. Moore, T.M. Mertz, S.K. Binz, C.M. Stith, E.I. Stepchenkova, K.L. Wendt, P.M. Burgers, P.V. Shcherbakova, DNA polymerases ζ and Rev1 mediate error-prone bypass of non-B DNA structures, Nucleic Acids Res, 42 (2014) 290-306.

[50] P.A. Auerbach, B. Demple, Roles of Rev1, pol ζ, Pol32 and pol η in the bypass of chromosomal abasic sites in *Saccharomyces cerevisiae*, Mutagenesis, 25 (2010) 63-69.

[51] A.V. Makarova, P.M. Burgers, Eukaryotic DNA polymerase ζ, DNA Repair (Amst), (2015).

[52] P.A. Knobel, T.M. Marti, Translesion DNA synthesis in the context of cancer research, Cancer Cell International, 11 (2011) 1-19.

[53] L.J. Stallons, W.G. McGregor, Translesion synthesis polymerases in the prevention and promotion of carcinogenesis, Journal of Nucleic Acids, (2010) 1-10.

[54] J.P. Wittschieben, S.C. Reshmi, S.M. Gollin, R.D. Wood, Loss of DNA polymerase ζ causes chromosomal instability in mammalian cells, Cancer Res, 66 (2006) 134-142.

[55] F. Wu, X. Lin, T. Okuda, S. Howell, DNA polymerase ζ regulates cisplatin cytotoxicity, mutagenicity, and development of cisplatin resistance, Cancer Research, 64 (2004) 8029-8035.

[56] Y.I. Pavlov, P.V. Shcherbakova, T.A. Kunkel, *In vivo* consequences of putative active site mutations in yeast DNA polymerases α, ε, δ, and ζ, Genetics, 159 (2001) 47-64.

[57] P.M. Burgers, Overexpression of multisubunit replication factors in yeast, METHODS: A Companion to Methods in Enzymology, 18 (1999) 349-355.

[58] H. Liu, J.H. Naismith, An efficient one-step site-directed deletion, insertion, single and multiple-site plasmid mutagenesis protocol, BMC Biotechnol, 8 (2008) 91.

[59] I. Saugar, J.L. Parker, S. Zhao, H.D. Ulrich, The genome maintenance factor Mgs1 is targeted to sites of replication stress by ubiquitylated PCNA, Nucleic Acids Res, 40 (2012) 245-257.

[60] P. Garg, C.M. Stith, J. Majka, P.M. Burgers, Proliferating cell nuclear antigen promotes translesion synthesis by DNA polymerase ζ, J Biol Chem, 280 (2005) 23446-23450.

[61] J.R. Nelson, C.W. Lawrence, D. Hinkle, Thymine-thymine dimer bypass by yeast DNA polymerase ζ, Science, 272 (1996) 1646-1649.

[62] T.L. Orr-Weaver, J.W. Szostak, Yeast recombination: The association between double-strand gap repair and crossing-over, PNAS, 80 (1983) 4417-4421.

[63] S.G. Kozmin, Y.I. Pavlov, T.A. Kunkel, E. Sage, Roles of *Saccharomyces cerevisiae* DNA polymerases polη and polζ in response to irradiation by simulated sunlight, Nucleic Acids Res, 31 (2003) 4541-4552.

[64] M.D. Rose, F. Winston, P. Hieter, Methods in yeast genetics, Cold Spring Harbor Laboratory Press, Cold Spring Harbor, NY, 1990.

[65] J.W. Drake, A constant rate of spontaneous mutation in DNA-based microbes, PNAS, 88 (1991) 7160-7164.

[66] W.J. Dixon, F.J. Massey, Introduction to statistical analysis, McGraw-Hill, NY, 1969.

[67] I.S. Waisertreiger, V.G. Liston, M.R. Menezes, H.M. Kim, K.S. Lobachev, E.I. Stepchenkova, T.H. Tahirov, I.B. Rogozin, Y.I. Pavlov, Modulation of mutagenesis in eukaryotes by DNA replication fork dynamics and quality of nucleotide pools, Environ Mol Mutagen, 53 (2012) 699-724.

[68] K. Bebenek, T.A. Kunkel, Family growth: The eukaryotic DNA polymerase revolution, Cell. Mol. Life Sci., 59 (2002) 54-57.

[69] P.V. Shcherbakova, K. Bebenek, T.A. Kunkel, Functions of eukaryotic DNA polymerases, science of Aging Knowledge Environment, (2003) 1-11.

[70] Y.I. Pavlov, P.V. Shcherbakova, DNA polymerases at the eukaryotic fork-20 years later, Mutat Res, 685 (2010) 45-53.

[71] T.A. Kunkel, P.M. Burgers, Delivering nonidentical twins, Nat Struct Mol Biol, 21 (2014) 649-651.

[72] T.A. Kunkel, P.M. Burgers, Dividing the workload at a eukaryotic replication fork, Trends Cell Biol, 18 (2008) 521-527.

[73] M.R. Northam, H.A. Robinson, O.V. Kochenova, P.V. Shcherbakova, Participation of DNA polymerase ζ in replication of undamaged DNA in *Saccharomyces cerevisiae*, Genetics, 184 (2010) 27-42.

[74] T.A. Kunkel, DNA replication fidelity, Journal of Biological Chemistry, 279 (2004) 16895-16898.

[75] T.H. Tahirov, Structure and function of eukaryotic DNA polymerase δ, Subcell Biochem, 62 (2012) 217-236.

[76] K. Hirota, K. Yoshikiyo, G. Guilbaud, T. Tsurimoto, J. Murai, M. Tsuda, L.G. Phillips, T. Narita, K. Nishihara, K. Kobayashi, K. Yamada, J. Nakamura, Y. Pommier, A. Lehmann, J.E. Sale, S. Takeda, The pold3 subunit of DNA polymerase δ can promote translesion synthesis independently of DNA polymerase ζ, Nucleic Acids Res, 43 (2015) 1671-1683.

[77] K.J. Gerik, X. Li, A. Pautz, P.M. Burgers, Characterization of the two small subunits of *Saccharomyces cerevisiae* DNA polymerase δ, 273 (1998) 19747-19755.

[78] A.G. Baranovskiy, A.G. Lada, H.M. Siebler, Y. Zhang, Y.I. Pavlov, T.H. Tahirov, DNA polymerases delta and zeta switch by sharing accessory subunits of DNA polymerase delta, Journal of Biological Chemistry, 287 (2012) 17281-17287.

[79] Y. Lee, M.T. Gregory, W. Yang, Human pol ζ purified with accessory subunits is active in translesion DNA synthesis and complements pol η in cisplatin bypass, PNAS, 111 (2014) 2954-2959.

[80] R.E. Johnson, L. Prakash, S. Prakash, Pol31 and Pol32 subunits of yeast DNA polymerase δ are also essential subunits of DNA polymerase ζ, Proc Natl Acad Sci U S A, 109 (2012) 12455-12460.

[81] A.V. Makarova, J.L. Stodola, P.M. Burgers, A four-subunit DNA polymerase ζ complex containing pol δ accessory subunits is essential for PCNA-mediated mutagenesis, Nucleic Acids Res, 40 (2012) 11618-11626.

[82] L.D. Langston, M. O'Donnell, Subunit sharing among high- and low-fidelity DNA polymerases, Proc Natl Acad Sci U S A, 109 (2012) 12268-12269.

[83] A.G. Baranovskiy, N.D. Babayeva, V.G. Listen, I.B. Rogozin, E.V. Koonin, Y.I. Pavlov, D.G. Vassylyev, T.H. Tahirov, X-ray structure of the complex of regulatory subunits of human DNA polymerase δ, Cell Cycle, 7 (2008) 3026-3036.

[84] T.H. Tahirov, Structure and function of eukaryotic DNA polymerase δ, Subcell Biochem, 62 (2012) 217-236.

[85] Y. Gomez-Llorente, R. Malik, R. Jain, J.R. Choudhury, R.E. Johnson, L. Prakash, S. Prakash, I. Ubarretxena-Belandia, A.K. Aggarwal, The architecture of yeast DNA polymerase ζ, Cell Rep, 5 (2013) 79-86.

[86] S. Klinge, R. Nunez-Ramirez, O. Llorca, L. Pellegrini, 3D architecture of DNA pol α reveals the functional core of multi-subunit replicative polymerases, EMBO J, 28 (2009) 1978-1987.

[87] D.J. Netz, C.M. Stith, M. Stumpfig, G. Kopf, D. Vogel, H.M. Genau, J.L. Stodola, R. Lill, P.M. Burgers, A.J. Pierik, Eukaryotic DNA polymerases require an iron-sulfur cluster for the formation of active complexes, Nat Chem Biol, 8 (2012) 125-132.

[88] B. Py, P.L. Moreau, F. Barras, Fe-S clusters, fragile sentinels of the cell, Curr Opin Microbiol, 14 (2011) 218-223.

[89] D.C. Johnson, D.R. Dean, A.D. Smith, M.K. Johnson, Structure, function, and formation of biological iron-sulfur clusters, Annu Rev Biochem, 74 (2005) 247-281.

[90] K. Brzoska, S. Meczynska, M. Kruszewski, Iron-sulfur cluster proteins: Electron transfer and beyond, Acta Biochimica Polonica, 53 (2006) 685-691.

[91] W.I. Whelan, E. Gocke, T.R. Manney, The *CAN1* locus of *Saccharomyces cerevisiae*: Fine-structure analysis and forward mutation rates, Genetics, 91 (1979) 35-51.

[92] T.H. Tahirov, K.S. Makarova, I.B. Rogozin, Y.I. Pavlov, E.V. Koonin, Evolution of DNA polymerases: An inactivated polymerase-exonuclease module in pol ε and a chimeric origin of eukaryotic polymerases from two classes of archaeal ancestors, Biol Direct, 4 (2009) 11.

[93] H.M. Siebler, A.G. Lada, A.G. Baranovskiy, T.H. Tahirov, Y.I. Pavlov, A novel variant of DNA polymerase ζ, rev3ΔC, highlights differential regulation of Pol32 as a subunit of polymerase δ versus ζ in *Saccharomyces cerevisiae*, DNA Repair (Amst), 24 (2014) 138-149.

[94] A. Umar, A.B. Buermeyer, J.A. Simon, D.C. Thomas, A.B. Clark, R.M. Liskay, T.A. Kunkel, Requirement for PCNA in DNA mismatch repair at a step preceding DNA resynthesis, Cell, 87 (1996) 65-73.

[95] L. Haracska, C.A. Torres-Ramos, R.E. Johnson, S. Prakash, L. Prakash, Opposing effects of ubiquitin conjugation and SUMO modification of PCNA on replicational bypass of DNA lesions in *Saccharomyces cerevisiae*, Molecular and Cellular Biology, 24 (2004) 4267-4274.

[96] C.W. Lawrence, Cellular functions of DNA polymerase ζ and Rev1 protein, Advances in Protein Biochemistry, 69 (2004) 167-203.

[97] M.T. Washington, K.D. Carlson, B.D. Freudenthal, J.M. Pryor, Variations on a theme: Eukaryotic Y-family DNA polymerases, Biochim Biophys Acta, 1804 (2010) 1113-1123.

[98] M. Huang, A. Rio, M. Galibert, F. Galibert, Pol32, a subunit of *Saccharomyces cerevisiae* DNA polymerase δ, suppresses genomic deletions and is involved in the mutagenic bypass pathway, Genetics, 160 (2002) 1409-1422.

[99] A. Daraba, V.K. Gali, M. Halmai, L. Haracska, I. Unk, Def1 promotes the degradation of Pol3 for polymerase exchange to occur during DNA-damaged-induced mutagenesis in *Saccharomyces cerevisiae*, PLOS Biology, 12 (2014) 1-11.

[100] T. Hishida, H. Iwasaki, T. Ohno, T. Morishita, H. Shinagawa, A yeast gene, MGS1, encoding a DNA-dependent AAA(+) ATPase is required to maintain genome stability, Proc Natl Acad Sci U S A, 98 (2001) 8283-8289.

[101] H. Nomura, A. Yoshimura, T. Edo, S. Kanno, S. Tada, M. Seki, A. Yasui, T. Enomoto, WRNIP1 accumulates at laser light irradiated sites rapidly via its ubiquitin-binding zinc finger domain and independently from its ATPase domain, Biochem Biophys Res Commun, 417 (2012) 1145-1150.

[102] T. Tsurimoto, A. Shinozaki, M. Yano, M. Seki, T. Enomoto, Human Werner helicase interacting protein 1 (WRNIP1) functions as a novel modulator for DNA polymerase δ, Genes to Cells, 10 (2005) 13-22.

[103] L. Barbour, Regulation of alternative replication bypass pathways at stalled replication forks and its effects on genome stability: A yeast model, Mutation Research/Fundamental and Molecular Mechanisms of Mutagenesis, 532 (2003) 137-155.

[104] D. Branzei, M. Seki, F. Onoda, T. Enomoto, The product of *Saccharomyces cerevisiae* whip/MGS1, a gene related to replication factor C genes, interacts functionally with DNA polymerase δ, Mol Genet Genomics, 268 (2002) 371-386.

[105] M. Smirnova, Role of the error-free damage bypass postreplication repair pathway in the maintenance of genomic stability, Mutation Research/Fundamental and Molecular Mechanisms of Mutagenesis, 532 (2003) 117-135.

[106] T. Hishida, T. Ohno, H. Iwasaki, H. Shinagawa, *Saccharomyces cerevisiae MGS1* is essential in strains deficient in the *RAD6*-dependent DNA damage tolerance pathway, EMBO, 21 (2002) 2019-2029.

[107] J.H. Kim, Y.H. Kang, H.J. Kang, D.H. Kim, G.H. Ryu, M.J. Kang, Y.S. Seo, *In vivo* and *in vitro* studies of Mgs1 suggest a link between genome instability and okazaki fragment processing, Nucleic Acids Res, 33 (2005) 6137-6150.

[108] M. Huang, A. Calignon, A. Nicolas, F. Galibert, *Pol32*, a subunit of the *Saccharomyces cerevisiae* DNA polymerase δ, defines a link between DNA replication and the mutagenic bypass repair pathway, Curr Genet, 38 (2000) 178-187.

[109] N. Acharya, L. Haracska, R.E. Johnson, I. Unk, S. Prakash, L. Prakash, Complex formation of yeast Rev1 and Rev7 proteins: A novel role for the polymerase-associated domain, Mol Cell Biol, 25 (2005) 9734-9740.

[110] T. Hishida, T. Ohya, Y. Kubota, Y. Kamada, H. Shinagawa, Functional and physical interaction of yeast Mgs1 with PCNA: Impact on Rad6-dependent DNA damage tolerance, Mol Cell Biol, 26 (2006) 5509-5517.

[111] Y. Lee, M.T. Gregory, W. Yang, Human pol ζ purified with accessory subunits is active in translesion DNA synthesis and complements pol η in cisplatin bypass, PNAS, 111 (2013) 2954-2959.

[112] L. Giot, R. Chanet, M. Simon, C. Facca, G. Faye, Involvement of the yeast DNA polymerase δ in DNA repair *in vivo*, Genetics, 146 (1997) 1239-1251.

[113] V. Pages, R.E. Johnson, L. Prakash, S. Prakash, Mutational specificity and genetic control of replicative bypass of an abasic site in yeast, Proc Natl Acad Sci U S A, 105 (2008) 1170-1175.

[114] S. Kikuchi, K. Hara, T. Shimizu, M. Sato, H. Hashimoto, Structural basis of recruitment of DNA polymerase ζ by interaction between Rev1 and Rev7 proteins, J Biol Chem, 287 (2012) 33847–33852.

[115] N. Acharya, R.E. Johnson, V. Pages, L. Prakash, S. Prakash, Yeast Rev1 protein promotes complex formation of DNA polymerase ζ with Pol32 subunit of DNA polymerase δ, Proc Natl Acad Sci U S A, 106 (2009) 9631-9636.

[116] A. Yoshimura, Y. Kobayashi, S. Tada, M. Seki, T. Enomoto, WRNIP1 functions upstream of DNA polymerase η in the UV-induced DNA damage response, Biochem Biophys Res Commun, 452 (2014) 48-52.

[117] R.P. Rastogi, Richa, A. Kumar, M.B. Tyagi, R.P. Sinha, Molecular mechanisms of ultraviolet radiation-induced DNA damage and repair, Journal of Nucleic Acids, 2010 (2010) 1-32.

[118] W. Yang, Surviving the sun: Repair and bypass of DNA UV lesions, Protein Science, 20 (2011) 1781.

[119] D.L. Narayanan, R.N. Saladi, J.L. Fox, Ultraviolet radiation and skin cancer, International Journal of Dermatology, 49 (2010) 978-986.

[120] K.M. Hanson, R.M. Clegg, Observation and quantification of ultraviolet-induced reactive oxygen species in *ex vivo* human skin, Photochemistry and Photobiology, 76 (2002) 57-63.

[121] H. Masaki, T. Atsumi, H. Sakurai, Detection of hydrogen peroxide and hydroxyl radicals in murine skin fibroblasts under UVB radiation Biochemical and Biophysical Research Communications, 206 (1995) 474-479.

[122] J. Ravanat, T. Douki, J. Cadet, Direct and indirect effects of UV radiation on DNA and its components, Journal of Photochemistry and Photobiology B: Biology, 63 (2001) 88-102.

[123] K.R. Solomon, Effects of ozone depletion and UV-B radiation on humans and the environment, Atmosphere-Ocean, 46 (2008) 185-202.

[124] J.B. Kerr, C.T. McElroy, Evidence for large upward trends of ultraviolet-B radiation linked to ozone depletion, Science, 262 (1993) 1032-1034.

[125] K.M. de Lima-Bessa, M.G. Armelini, V. Chigancas, J.F. Jacysyn, G.P. Amarante-Mendes, A. Sarasin, C.F. Menck, Cpds and 6-4PPs play different roles in UV-induced cell death in normal and NER-deficient human cells, DNA Repair (Amst), 7 (2008) 303-312.

[126] K. McAteer, Y. Jing, J. Kao, T. J.-S., M.A. Kennedy, Solution-state structure of a DNA dodecamer duplex containing a *cis-syn* thymine cyclobutane dimer, the major UV photoproduct of DNA, Journal of Molecular Biology, 282 (1998) 1013-1032.

[127] H. Park, K. Zhang, Y. Ren, S. Nadji, N. Sinha, J.S. Taylor, C. Kang, Crystal structure of a DNA decamer containing a cis-syn thymine dimer, Proc Natl Acad Sci U S A, 99 (2002) 15965-15970.

[128] J.-K. Kim, B.-S. Choi, The solution structure of DNA duplex-decamer containing the (6-4) photoproduct of thymidylyl(3'-5')thymidine by NMR and relaxation matrix refinement, Eur. J. Biochem., 228 (1995) 849-854.

[129] J. Li, T. Uchida, T. Todo, T. Kitagawa, Similarities and differences between cyclobutane pyrimidine dimer photolyase and (6-4) photolyase as revealed by resonance raman spectroscopy: Electron transfer from the FAD cofactor to ultraviolet-damaged DNA, J Biol Chem, 281 (2006) 25551-25559.

[130] P.H. Clingen, C.F. Arlett, L. Roza, T. Mori, O. Nikaido, M.H.L. Green, Induction of cyclobutane pyrimidine dimers, pyrimidine(6-4)pyrimidone photoproducts, and dewar valence isomers by natural sunlight in normal human mononuclear cells, Cancer Research, 55 (1995) 2245-2248.

[131] A.F. Glas, S. Schneider, M.J. Maul, U. Hennecke, T. Carell, Crystal structure of the T(6-4)C lesion in complex with a (6-4) DNA photolyase and repair of UV-induced (6-4) and dewar photolesions, Chemistry, 15 (2009) 10387-10396.

[132] J.-S. Taylor, H.-F. Lu, J.J. Kotyk, Quantitative coversion of the (6-4) photoproduct of TpdC to its dewar valence isomer upon exposure to simulated sunlight, Photochemistry and Photobiology, 51 (1990) 161-167.

[133] J.-H. Lee, G.-S. Hwang, J.-K. Kim, B.-S. Choi, The solution structure of DNA decamer duplex containing the dewar product of thymidylyl(3'-5')thymidine by NMR and full relaxation matrix refinement, FEBS Lett, 428 (1998) 269-274.

[134] D.E. Brash, W.A. Haseltine, UV-induced mutation hotspots occur at DNA damage hotspots, Nature, 298 (1982) 189-192.

[135] P.W. Doetsch, T.H. Zastawny, A.M. Martin, M. Dizdaroglu, Monomeric base damage products from adenine, guanine, and thymine induced by exposure of DNA to ultraviolet radiation, Biochemistry, 34 (1995) 737-742.

[136] D. Kulms, E. Zeise, B. Poppelmann, T. Schwartz, DNA damage, death receptor activation and reactive oxygen species contribute to ultraviolet radiation-induced apoptosis in an essential and independent way, Oncogene, 21 (2002) 5844-5851.

[137] N.J. Duker, P.E. Gallagher, Purine photoproducts, Photochemistry and Photobiology, 48 (1988) 35-39.

[138] L.F. Batista, B. Kaina, R. Meneghini, C.F. Menck, How DNA lesions are turned into powerful killing structures: Insights from UV-induced apoptosis, Mutat Res, 681 (2009) 197-208.

[139] G.B. Sancar, Enzymatic photoreactivation: 50 years and counting, Mutation Research, 451 (2000) 25-37.

[140] C.F. Menck, Shining a light on photolyases, Nature Genetics, 32 (2002) 338-339.

[141] C. Luo, R. Krishnasamy, A.K. Basu, Y. Zou, Recognition and incision of site-specifically modified C8 guanine adducts formed by 2-aminofluorene, *n*-acetyl-2-aminofluorene and 1-nitropyrene by uvrabc nuclease, Nucleic Acids Res, 28 (2000) 3719-3724.

[142] D. Chandrasekhar, B. Van Houten, *In vivo* formation and repair of cyclobutane pyrimidine dimers and 6-4 photoproducts measured at the gene and nucleotide level in *Escherichia coli*, Mutation Research, 450 (2000) 19-40.

[143] D.G. Vassylyev, T. Kashiwagi, Y. Mikami, M. Ariyoshi, S. Iwai, E. Ohtsuka, K. Morikawa, Atomic model of a pyrimidine dimer excision repair enzyme complexed with a DNA substrate: Structural basis for damaged DNA recognition, Cell, 83 (1995) 773-782.

[144] B.J. Vande Berg, G.B. Sancar, Evidence for dinucleotide flipping by DNA photolyase, J Biol Chem, 273 (1998) 20276-20284.

[145] S.D. McCulloch, R.J. Kokoska, C. Masutani, S. Iwai, F. Hanaoka, T.A. Kunkel, Preferential *cis-syn* thymine dimer bypass by DNA polymerase η occurs with biased fidelity Nature, 428 (2004) 87-100.

[146] R.E. Johnson, S. Prakash, L. Prakash, Efficient bypass of a thymine-thymine dimer by yeast DNA polymerase, polη, Science, 283 (1999) 1001-1004.

[147] A.L. Abdulovic, S. Jinks-Robertson, The *in vivo* characterization of translesion synthesis across UV-induced lesions in *Saccharomyces cerevisiae*: Insights into polζ- and polη-dependent frameshift mutagenesis, Genetics, 172 (2006) 1487-1498.

[148] P.E. Gibbs, J. McDonald, R. Woodgate, C.W. Lawrence, The relative roles *in vivo* of *Saccharomyces cerevisiae* pol η, pol ζ, Rev1 protein and Pol32 in the bypass and mutation induction of an abasic site, T-T (6-4) photoadduct and T-T cis-syn cyclobutane dimer, Genetics, 169 (2005) 575-582.

[149] A. Bresson, R.P. Fuchs, Lesion bypass in yeast cells: Pol η participates in a multi-DNA polymerase process, The EMBO Journal, 21 (2002) 3881-3887.

[150] J.R. Nelson, C.W. Lawrence, D.C. Hinkle, Thymine-thymine dimer bypass by yeast DNA polymerase ζ, Science, 272 (1996) 1646-1649.

[151] I.B. Rogozin, B.A. Malyarchuk, Y.I. Pavlov, L. Milanesi, From context-dependence of mutations to molecular mechanisms of mutagenesis, Pac Symp Biocomput. , (2005) 409-420.

[152] E. Dogliotti, P. Hainaut, T. Hernandez, M. D'Errico, D.M. DeMarini, Mutation spectra resulting from carcinogenic exposure: From model systems to cancer-related genes, Recent Results in Cancer Research, 154 (1998) 97-124.

[153] G. Giglia-Mari, A. Sarasin, TP53 mutations in human skin cancers, Human Mutation, 21 (2003) 217-228.

[154] L. Daya-Grosjean, N. Dumaz, A. Sarasin, The specificity of p53 mutation spectra in sunlight induced human cancers, Journal of Photochemistry and Photobiology, 28 (1995) 115-124.

[155] A. Inga, G. Scott, P. Monti, A. Aprile, A. Abbondandolo, P.A. Burns, G. Fronza, Ultraviolet-light induced p53 mutational spectrum in yeast is indistinguishable from p53 mutations in human skin cancer, Carcinogenesis, 19 (1998) 741-746.

[156] R. Srivas, T. Costelloe, A. Carvunis, S. Sarkar, E. Malta, S.M. Sun, M. Pool, K. Licon, T. Welsem, F. Leeuwen, P.J. McHugh, H. Attikum, A UV-induced genetic network links the RSC complex to nucleotide excision repair and shows dose-dependent rewiring, Cell Reports, 5 (2013) 1714-1724.

[157] D.E. Brash, W.A. Franklin, G.B. Sancar, A. Sancar, W.A. Haseltine, *Escherichia coli* DNA photolyase reverses cyclobutane pyrimidine dimers but not pyrimidine-pyrimidone (6-4) photoproducts, J Biol Chem, 260 (1985) 11438-11441.

[158] T. Todo, H. Takemori, H. Ryo, M. Ihara, T. Matsundaga, O. Nikaido, K. Sato, T. Nomura, A new photoreactivating enzyme that specifically repairs ultraviolet light-induced (6-4)photoproducts, Nature, 361 (1993) 371-374.

8 Appendices

8.1 Appendix A: Abbreviations

6-4PP – 6-4 photoproduct

8-oxoG – 8-oxoguanine

AAF – N-2-acetyl-2-aminoflurene

AP site – apurinic/apyrimidinic site

BER – base excision repair

bp – base pairs

Can - canavanine

CPD – cyclobutane pyrimidine dimer

CTD - C-terminal domain

DDR – DNA damage response

DNA – deoxyribonucleic acid

DP - dipyrimidine

DRIM – defective replisome-induced mutagenesis

DSB – double strand break

FRET – fluorescence resonance energy transfer

GG-NER – global genome nucleotide excision repair

HR – homologous recombination

HU - hydroxyurea

ICL – interstrand crosslink

MBS1/MBS2 – metal binding site 1/2

MEFs – mouse embryonic fibroblasts

Mgs1 – maintenance of genome stability 1

MMR – mismatch repair

MMS – methyl methanesulfonate

NER – nucleotide excision repair

NHEJ – non-homologous end joining

NTS – non-transcribed strand

ORF – open reading frame

PAD – polymerase associated domain

PCNA – proliferating cell nuclear antigen

PCR – polymerase chain reaction

PRR – post-replicative repair

RFC – replication factor C

RNA – ribonucleic acid

ROS – reactive oxygen species

RPA – replication protein A

SC – synthetic complete

SGD – saccharomyces genome database

SSB – single strand break

TC-NER – transcription coupled nucleotide excision repair

TLS – translesion DNA synthesis

TS – transcribed strand

UVR – ultraviolet radiation

WNRIP1 – Werner interacting protein 1

WT – wild type

XP – xeroderma pigmentosum

XPV – xeroderma pigmentosum Variant

ZnF – zinc finger

8.2 Appendix B: Primer Sequences

Table B1: Primer sequences

Primer Set	Function	Sequence (5'-3')
CAN1extF2 CAN1extR2	PCR amplification of *CAN1* gene for spectra	F2 - TCTTCAGACTTCTTAACTCC R2 - ATAGTAAGCTCATTGATCCC
CAN1seq520F CAN1seq699R CAN1seq2094R	*CAN1* sequencing primers for spectra	520F – TGGTTTTCTTGGGCAATCAC 699R - GATGGAAGCGACCCAGAAC 2094R - CATTGATCCCTTAAACTTTCTTTTC
Rev3DDmuta Rev3DDmutaRC	Creation of *rev3-dd* mutant using SDM	GAACGCCAAAGTTGTCTATGGAGCCA CAGCTAGTTTATTTGTATATC RC - Reverse complement of above
Rev1/US-300-F Rev1/US-300-R	Amplification of Rev1 deletion cassette	F - CAAGACGGAAAAAAGTAGCT R - GGTGAGGATGTTCATAGGCG
Pol32-ups-F Pol32-down-R	Amplification of Pol32 deletion cassette	F - GATGTCCTCGGATCGAAACC R - GTGGCGACAGTCATTGAA
ZnF1SDF ZnF1SDR	Creation of *rev3-ZnF* mutant using SDM	F – GAATTGACTAAAATATGTTCACTTCA GTTAGCTGATGACGCTTTAGAG R – GTGAACATATTTTAGTCAATTCTTCA CCAGCATTACAAGCTGTTG
ZnF2-1SDF ZnF2-2SDF ZnF2-2SDR	Creation of *rev3-FeS* mutant using SDM	F1 – TGGCCAGGACGGCCAGTTATCGTTA CACTTCCGATGCAG F2 – AGCCAATTCATATGACGCTCCAGTA TTTTACTCTCGTGTCAAAG R – GAGCGTCATATGAATTGGCTTTACTA GCTATATGGTCATTTTCGATG

*GR – gap repair, SDM – site directed mutagenesis

8.3 Appendix C: Additional Data

8.3.1 Figure C1 - Mutational spectra mapped to *CAN1* gene for WT and *rev3*Δ*C* strains

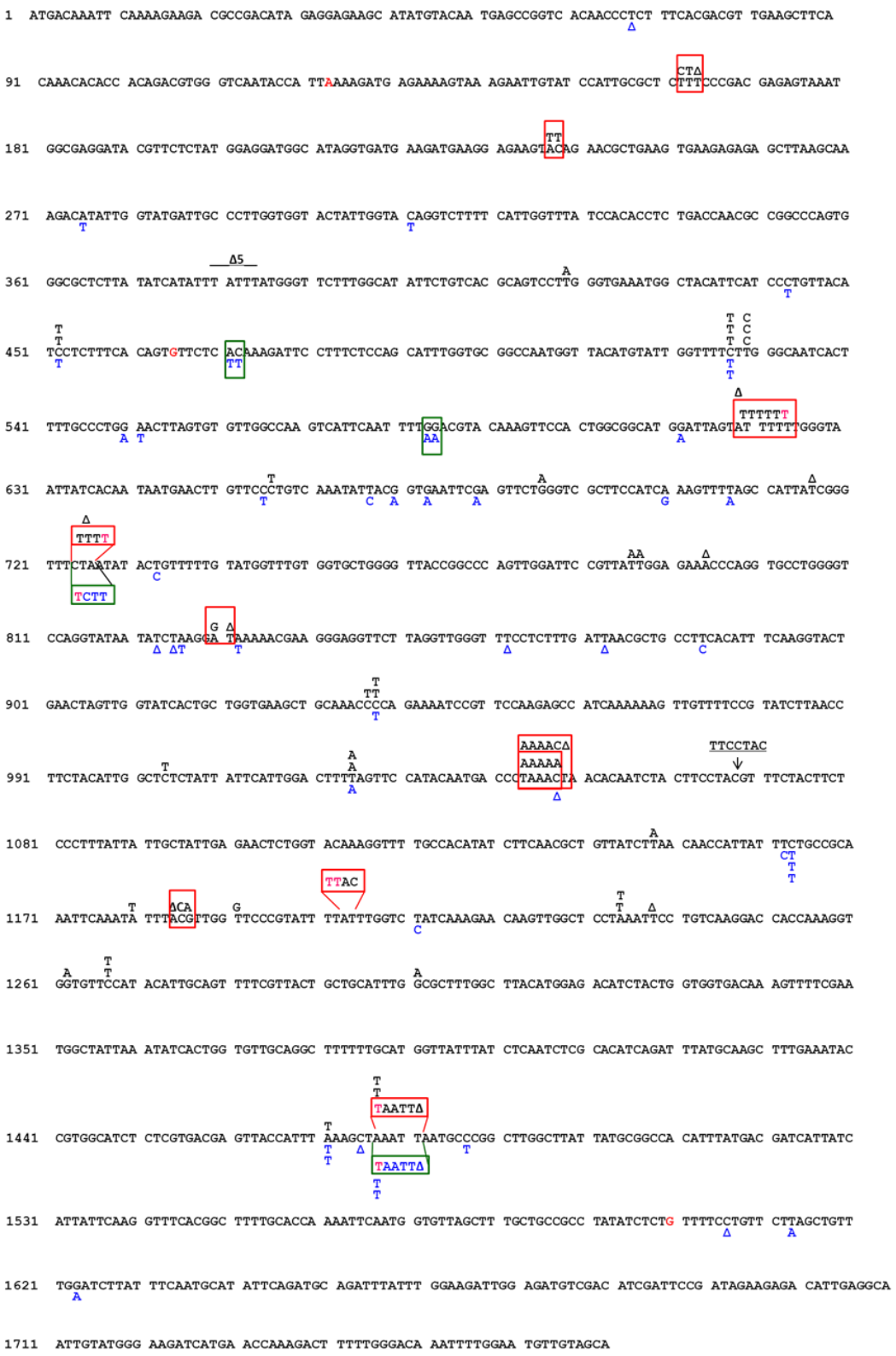
1 ATGACAAATT CAAAAGAAGA CGCCGACATA GAGGAGAAGC ATATGTACAA TGAGCCGGTC ACAACCCTCT TTCACGACGT TGAAGCTTCA
91 CAAACACACC ACAGACGTGG GTCAATACCA TTAAAAGATG AGAAAAGTAA AGAATTGTAT CCATTGCGCT CTTTCCCGAC GAGAGTAAAT
181 GGCGAGGATA CGTTCTCTAT GGAGGATGGC ATAGGTGATG AAGATGAAGG AGAAGTACAG AACGCTGAAG TGAAGAGAGA GCTTAAGCAA
271 AGACATATTG GTATGATTGC CCTTGGTGGT ACTATTGGTA CAGGTCTTTT CATTGGTTTA TCCACACCTC TGACCAACGC CGGCCCAGTG
361 GGCGCTCTTA TATCATATTT ATTTATGGGT TCTTTGGCAT ATTCTGTCAC GCAGTCCTTG GGTGAAATGG CTACATTCAT CCCTGTTACA
451 TCCTCTTTCA CAGTGTTCTC ACAAAGATTC CTTTCTCCAG CATTTGGTGC GGCCAATGGT TACATGTATT GGTTTTCTTG GGCAATCACT
541 TTTGCCCTGG AACTTAGTGT GTTGGCCAA GTCATTCAAT TTTGGACGTA CAAAGTTCCA CTGGCGGCAT GGATTAGTAT TTTTTGGGTA
631 ATTATCACAA TAATGAACTT GTTCCCTGTC AAATATTACG GTGAATTCGA GTTCTGGGTC GCTTCCATCA AAGTTTTAGC CATTATCGGG
721 TTTCTAATAT ACTGTTTTTG TATGGTTTGT GGTGCTGGGG TTACCGGCCC AGTTGGATTC CGTTATTGGA GAAACCCAGG TGCCTGGGGT
811 CCAGGTATAA TATCTAAGGA TAAAAACGAA GGGAGGTTCT TAGGTTGGGT TTCCTCTTTG ATTAACGCTG CCTTCACATT TCAAGGTACT
901 GAACTAGTTG GTATCACTGC TGGTGAAGCT GCAAACCCCA GAAAATCCGT TCCAAGAGCC ATCAAAAAAG TTGTTTTCCG TATCTTAACC
991 TTCTACATTG GCTCTCTATT ATTCATTGGA CTTTTAGTTC CATACAATGA CCCTAAACTA ACACAATCTA CTTCCTACGT TTCTACTTCT
1081 CCCTTTATTA TTGCTATTGA GAACTCTGGT ACAAAGGTTT TGCCACATAT CTTCAACGCT GTTATCTTAA CAACCATTAT TTCTGCCGCA
1171 AATTCAAATA TTTACGTTGG TTCCCGTATT TTATTTGGTC TATCAAAGAA CAAGTTGGCT CCTAAATTCC TGTCAAGGAC CACCAAAGGT
1261 GGTGTTCCAT ACATTGCAGT TTTCGTTACT GCTGCATTTG GCGCTTTGGC TTACATGGAG ACATCTACTG GTGGTGACAA AGTTTTCGAA
1351 TGGCTATTAA ATATCACTGG TGTTGCAGGC TTTTTTGCAT GGTTATTTAT CTCAATCTCG CACATCAGAT TTATGCAAGC TTTGAAATAC
1441 CGTGGCATCT CTCGTGACGA GTTACCATTT AAAGCTAAAT TAATGCCCGG CTTGGCTTAT TATGCGGCCA CATTTATGAC GATCATTATC
1531 ATTATTCAAG GTTTCACGGC TTTTGCACCA AAATTCAATG GTGTTAGCTT TGCTGCCGCC TATATCTCTG TTTTCCTGTT CTTAGCTGTT
1621 TGGATCTTAT TTCAATGCAT ATTCAGATGC AGATTTATTT GGAAGATTGG AGATGTCGAC ATCGATTCCG ATAGAAGAGA CATTGAGGCA
1711 ATTGTATGGG AAGATCATGA ACCAAAGACT TTTTGGGACA AATTTTGGAA TGTTGTAGCA

Figure C.1 Mutational Spectra of WT and *rev3*Δ*C* at 20 J/m^2 mapped to *CAN1* gene

Black continuous text represents the sequence of the *CAN1* gene in budding yeast. Black text/bases above *CAN1* represent mutations found in WT clones and blue text/bases below *CAN1* indicate mutations found in *rev3*Δ*C* clones. Red boxes encase WT complex mutations and green boxes encase *rev3*Δ*C* complex mutations. Triangles represent deletions, if a number is present it indicates how many bases were deleted otherwise it was one base. Red bases in the *CAN1* sequence are polymorphisms found in the 8C strain that differ from the reference strain deposited in the Saccharomyces Genome Database.

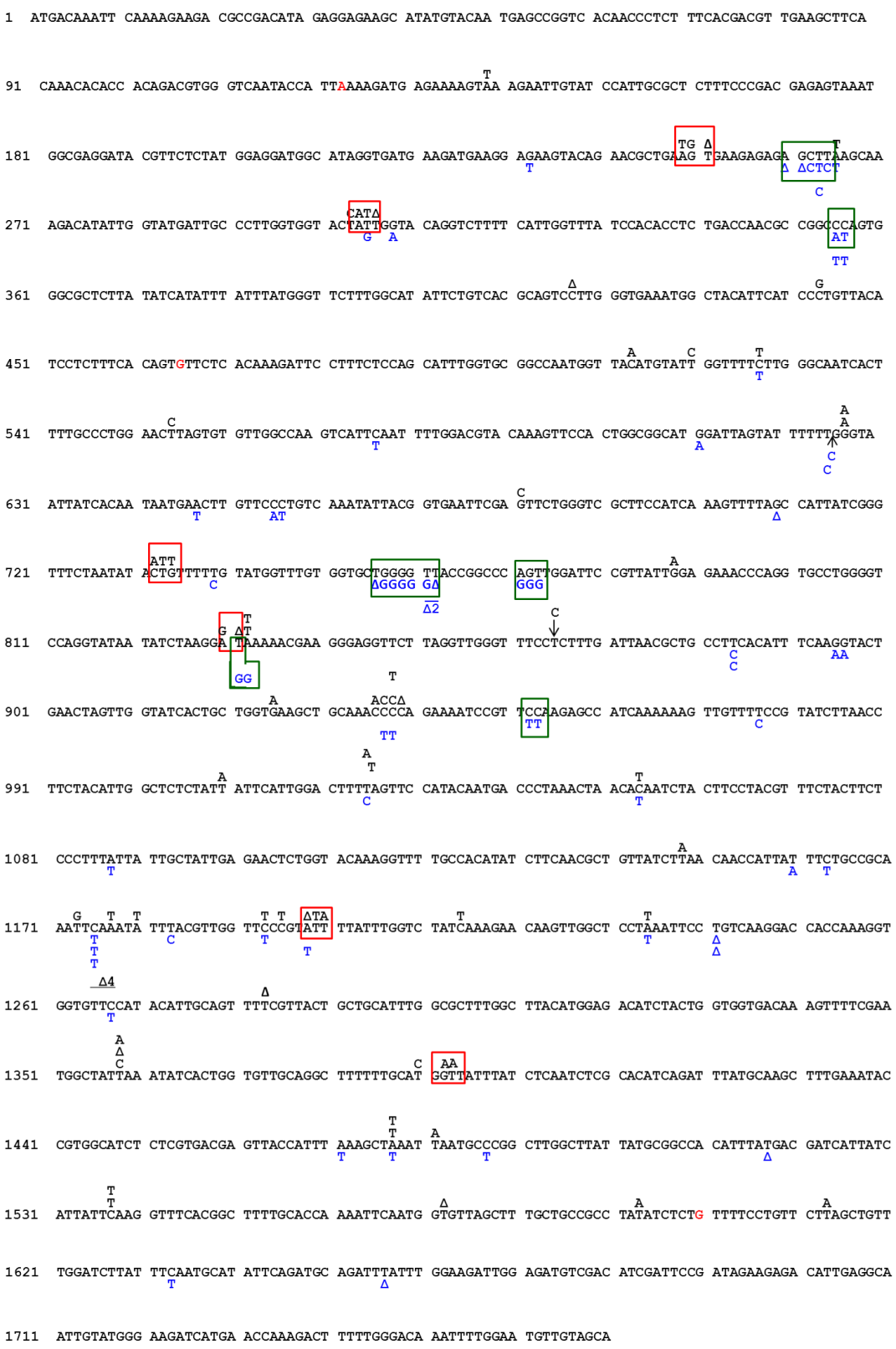
1 ATGACAAATT CAAAAGAAGA CGCCGACATA GAGGAGAAGC ATATGTACAA TGAGCCGGTC ACAACCCTCT TTCACGACGT TGAAGCTTCA
91 CAAACACACC ACAGACGTGG GTCAATACCA TTAAAAGATG AGAAAAGTAA AGAATTGTAT CCATTGCGCT CTTTCCCGAC GAGAGTAAAT
181 GGCGAGGATA CGTTCTCTAT GGAGGATGGC ATAGGTGATG AAGATGAAGG AGAAGTACAG AACGCTGAAG TGAAGAGAGA GCTTAAGCAA
271 AGACATATTG GTATGATTGC CCTTGGTGGT ACTATTGGTA CAGGTCTTTT CATTGGTTTA TCCACACCTC TGACCAACGC CGGCCCAGTG
361 GGCGCTCTTA TATCATATTT ATTTATGGGT TCTTTGGCAT ATTCTGTCAC GCAGTCCTTG GGTGAAATGG CTACATTCAT CCCTGTTACA
451 TCCTCTTTCA CAGTGTTCTC ACAAAGATTC CTTTCTCCAG CATTTGGTGC GGCCAATGGT TACATGTATT GGTTTTCTTG GGCAATCACT
541 TTTGCCCTGG AACTTAGTGT GTTGGCCAA GTCATTCAAT TTTGGACGTA CAAAGTTCCA CTGGCGGCAT GGATTAGTAT TTTTTGGGTA
631 ATTATCACAA TAATGAACTT GTTCCCTGTC AAATATTACG GTGAATTCGA GTTCTGGGTC GCTTCCATCA AAGTTTTAGC CATTATCGGG
721 TTTCTAATAT ACTGTTTTTG TATGGTTTGT GGTGCTGGGG TTACCGGCCC AGTTGGATTC CGTTATTGGA GAAACCCAGG TGCCTGGGGT
811 CCAGGTATAA TATCTAAGGA TAAAAACGAA GGGAGGTTCT TAGGTTGGGT TTCCTCTTTG ATTAACGCTG CCTTCACATT TCAAGGTACT
901 GAACTAGTTG GTATCACTGC TGGTGAAGCT GCAAACCCCA GAAAATCCGT TCCAAGAGCC ATCAAAAAAG TTGTTTTCCG TATCTTAACC
991 TTCTACATTG GCTCTCTATT ATTCATTGGA CTTTTAGTTC CATACAATGA CCCTAAACTA ACACAATCTA CTTCCTACGT TTCTACTTCT
1081 CCCTTTATTA TTGCTATTGA GAACTCTGGT ACAAAGGTTT TGCCACATAT CTTCAACGCT GTTATCTTAA CAACCATTAT TTCTGCCGCA
1171 AATTCAAATA TTTACGTTGG TTCCCGTATT TTATTTGGTC TATCAAAGAA CAAGTTGGCT CCTAAATTCC TGTCAAGGAC CACCAAAGGT
1261 GGTGTTCCAT ACATTGCAGT TTTCGTTACT GCTGCATTTG GCGCTTTGGC TTACATGGAG ACATCTACTG GTGGTGACAA AGTTTTCGAA
1351 TGGCTATTAA ATATCACTGG TGTTGCAGGC TTTTTTGCAT GGTTATTTAT CTCAATCTCG CACATCAGAT TTATGCAAGC TTTGAAATAC
1441 CGTGGCATCT CTCGTGACGA GTTACCATTT AAAGCTAAAT TAATGCCCGG CTTGGCTTAT TATGCGGCCA CATTTATGAC GATCATTATC
1531 ATTATTCAAG GTTTCACGGC TTTTGCACCA AAATTCAATG GTGTTAGCTT TGCTGCCGCC TATATCTCTG TTTTCCTGTT CTTAGCTGTT
1621 TGGATCTTAT TTCAATGCAT ATTCAGATGC AGATTTATTT GGAAGATTGG AGATGTCGAC ATCGATTCCG ATAGAAGAGA CATTGAGGCA
1711 ATTGTATGGG AAGATCATGA ACCAAAGACT TTTTGGGACA AATTTTGGAA TGTTGTAGCA

Figure C.2 Mutational Spectra of WT and *rev3ΔC* at 40 J/m^2 mapped to *CAN1* gene

Black continuous text represents the sequence of the *CAN1* gene in budding yeast. Black text/bases above *CAN1* represent mutations found in WT clones and blue text/bases below *CAN1* indicate mutations found in *rev3ΔC* clones. Red boxes encase WT complex mutations and green boxes encase *rev3ΔC* complex mutations. Triangles represent deletions, if a number is present it indicates how many bases were deleted otherwise it was one base. Red bases in the *CAN1* sequence are polymorphisms found in the 8C strain that differ from the reference strain deposited in the Saccharomyces Genome Database.

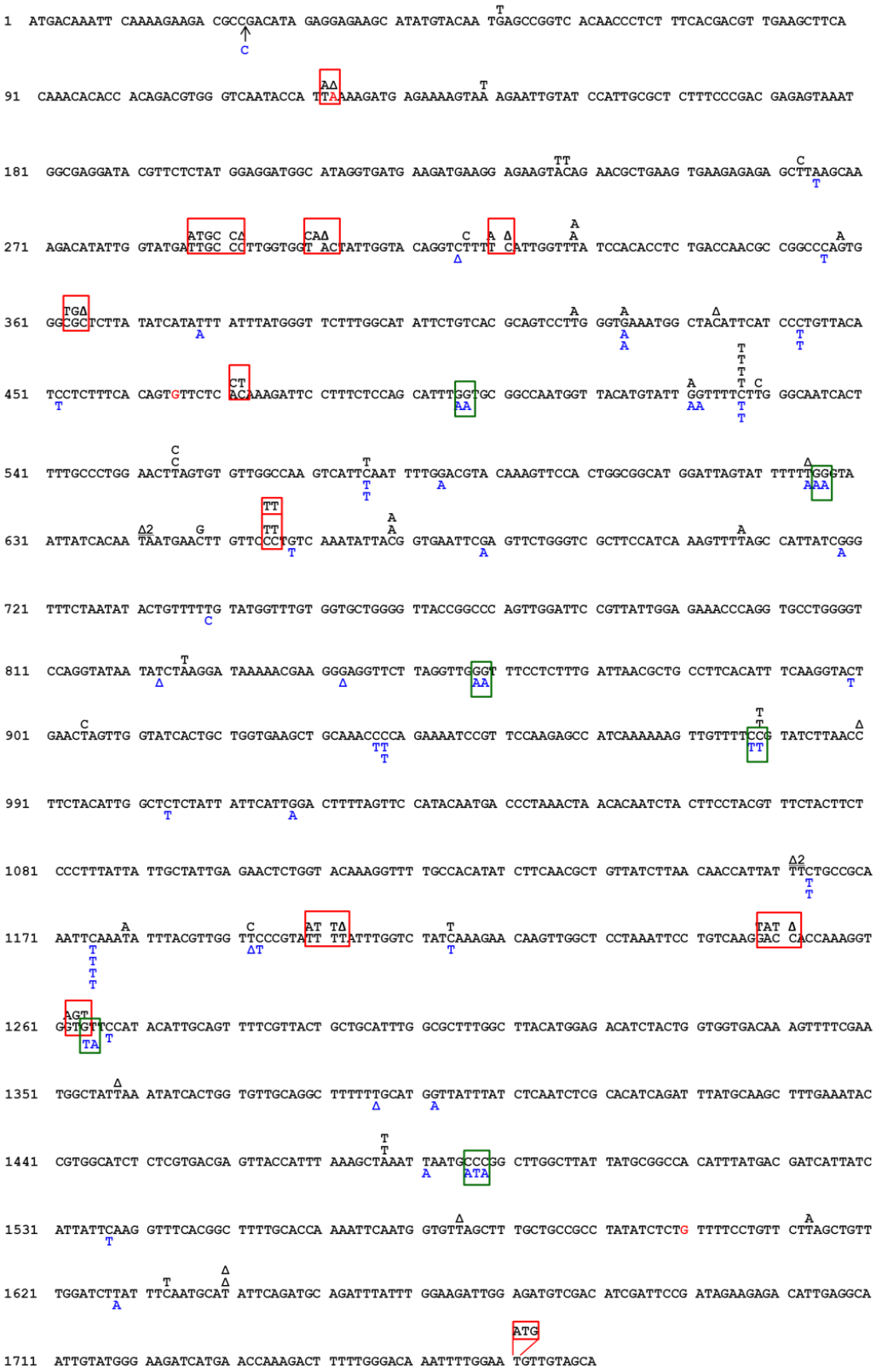
1 ATGACAAATT CAAAAGAAGA CGCCGACATA GAGGAGAAGC ATATGTACAA TGAGCCGGTC ACAACCCTCT TTCACGACGT TGAAGCTTCA
91 CAAACACACC ACAGACGTGG GTCAATACCA TTAAAAGATG AGAAAAGTAA AGAATTGTAT CCATTGCGCT CTTTCCCGAC GAGAGTAAAT
181 GGCGAGGATA CGTTCTCTAT GGAGGATGGC ATAGGTGATG AAGATGAAGG AGAAGTACAG AACGCTGAAG TGAAGAGAGA GCTTAAGCAA
271 AGACATATTG GTATGATTGC CCTTGGTGGT ACTATTGGTA CAGGTCTTTT CATTGGTTTA TCCACACCTC TGACCAACGC CGGCCCAGTG
361 GGCGCTCTTA TATCATATTT ATTTATGGGT TCTTTGGCAT ATTCTGTCAC GCAGTCCTTG GGTGAAATGG CTACATTCAT CCCTGTTACA
451 TCCTCTTTCA CAGTGTTCTC ACAAAGATTC CTTTCTCCAG CATTTGGTGC GGCCAATGGT TACATGTATT GGTTTTCTTG GGCAATCACT
541 TTTGCCCTGG AACTTAGTGT GTTGGCCAA GTCATTCAAT TTTGGACGTA CAAAGTTCCA CTGGCGGCAT GGATTAGTAT TTTTTGGGTA
631 ATTATCACAA TAATGAACTT GTTCCCTGTC AAATATTACG GTGAATTCGA GTTCTGGGTC GCTTCCATCA AAGTTTTAGC CATTATCGGG
721 TTTCTAATAT ACTGTTTTTG TATGGTTTGT GGTGCTGGGG TTACCGGCCC AGTTGGATTC CGTTATTGGA GAAACCCAGG TGCCTGGGGT
811 CCAGGTATAA TATCTAAGGA TAAAAACGAA GGGAGGTTCT TAGGTTGGGT TTCCTCTTTG ATTAACGCTG CCTTCACATT TCAAGGTACT
901 GAACTAGTTG GTATCACTGC TGGTGAAGCT GCAAACCCCA GAAAATCCGT TCCAAGAGCC ATCAAAAAAG TTGTTTTCCG TATCTTAACC
991 TTCTACATTG GCTCTCTATT ATTCATTGGA CTTTTAGTTC CATACAATGA CCCTAAACTA ACACAATCTA CTTCCTACGT TTCTACTTCT
1081 CCCTTTATTA TTGCTATTGA GAACTCTGGT ACAAAGGTTT TGCCACATAT CTTCAACGCT GTTATCTTAA CAACCATTAT TTCTGCCGCA
1171 AATTCAAATA TTTACGTTGG TTCCCGTATT TTATTTGGTC TATCAAAGAA CAAGTTGGCT CCTAAATTCC TGTCAAGGAC CACCAAAGGT
1261 GGTGTTCCAT ACATTGCAGT TTTCGTTACT GCTGCATTTG GCGCTTTGGC TTACATGGAG ACATCTACTG GTGGTGACAA AGTTTTCGAA
1351 TGGCTATTAA ATATCACTGG TGTTGCAGGC TTTTTTGCAT GGTTATTTAT CTCAATCTCG CACATCAGAT TTATGCAAGC TTTGAAATAC
1441 CGTGGCATCT CTCGTGACGA GTTACCATTT AAAGCTAAAT TAATGCCCGG CTTGGCTTAT TATGCGGCCA CATTTATGAC GATCATTATC
1531 ATTATTCAAG GTTTCACGGC TTTTGCACCA AAATTCAATG GTGTTAGCTT TGCTGCCGCC TATATCTCTG TTTTCCTGTT CTTAGCTGTT
1621 TGGATCTTAT TTCAATGCAT ATTCAGATGC AGATTTATTT GGAAGATTGG AGATGTCGAC ATCGATTCCG ATAGAAGAGA CATTGAGGCA
1711 ATTGTATGGG AAGATCATGA ACCAAAGACT TTTTGGGACA AATTTTGGAA TGTTGTAGCA

Figure C.3 Mutational Spectra of WT and *rev3*Δ*C* at 60 J/m^2 mapped to *CAN1* gene

Black continuous text represents the sequence of the *CAN1* gene in budding yeast. Black text/bases above *CAN1* represent mutations found in WT clones and blue text/bases below *CAN1* indicate mutations found in *rev3*Δ*C* clones. Red boxes encase WT complex mutations and green boxes encase *rev3*Δ*C* complex mutations. Triangles represent deletions, if a number is present it indicates how many bases were deleted otherwise it was one base. Red bases in the *CAN1* sequence are polymorphisms found in the 8C strain that differ from the reference strain deposited in the Saccharomyces Genome Database.

8.4 Appendix D: Breakdown of DP Sites in *CAN1*

Table D1: Number of sites of each DP site present on each strand in *CAN1*

Type of DP	# of sites in *CAN1*	Total per strand
TT	225	
TC	105	NTS
CT	111	518
CC	77	
AA	136	
AG	92	TS
GA	87	418
GG	103	

*DP – dipyrimidine, NTS – non-transcribed strand
TS – transcribed strand

Table D2: Number of sites of each overlapping DP site present on each strand in *CAN1*

Type of OVL DP	# of sites in *CAN1*	Total per strand
TTC	38	NTS 186
CTT	50	
CCT	26	
TCT	35	
TCC	20	
CTC	17	
AAG	29	TS 157
GAA	37	
GGA	19	
AGA	31	
AGG	21	
GAG	20	

*OVL – overlapping, DP – dipyrimidine
NTS – non-transcribed strand, TS – transcribed strand